博 士 学 位 論 文
Doctoral Dissertation

The Impact of Changes in Anthropogenic Activity

Caused by COVID-19 Lockdown on Reducing Air Pollution

Levels

(COVID-19 ロックダウンによって生じた人間活動の変化の大気汚染

レベルへの影響)

東北大学大学院環境科学研究科

Graduate School of Environmental Studies, Tohoku University

	先端環境創成学専攻 文化環境学コース	専攻major／ コースcourse
学籍番号 Student ID No.	C0GD4502	
氏　名 Name	ナトラリ トングルエン	

<table>
<tr><td>指　導　教　員
Supervisor at Tohoku Univ.</td><td colspan="2">教授　中谷　友樹</td></tr>
<tr><td>研 究 指 導 教 員
Research Advisor at Tohoku Univ.</td><td colspan="2"></td></tr>
<tr><td rowspan="4">審　査　委　員
（○印は主査）
Dissertation Committee Members
Name marked with “○” is the Chief Examiner</td><td colspan="2">○　教授　中谷　友樹</td></tr>
<tr><td>1　教授　松八重　一代</td><td>2　准教授　磯田　弦
（理学研究科）</td></tr>
<tr><td>3　准教授　堤田　成政
（埼玉大学）</td><td>4</td></tr>
<tr><td>5</td><td>6</td></tr>
</table>

ACKNOWLEDGMENTS

I would like to express my sincere gratitude to my supervisor, Dr. Tomoki Nakaya, for his invaluable guidance, encouragement, and support throughout my PhD journey. His expert insights, constructive feedback, and unwavering dedication to my success have been instrumental in shaping my research and helping me overcome the various challenges I encountered along the way.

I would like to show my sincere gratitude to the co-author of this study, Dr. Narumasa Tsutsumida for his valuable feedback and constructive criticism, which helped me refine my ideas and improve the quality of my work.

I would also like to thank the committee members of my dissertation committee, Dr.Yuzuru Isoda, and Dr. Kazuyo Matsubae for their guidance, advice and valuable suggestion regarding my dissertation.

I would like to thank the members of Environmental Geography Laboratory and the Human Geography Group at Tohoku University for their support, stimulating discussions, and encouragement throughout the years.

I would like to express my heartfelt gratitude to my family and my parents, Mrs. Siriluk and Mr. Somkuan, for their unwavering support, encouragement, and sacrifices throughout my academic journey. Without their love and support, this achievement would not have been possible.

I also want to give a special thanks to Mr. Jesse Dean Ludick and my friends, for providing emotional support during stressful times. They have listened to my ideas, celebrated my successes, and helped me navigate the challenges and setbacks along the way. I could not have completed this degree without their love and encouragement.

Last but not the least, I gratefully appreciate to Japanese Government (MEXT) Scholarship which gave the opportunities of education to me with scholarships.

ABSTRACT

Coronavirus disease (COVID-19)[1] was first identified in Wuhan, China, in 2019, and has since become a pandemic. To reduce the risk of COVID-19 infection, most countries implemented non-pharmaceutical interventions (NPIs), such as lockdown measures, restrictions on various anthropogenic practices, and reduced inter-provincial transportation. This resulted in an unintended decrease in air pollution. The primary goal of this thesis is to investigate the geographic contextualities of the impact of the changes in human activities caused by the NPIs, particularly COVID-19 lockdown measure, on air pollution levels in Thailand and other Southeast Asian and South Asian countries.

First, this study examines the impact of the COVID-19 lockdown on air pollution and human activity in the Bangkok Metropolitan Region (BMR) in Thailand. Ground-based air pollutant data was analyzed to compare pollutant levels during the first lockdown period in 2020 with the baseline period of 2017-2019. This study found substantial reductions in NO_2, SO_2, PM_{10}, and $PM_{2.5}$ concentrations during the lockdown period due to a halt in anthropogenic activities such as transportation and industrial operations. Only O_3 levels rose, possibly due to lowered emissions of its precursors. The study identified a strong temporal correlation between the intensity of Nighttime Lights (NTL) and NO_2 levels in the BMR. In comparison to other measures of human activity in the BMR, the NTL has the highest sensitivity to the temporal fluctuations of air pollutants. This indicates that monitoring the temporal changes or regional differences in NTL intensity is promising to assess temporal or regional variations in air pollution level, particularly NO_2.

Second, based on the findings of the above, we used satellite-based NTL intensity as an indicator of human activity and expand the study area from the BMR to the entire country of Thailand, with a focus on the lockdown period, in order to investigate the contextuality of the association between the changes in human activity and air pollution. There are few studies on the relationship between NO_2 and human activity

[1] COVID-19: coronavirus disease, WHO: World Health Organization, NASA: National Aeronautics and Space Administration, NO_2: nitrogen dioxide, NTL: night-time light, GWR: geographically weighted regression, S5P: Sentinel-5 Precursor, GEE: Google Earth Engine, TROPOMI: Tropospheric Monitoring Instrument, Suomi-NPP: Suomi National Polar-orbiting Partnership, VIIRS-DNB: Visible Infrared Imaging Radiometer Suite Day/Night Band, and BMR: Bangkok Metropolitan Region.

measurements in developing countries, owing to the difficulty in identifying changes in anthropogenic activity at a high geographical resolution. We focused on satellite-based NTL as an indicator of anthropogenic activity and investigated the relationship between the NTL and NO_2 reductions captured by Sentinel-5 Precursor satellite observations during Thailand's first lockdown period in 2020. Using geographically weighted regression (GWR), we examined the regional relationship between NTL and NO_2 changes during the first lockdown because the contributions of NTL to NO_2 concentration in the air may vary over space depending on types of local anthropogenic activity. According to the satellite-based percentage changes in NO_2 levels during the lockdown period in 2020 decreased by 10.36% when compared to the same period in 2019. Such decreases in NTL were prominent in major urban and built-up areas (31.66%). According to the GWR result, the NTL and NO_2 have a positive local association around the country's central, western, and northern regions, while negative associations were found in the peripheral regions. The positive association was most salient around the BMR in the central part of Thailand. These findings indicate that NTL observations can be used to monitor the NO_2 changes caused by the anthropogenic activity changes in urban areas.

Finally, this study broadens the study area to include major cities in South Asia (SA) and Southeast Asia (SEA) to examine the contextualized effect of human activity changes caused by COVID-19 lockdown measures on changes in NO_2 levels in a wider international context. The results showed that in most of cities NO_2 concentration decreased during the lockdown period in 2020 compared to the same period in 2019. Comparing detailed element of implemented NPIs between the cities, we found that strict restrictions led to substantial reductions in human activity, particularly in the transportation and industrial sectors, resulting in lower NO_2 emissions. Furthermore, variations in NTL intensity during the lockdown period were observed among the cities, most likely due to differences in lockdown duration, policies, and economic activity within each country. The severity and enforcement of lockdown policies varied across the countries studied, resulting in differences in economic activity and energy consumption. These variations emphasize the importance of considering regional and country-specific factors into account when analyzing the relationship between NTL intensity, NO_2 concentrations, and the impact of COVID-19 lockdown measures. Furthermore, this study revealed that NTL is useful for monitoring the impact of a

sudden decrease in human activities on air pollution in cities with large populations and more advanced economic activities, while NTL does not function well in cities with less developed and smaller populations.

CONTENTS

Page

ABSTRACT **iv**

CONTENTS **viii**

LIST OF TABLES **x**

LIST OF FIGURES **xi**

Figures **Page**

xi

LIST OF ABBREVIATIONS **xiii**

CHAPTER 1 INTRODUCTION **1**

1.1 Air pollution situation before COVID-19 pandemic 1

1.2 COVID-19 lockdown and air pollution 3

1.3 Nighttime light remote sensing 5

1.4 Objectives of the Study 6

1.5 Chapter Overview 7

CHAPTER 2 Examining the change in air pollutants during COVID-19 lockdown in Bangkok Metropolitan Region, Thailand **10**

2.1 Introduction 10

2.2 Materials and methods 11

2.2.1 Study area11

2.2.2 Data collection 13

2.2.3 Statistical Analysis 16

2.3 Results 19

2.3.1 Air pollution assessment during COVID-19 19

2.3.2 Correlation between human activities and air pollutants in the Bangkok Metropolitan Region 29

2.3.3 Multiple regression analysis between human activities and air pollution changes in the Bangkok Metropolitan Region 32

2.4 Discussion 35

2.5 Conclusion 37

CHAPTER 3 The Impact of Changes in Anthropogenic Activity Caused by COVID-19 Lockdown on Reducing Nitrogen Dioxide Levels in Thailand Using Nighttime Light Intensity **38**
3.1 Introduction 38
3.2.1 Data Sources and Preparation 42
3.2.2 Estimation of Air Pollution Emission and Its Relationship with Anthropogenic Activities 43
3.2 Results 44
3.2.1 NO_2 Level and NTL Intensity Change in Thailand 44
3.2.2 Association between the NTL and NO_2 Levels 51
3.3 Discussion 53
3.4 Conclusion 55
CHAPTER 4 **56**
The Effect of Anthropogenic Activity Caused by COVID-19 Lockdown Resulting in Changes in Nitrogen Dioxide Levels Using Nighttime Light Intensity in South and Southeast Asia **56**
4.1 Introduction 56
4.2 Materials and Methods 57
4.2.1 Study area57
4.2.2 Data collection 62
4.2.3 Statistical Analysis 62
4.3 Results 64
4.3.1 NO_2 Level and NTL Intensity Change in the 7 Cities in Southeast Asia 64
4.3.2 NO_2 Level and NTL Intensity Change in the 11 Cities in Southeast Asia 69
4.3.3 The different experiences among the study cities during the lockdown period 77
4.3.4 Description of boxplots and graphs analysis 81
4.4 Discussion 87
4.5 Conclusion 89
CHAPTER 5 Summary and Conclusion **91**
List of Publication **95**
REFERENCES **96**

LIST OF TABLES

Tables **Page**

Table 2.1 *Descriptive of air pollution monitoring sites in the Bangkok Metropolitan Region* 15

Table 2.2 *Descriptive statistics of air pollutant concentrations, expressway traffic volume and public transport ridership data across the Bangkok Metropolitan Region in year 2017 to 2020* 19

Table 2.3 *Average air pollutant concentrations and human activities during the first lockdown and same period in 2017 to 2019 in the Bangkok Metropolitan Region* 20

Table 2.4 *Descriptive of correlation between expressway traffic volume and air pollutants in the Bangkok Metropolitan Region* 30

Table 2.5 *Descriptive of correlation between public transportation and air pollutants in the Bangkok Metropolitan Region* 31

Table 2.6 *Descriptive of correlation between nighttime light and air pollutants in the Bangkok Metropolitan Region* 32

Table 2.7 *Multiple regression analysis between air pollutants and measure of human activities in the Bangkok Metropolitan Region during the lockdown period* 34

Table 3.1 *Land cover types in NO_2 and nighttime light intensity reduction areas* 49

Table 4.1*The study area description* 58

Table 4.2 *Description of study cities* 76

LIST OF FIGURES

Figures **Page**

Figure 1.1 *Structure of this thesis* 8
Figure 2.1 *The Bangkok Metropolitan Region map and COVID-19 case per 1,000 people during the 1st lockdo* 12
Figure 2.2 *The Bangkok Metropolitan Region's population density (per square kilometer)* 13
Figure 2.3 *Spatial distribution of air pollution monitoring sites located in the Bangkok Metropolitan Region* 14
Figure 2.4 *Time-trends of monthly averaged of NO_2 concentration between 2017 to 2020* 21
Figure 2.5 *Time-trends of monthly averaged of SO_2 concentration between 2017 to 2020* 22
Figure 2.6 *Time-trends of monthly averaged of CO concentration between 2017 to 2020* 23
Figure 2.7 *Time-trends of monthly averaged of O_3 concentration between 2017 to 2020* 24
Figure 2.8 *Time-trends of monthly averaged of PM_{10} concentration between 2017 to 2020* 25
Figure 2.9 *Time-trends of monthly averaged of $PM_{2.5}$ concentration between 2017 to 2020* 26
Figure 2.10 *Time-trends of monthly averaged of expressway traffic volume concentration between 2017 to 2020* 27
Figure 2.11 *Time-trends of monthly averaged of public transport ridership concentration between 2017 to 2020* 28
Figure 2.12 *Time-trends of monthly averaged of nighttime light concentration between 2017 to 2020* 29
Figure 3.1 *Population density of Thailand* 39
Figure 3.2 *COVID-19 cases per 1000 people during the first lockdown and COVID-19 situation administration zoning map (March 18 to June 30, 2020).* 40

Figure 3.3 *Monthly trends of nighttime light (a) and NO_2 (b) in 2019 and 2020 in Thailand.* 46
Figure 3.4 *Spatial distribution of the change in NO_2 levels during the first lockdown period in 2020 compared to the same period in 2019.* 47
Figure 3.5 *Spatial distribution of the difference in nighttime light intensity between the first lockdown period in 2020 and the same period in 2019.* 48
Figure 3.6 *Land cover types in reduction areas* 50
Figure 3.7 *Geographically weighted regression (GWR) estimates of the slope coefficient.* 52
Figure 4.1 *South Asia region map* 60
Figure 4.2 *Southeast Asia region map* 61
Figure 4.3 *Monthly trends of NO_2 of 7 cities in South Asia in 2019 and 2020* 65
Figure 4.4 *Monthly trends of Nighttime light of 7 cities in South Asia in 2019 and 2020* 67
Figure 4.5 *Monthly trends of NO_2 of 11 cities in Southeast Asia in 2019 and 2020* 70
Figure 4.6 *Monthly trends of nighttime light of 11 cities in Southeast Asia in 2019 and 2020* 73
Figure 4.7 *Hierarchical Clustering Dendrogram of percentage reduction of nighttime light and percentage reduction of NO_2 during the lockdown period in 18 cities* 78
Figure 4.8 *Scatter diagram of percentage reduction of nighttime light and percentage reduction of NO_2 during the lockdown period in 18 cities* 79
Figure 4.9 *Boxplot of GDP per capita by group of percentage of nighttime light and NO_2 reduction* 82
Figure 4.10 *Boxplot of area size by group of percentage of nighttime light and NO_2 reduction* 83
Figure 4.11 *Boxplot of estimated population by group of percentage of nighttime light and NO_2 reduction* 84
Figure 4.12 *Bar plot of stay-at-home policy restriction levels by group of percentage of nighttime light and NO_2 reduction* 85
Figure 4.13 *Bar plot of internal movement policy restriction levels by group of percentage of nighttime light and NO_2 reduction* 86
Figure 4.14 *Bar plot of cancelation of public events policy restriction levels by group of percentage of nighttime light and NO_2 reduction* 87

LIST OF ABBREVIATIONS

BMR	= Bangkok Metropolitan Region
CO	= carbon monoxide
CO_2	= carbon dioxide
COVID-19	= Coronavirus disease 2019
DMSP-OLS	= Defense Meteorological Satellite Program's Operational Line Scan System
DNB	= day/night band
GEE	= Google Earth Engine
GWR	= geographically weighted regression
MRT	= mass rapid transit
NO_2	= nitrogen dioxide
NTL	= nighttime light
O_3	= ozone
PCD	= Pollution Control Department
$PM_{2.5}$	= particulate matter 2.5
PM_{10}	= particulate matter 10
SA	= South Asia
SEA	= Southeast Asia
S-NPP	= Suomi National Polar-orbiting Partnership

SO_2 = sulphur dioxide

S5P = Sentinel-5 Precursor

VIIRS = Visible Infrared Imaging Radiometer Suite

WHO = World Health Organization

CHAPTER 1
INTRODUCTION

1.1 Air pollution situation before COVID-19 pandemic

Many global citizens lived in a rapidly industrializing and urbanizing world in the years preceding the emergence of the 2019 Coronavirus disease (COVID-19) and the period of intense global lockdowns. Obviously, the rate of development varied according to each nation's social, economic, and geopolitical circumstances. Regardless of these distinctions, the nature of industrial society encourages daily activities that influence global air pollution trends, such as the use of biomass and other energy and transportation fuels. Current estimates place the global population at 8 billion, with an annual increase of more than 33 million (Worldometer, 2023). The global population's rapid growth necessitates an increase in the production of food, shelter, and other essential services (Helin and Weikard, 2019). As a result, anthropogenic activities such as industrial and processing operations face increased demand (Subramaniam et al., 2020), posing a substantial threat to the Earth's ecosystem long-term viability (Iqbal et al., 2018). Power generation, industry, transportation demand, and transport volume have all increased in tandem with population growth. The massive anthropogenic emissions from these sectors have caused numerous of environmental issues, including detrimental effects on human health (Lelieveld et al, 2015; Kim et al., 2015), decreased outdoor air quality (Gu et al., 2015), and a changed climate system (Ramanathan and Feng, 2009).

Environmental impacts are one of the most important factors influencing human health (Wong et al., 2008). Monitoring air quality is critical for ecosystems and public health. Air pollutants like sulfur dioxide (SO_2), carbon monoxide (CO), ozone (O_3), and nitrogen dioxide (NO_2), on the other hand, are poisoning the air at previously unheard-of levels, endangering human health (Chen et al., 2007). Environmental pollution has been linked to a variety of acute and terminal illnesses, including lung aging, asthma, emphysema, bronchitis, and cancer (Hamra et al., 2015). Air pollution claims a significant number of lives each year, with the severity of the problem worsening over time. Elevated NO_2 and other pollutants level present in the atmosphere are responsible for nearly seven million deaths reported by health authorities each year (Khoder, 2002).

According to the World Health Organization (WHO), the adverse effects of poor air quality are responsible for the death of more than 4.6 million people annually. In densely populated areas, urban aerosols and atmospheric NO_2 are widely recognized as significant and hazardous air pollutants (Cohen et al., 2017). The primary source of these pollutants is the combustion of fossil fuels in the industrial, transportation, and social sectors (Seinfeld and Pandis, 2016). In recent years, there has been a greater emphasis placed on reducing air pollution. Global legislation has seen a concerted effort to reduce waste and pollution. Nonetheless, progress in reducing pollution levels has been relatively limited.

There is a notable occurrence of development in South Asia (SA) and Southeast Asia (SEA) regions that exacerbates various challenges associated with rapid urbanization and pollution, such as vehicular emissions and biomass burning. According to studies conducted by Beig et al. (2020) and Conticini et al. (2020), in Asia harbor cities with high population densities and substantial levels of pollution, the elevated levels of air pollution in urban areas can cause cellular inflammation, severe respiratory problems, bronchial hyperresponsiveness, and potentially fatal outcomes (Lippmann and Leikauf, 2020).

Exploring SA in more detail, nations such as India, Bangladesh, and Iran are of particular interest because they use and consume the most energy in an area where regional air pollution is expected to rise steadily. India, being the most densely populated country in the region, with notably rapid urbanization and population growth, becomes a prime example for investigating the various contributing factors to air pollution. India relies on the combustion of various fuels for the supply of electricity, heating, cooking and other industries. In 2017, India was the world's second largest producer, consumer, and importer of coal (IEA, 2018). Coal is the most carbon-intensive and polluting fossil fuel. According to the Central Electricity Authority (2017), coal accounted for 72% of India's electricity generation and 65% of its CO_2 emissions. Bangladesh like the rest of the region yields similar results. Vehicular and industrial emissions and biomass burning release the highest amounts of pollutants into the air.

SEA countries contribute similarly to air pollution as SA countries do. SEA has a large area of tropical forests and other fire-prone biomes, in addition to a growing

demand for pollutant-causing resources resulting from rapid urbanization, particularly, the burning of Indonesian peatlands and forests, contribute significantly to global CO_2 emissions (Jaenicke et al., 2008). Other Southeast Asian countries, including Vietnam, Laos, Thailand, Cambodia, Myanmar, and Malaysia, have up to 50% of their land covered by forests, peatlands, and other undeveloped environments that are vulnerable to fire (Fujisaka et al., 1996). To summarize, these countries are impacted by both natural and man-made pollution sources.

1.2 COVID-19 lockdown and air pollution

Coronavirus disease 2019 (COVID-19) was first identified in Wuhan, China, and has since spread to many countries worldwide (Cucinotta and Vanelli, 2020). According to the World Health Organization (WHO), there have been 394,381,395 confirmed cases and 5,735,179 deaths of COVID-19 worldwide as of February 7, 2022 (WHO, 2020). Most countries have implemented non-pharmaceutical interventions, including lockdowns, to reduce the risk of disease spread and save human lives (Hong et al., 2021). Since the early stages of the pandemic outbreak, the implementation of lockdown measures had profound effects on individuals and industries, leading to a notable reduction in atmospheric pollutant concentrations (Wang et al., 2020).

The global response to the COVID-19 pandemic has had far-reaching consequences for the global economy and human mobility, causing widespread disruption and chaos. The global pandemic outbreak has had a substantial impact on global economic development (Rajput et al., 2020). According to an International Monetary Fund (IMF) report, the outbreak of the COVID-19 pandemic caused a global economic recession in 2020, resulting in a four percentage point reduction in economic growth (ABD, 2020).

At the same time, many studies have been conducted to investigate the impact of the COVID-19 outbreak on changes in air quality improvement due to the emission reduction (Mahato et al., 2020; Sharma et al., 2020; Tobías et al., 2020; Chauhan and Singh, 2020). As a result, air pollution levels have been significantly reduced in over 34 countries globally (Venter et al., 2021). According to Patel (2020), NASA Earth Observatory data show a 10–30% decrease in NO_2 concentration in eastern and central China in 2020 compared to 2019. Pacheco et al. (2020) identified a significant improvement in Ecuador's air quality during the lockdown, as evidenced by a 23%

reduction in NO_2 levels. Similarly, Lokhandwala and Gautam (2020) found the improvements of the air quality index in a heavily polluted urban area in India. Similarly, several countries experienced a substantial decrease in atmospheric pollution during the pandemic (Doi et al., 2022; Kanniah et al., 2020). Sicad et al. (2020) investigated how NO_2 and O_3 concentrations changed during lockdowns in four European cities and Wuhan. They reported a significant improvement in air quality and an increase in O_3 production in cities under consideration. Furthermore, Kanniah et al. (2020) reported a 27–34% decrease in aerosol optical depth and NO_2 concentration in Malaysian urban areas that was unaffected by seasonal biomass burning. Sharma et al. (2020) reported that $PM_{2.5}$, PM_{10}, CO, and NO_2 emission levels decreased in 22 Indian cities, resulting in improved air quality. Similarly, Velásquez and Lara (2020) employed a Gaussian Process Regression to ascertain the probability and association between case of COVID-19 and the concentration of NO_2 in Lima. In their study, Roy et al. (2021) conducted an observation of NO_2 concentration reductions in several cities in SA during the lockdown period in 2020, specifically in Dhaka, Kathmandu, Jakarta, and Hanoi. The researchers found that these cities exhibited the highest reductions, ranging from approximately 40–47%, in comparison to the corresponding period in 2019. Pei et al. (2020) found that major air pollutants decreased significantly in three Chinese cities: Beijing, Wuhan, and Guangzhou. Krecl et al. (2020) investigated the impact of COVID-19 policy measures on the megacity of Sao Paulo during a period of closure. A notable reduction in the levels of nitrogen oxides (NOx) in urban areas was documented. The primary sources of NOx are combustion-related activities, such as vehicle emissions, residential heating, power plants, and industrial processes (Dumka et al., 2019). These compounds, which are initially released as nitrogen monoxide (NO), endure rapid oxidation reactions, resulting in the formation of NO_2. It should be noted that NO_2 is a widely recognized indicator of human-caused combustion and a precursor to the formation of nitrate aerosols and ozone (Zhang et al., 2020).

Zhang et al. (2020b) and Bauwens et al. (2020) suggested that the unprecedented reduction in human activity caused by lockdown measures had a significant impact on the reduction of global air pollutants. Stringent restrictions led to significant reductions in human activity, particularly in the transportation and industrial sectors. This reduction had a significant impact on many aspects of society, including transportation, manufacturing, commercial operations, institutions, and households (Venter et al.,

2020). Prior to the COVID-19 pandemic, the majority of countries identified these sectors as significant contributors to air pollution (Klimont et al., 2017). Pata (2020) investigated the impact of the COVID-19 pandemic on environmental pollution in eight different locations across the United States and found that the ongoing pandemic reduced $PM_{2.5}$ emissions in the US. Furthermore, Agarwal et al. (2020) investigated the impact of closure measures on air pollution in six Indian megacities and six Chinese cities, concluding that air pollution decreased dramatically in the cities studied. Due to severe restrictions on air travel, air quality in 44 cities in northern China improved during the initial phase of the lockdown (Bao and Zhang, 2020).

1.3 Nighttime light remote sensing

During the 20th century, the development of electric lighting and the rapid expansion of human habitation, transportation infrastructure, and economic activity resulted in the illumination of large portions of the globe at night by artificial light. In contrast to daytime remote sensing, which typically focuses on the physical attributes of land cover, nighttime light (NTL) remote sensing provides a distinct and direct perspective on human activities, particularly those related to artificial light during the night. The use of nighttime light remote sensing has become common in many disciplines including human geography, demography, economics, sociology, fisheries, ecology, light pollution, and human rights.

The Defense Meteorological Satellite Program's Operational Line Scan System (DMSP-OLS) and the Visible Infrared Imaging Radiometer Suite (VIIRS) Day-Night Band (DNB) aboard the Suomi National Polar-orbiting Partnership (S-NPP) satellite are two of the most common NTL data sources. Since the early 1970s, DMSP-OLS has been acquiring NTL imagery. Nevertheless, the system has certain drawbacks such as low spatial resolution, coarse radiometric accuracy, lack of onboard calibration, and a restricted dynamic range (Elvidge, 2007). The latest generation of NPP-VIIRS DNB data provides unprecedented capabilities for observing NTL, surpassing some of the limitations of DMSP-OLS images (Elvidge, 2017). The use of the artificial light distribution depicted in these images has been used as a substitute measure for variety of factors including electric power consumption (Elvidge et al., 2001), economic activity (Ghosh et al., 2010; Chen and Nordhaus, 2011), population density (Amaral et

al., 2006), urbanization (Sutton, 2003), armed conflict (Agnew, 2008), natural disaster (Zhao et al., 2018) and the evaluation of the geographical scope of light pollution (Butt, 2012).

Human activity analysis includes a variety of data sources, such as mobility data, which can provide valuable insights into the relationship between anthropogenic activities and air pollution. However, it should be noted that these data sources do not provide comprehensive coverage across all regions, particularly in developing and underdeveloped countries such as Thailand, as well as other countries within SA and SEA countries. Thus, while mobility data presents a potential avenue for assessing levels of human activity, its applicability is limited in the current context. As a result, this study chose to rely on NTL data instead. This method can be applied to other countries by employing the same methodology with NTL data.

So far, few studies have been conducted on the relationship between changes in air pollution and NTL caused by COVID-19 lockdown, owing to the difficulty in identifying changes in anthropogenic activities at a high geographical resolution. Hence, the primary objective of this study is to examine the impact of NTL change from the COVID-19 lockdown on air pollution. It should be also mentioned that previous studies have primarily focused on analyzing changes in NTL in a small number of cities within a single country, with no international comparisons. To overcome this limitation, this study focuses on different geographical scales of analysis, including the city-wide scale of the Bangkok Metropolitan Region (BMR), the national scale of Thailand, and an international scale composing of a selection of 18 major cities within SA and SEA. A comprehensive description and outline of the objectives of this thesis will be presented in the subsequent section.

1.4 Objectives of the Study

The overall objective of this thesis is to investigate the geographic contextualities of the impact of the changes in human activities caused by the NPIs, particularly COVID-19 lockdown measure, on air pollution levels in Thailand and other South Asian and Southeast Asian countries. First, this study compares the changes of air pollutants and human activities in the BMR during COVID-19 compared to the same period in 2017 through 2020 to investigate the relationship between human activities

and air pollutants in the BMR area. The study at this scale also intends to ascertain if NTL is a sensitive indicator to be related to changes in air pollution by comparing to other indicators of human activity for subsequent chapters' investigation of the effect of human activity on air pollution change caused by the COVID-19 lockdown.

Second, this study examines local associations between changes in human activity (i.e. NTL) and air pollution (NO_2) around the first lockdown period in entire Thailand in 2020 by using geographically weighted regression (GWR). It should be noted that there are few studies on such local association between NO_2 levels and human activity, owing to the difficulty of identifying changes in anthropogenic activities at a high geographical resolution. The GWR-based approach may highlight the importance of geographically contextualized relationship between changes in human activity and air pollution, meaning that the relationship may change depending on different local condition such as population, industry, and transportation.

Thirdly and lastly, the lockdown or similar policy implementation period, hereafter referred to as the "lockdown period". This study broadens the study area to include major cities in SA and SEA to examine the effect of human activity caused by COVID-19 lockdown resulting in changes in NO_2 levels to consider the contextualized relationship in a wider international context.

1.5 Chapter Overview

Figure 1.1 illustrates the dissertation's structure. This thesis is organized as follows:

In chapter 1 (Introduction), a concise introduction of the air pollution situation before the pandemic, COVID-19 lockdown and air pollution and NTL, the research gap, and the objective of the study are presented.

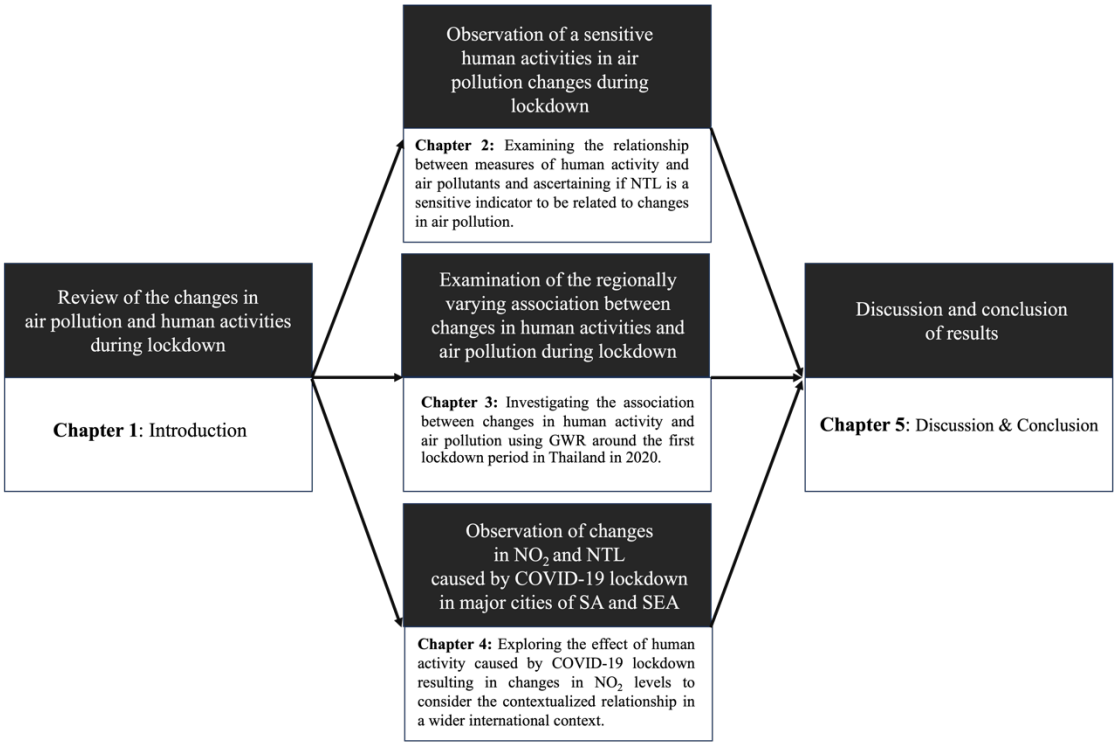

Figure 1.1 *Structure of this thesis*

Chapter 2 details the COVID-19 observations of changes in air pollutants and human activities in the BMR. The data on ground-based air pollutant concentrations (NO_2, SO_2, CO, O_3, $PM_{2.5}$, and PM_{10}) and human activities (expressway traffic volume, public transportation ridership and NTL) were used to conduct the comparative analysis. In order to determine which air pollutants have a stronger correlation with measure of human activities, it is necessary to provide insight into the potential connections between measure of human activity and pollutants. Thus, the relationship between measure of human activities and various air pollutants were investigated. Furthermore, this chapter intends to validate the use of NTL by confirming if NTL is a sensitive indicator by comparing to other indicators of human activity to be related to variations in air pollutants during the COVID-19 lockdown for investigating the effect of human activity on air pollution change caused by the COVID-19 lockdown in the subsequent chapters.

Chapter 3 examines the regionally varying association between human activity changes and air pollution changes in Thailand. The Sentinel-5 Precursor (S5P) satellite provided the NO_2 information is utilized in this chapter. Observations by the Suomi-NPP satellite provided the NTL intensity data. In addition, the land cover data used in

this analysis are obtained from the SERVIR-Mekong-managed land-cover portal website. This chapter uses GWR to investigate the contextuality of association between the changes in NTL and NO_2 around the first lockdown period in Thailand in 2020.

Chapter 4 to examine the relationship between the changes in NO_2 levels and NTL intensity observed during the COVID-19 lockdown in 18 cities across SA and SEA regions by using the same data source for Chapter 3. This chapter investigates how city attributes are related to the different NO_2 and NTL percentage change experiences among the study cities during the first wave of the pandemic.

Finally, Chapter 5 summarizes of the findings of this study based on previous chapters and draws the conclusions of this study with its implications and recommendation for future studies.

CHAPTER 2

Examining the change in air pollutants during COVID-19 lockdown in Bangkok Metropolitan Region, Thailand

The next three chapters, including the current one, are series of research findings on the impact of changes in human activities caused by COVID-19 lockdown on air pollution levels across diverse geographical scales. This chapter will first demonstrate how air pollutants and human activities changed in the Bangkok Metropolitan Region during the COVID-19 period. Furthermore, this study will demonstrate the sensitivity of indicators of human activity to variations in air pollution levels.

2.1 Introduction

Prior to the COVID-19 pandemic, air pollution in the BMR area was a major social concern as in the cases of many other Asian big cities. Rapidly growing metropolitan areas frequently have a significantly higher prevalence of vehicular traffic congestion than their counterparts. The inefficient combustion of fossil fuels is the primary source of air pollution. Numerous studies have been conducted to assess the potential health consequences of the rising number of fossil fuel-powered vehicles and traffic congestion worldwide. These studies have found a link between polluted urban air and adverse health effects (Janssen et al., 2003; Van Vliet et al., 1997). Air pollution has been a problem in Bangkok and surrounding provinces for decades, with hazardous levels of pollutants affecting air quality and posing health risks. Bangkok suffers from severe air pollution as a result of its rapid economic growth and urbanization. Vehicle emissions are the largest contributor to PM_{10} in the BMR, accounting for more than 30% (Chuersuwan et al., 2008). Vehicle emissions also produce additional gaseous pollutants such as NO_2, SO_2, and CO.

The emergence of the COVID-19 pandemic in early 2020 prompted unprecedented global responses, including lockdown measures and the implementation of social distancing as integral COVID-19 pandemic response strategies aimed at mitigating virus transmission. Thailand's government implemented a nationwide curfew beginning in mid-March 2020, as part of a comprehensive COVID-19 prevention plan. Consequently, these measures had an immediate impact on people's daily routines and lifestyle, leading to a paradigm shift towards remote working arrangements (including

working from home), the adoption of takeout-only policies for restaurants, and a transition to online learning in educational institutions. Moreover, there was a notable surge in online shopping and delivery services during this time period. Many studies have found that air pollution levels dropped during the lockdown. Compared to 2019, Wetchayint (2021) observed a substantial improvement in air quality in 2020, with reductions of 31.7% (PM_{10}), 15.8% ($PM_{2.5}$), 7.1% (O_3), and 8% (CO) during lockdown in Bangkok.

We compared the temporal variations in air pollutants and human activities in the BMR from March through June, 2020, compared to the same period from 2017 to 2019. Then, this study investigated which measure of human activity is most sensitive to air pollution reduction in order to select a measure of human activity for the subsequent chapters' investigation of the contextual nature of the association between changes in human activity and air pollution in larger areas.

2.2 Materials and methods

2.2.1 Study area

The BMR is an important geographical area located centrally in Thailand, encompassing the Bangkok Metropolitan Administration along with five neighboring provinces, namely Pathum Thani, Nonthaburi, Samut Prakarn, Samut Sakhon, and Nakhon Pathom. This region, depicted in Figure 2.1, covers a total land area of 7,762 square kilometers and is home to an estimated population of approximately 15.6 million people. The population of the BMR is made up of 10.8 million registered residents and 4.8 million unregistered residents. Consequently, the region has a high population density of approximately 2,009.79 people per square kilometer. The BMR encompasses a wide range of economic sectors, including urban, industrial, agricultural, and tourism activities, with Bangkok serving as a vital economic hub for the national economy. The BMR has significant traffic issues, ranking among the top ten most congested cities globally (Fuchs et al., 1994). Figure 2.2 presents the population density by subarea in the BMR.

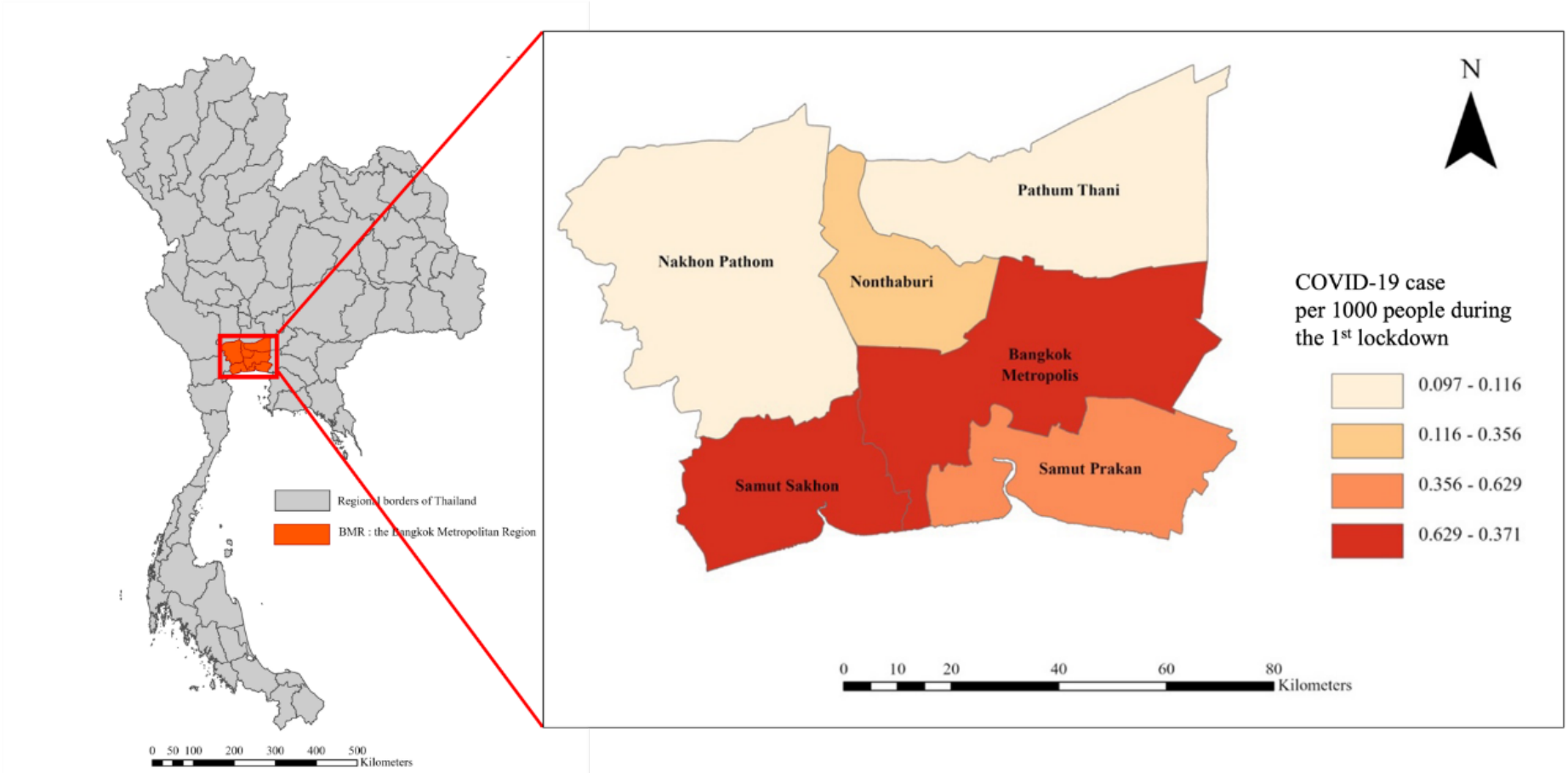

Figure 2.1 *The Bangkok Metropolitan Region map and COVID-19 case per 1,000 people during the 1st lockdo*

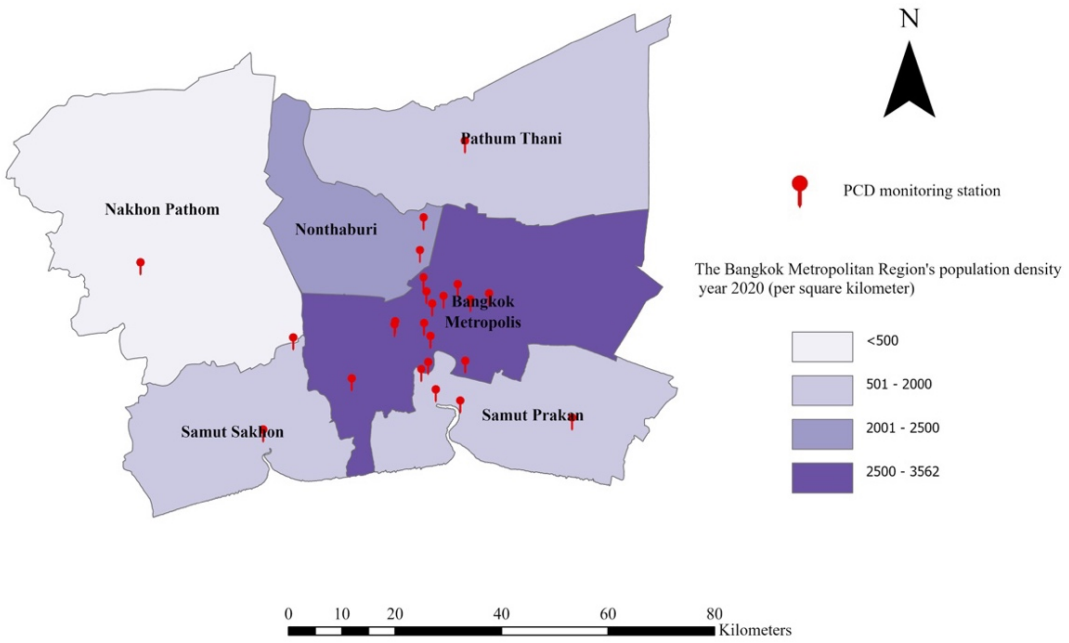

Figure 3.2 *The Bangkok Metropolitan Region's population density (per square kilometer)*

2.2.2 Data collection

The air pollution data for the period between 2017– 2020 were obtained from the Pollution Control Department (PCD), Ministry of Natural Resources and Environment of Thailand. The concentrations of air pollutants including NO_2, SO_2, CO, O_3, $PM_{2.5}$, and PM_{10} were measured hourly at 24 air pollution monitoring stations in the BMR. The daily value of air pollution is determined by calculating the mean of the values observed from the monitoring stations. As shown in Table 2.1, these stations were distributed as follows: thirteen in Bangkok, one in Nakhon Pathom, two in Nonthaburi, one in Pathum Thani, five in Samut Prakan, and two in Samut Sakhon provinces. Figure 2.3 depicts the geographical locations of these stations.

In this study, we considered three measures of human activities available in the study area: expressway traffic volume, public transportation ridership, and the intensity of NTL. Data on average monthly expressway traffic volume and public transportation ridership from 2017–2020 were obtained from the website of Bangkok Expressway and Metro Public Company Limited (BEM), which is a public transportation company in

charge of the operation and management of the mass transit systems in Bangkok, including the Mass Rapid Transit (MRT) system and expressways (https://investor.bemplc.co.th/). These transportation systems are critical in connecting the provinces of the BMR. It should be noted that the average public transportation ridership considered in this study is specific to MRT systems, whereas the expressway traffic volume data is specific to the daily expressway usage in Bangkok in order to link air pollution with people movements.

Suomi-NPP satellite observations were used to collect the NTL intensity data. The Suomi-NPP satellite's Visible Infrared Imaging Radiometer Suite (VIIRS), which is operated by NASA and the National Oceanic and Atmospheric Administration, includes a day/night band (DNB). This DNB permits the collection of multitemporal NTL data and facilitates near-real-time monitoring due to its high repetition frequency (Elvidge et al., 2013). The VIIRS sensor collects data while in a polar orbit, between midnight and one a.m., which is the best time to observe Thailand. We used the VIIRS Nighttime Day/Night Band Composites Version 1 in this study, which contains monthly averaged radiance composite images. We obtained monthly average stable composite data from the VIIRS-DNB data from 2017–2020 by using the Google Earth Engine (GEE) median reducer to remove the maximum value of NTL. From the composite VIIRS-DNB data, the average DNB radiance value within the BMR extent was selected for this study.

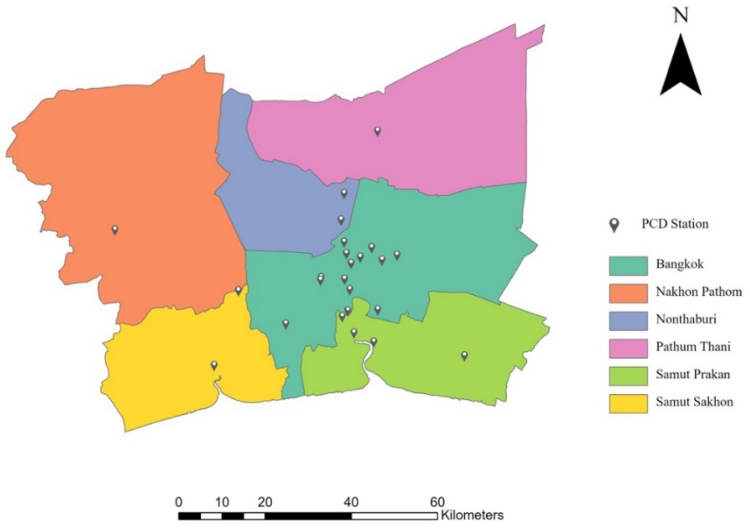

Figure 4.3 *Spatial distribution of air pollution monitoring sites located in the Bangkok Metropolitan Region*

Table 2.1 *Descriptive of air pollution monitoring sites in the Bangkok Metropolitan Region*

Province	District	Latitude	Longitude	Station name
Bangkok	Phaya Thai	13.78	100.54	The Public Relations Department
Bangkok	Thon Buri	13.73	100.49	Bansomdejchaopraya Rajabhat University
Bangkok	Bang Khun Thian	13.64	100.41	National Route 3902
Bangkok	Bangna	13.67	100.61	Thai Meteorological Department
Bangkok	Wang Thonglang	13.77	100.62	Bodindecha (Sing Singhaseni) School
Bangkok	Bangkapi	13.78	100.65	Klongjun NHA
Bangkok	Din Daeng	13.78	100.57	Huaykwang NHA
Bangkok	Yan Nawa	13.71	100.55	Nonsi Witthaya School
Bangkok	Pathum Wan	13.73	100.54	King Chulalongkorn Memorial Hospital
Bangkok	Thon Buri	13.79	100.59	Metropolitan Electricity Authority Substation Thon Buri
Bangkok	Wang Thonglang	13.73	100.49	Chok Chai Police Station
Bangkok	Din Daeng	13.76	100.55	National Housing Authority Public Community Din Daeng
Samut Prakan	Phra Pradaeng	13.66	100.54	Vocational Rehabilitation Center
Samut Prakan	Mueang Samut Prakan	13.62	100.56	South Bangkok Power Plant

Province	District	Latitude	Longitude	Station name
Samut Prakan	Phra Pradaeng	13.65	100.53	Residence for Dept of Primary Industries and mines
Samut Prakan	Mueang Samut Prakan	13.60	100.60	Samut Prakan Provincial Hall
Samut Prakan	Bangplee	13.57	100.79	Bangplee NHA
Nonthaburi	Bangkruai	13.81	100.54	EGAT
Nonthaburi	Mueang Nonthaburi	13.85	100.53	Department of Disease Control
Nonthaburi	Pak Kret	13.91	100.54	Sukhothai Thammathirat Open University
Samut Sakhon	Krathum Bean	13.71	100.32	Samut Sakhon Highway District of Highway
Samut Sakhon	Mueang Samut Sakhon	13.55	100.27	Samut Sakhon Wittayalai School
Pathum Thani	Khlong Luang	14.04	100.61	Bangkok University (Rangsit)
Nakhon Pathom	Mueang Nakhon Pathom	13.83	100.06	Prapa Nakhon Reservoir

2.2.3 Statistical Analysis

Data on ground-based air pollution concentrations and human activities (expressway traffic volume, public transportation ridership and NTL) were examined for a comparative analysis from 2017–2020. The primary focus was on comparing changes in air pollutant concentrations from March through June, 2020 lockdown period to the same period observed from 2017–2019.

To investigate the change in air pollutants and human activities between the baseline years of 2017–2019 and 2020, specifically during the first lockdown period, an analysis of percentage change from the baseline was performed. This analysis involved calculating the percentage change in each air pollutants and human activities during the first lockdown period of 2020, compared to the baseline years of 2017–2019. For example, the percentage change in NO_2 concentrations was calculated using the following formula (2.1):

$$PC_{NO_2} = \left(\left(NO_{2_{2020}} - NO_{2_{2017-2019}} \right) \div NO_{2_{2017-2019}} \right) \times 100 \quad (2.1)$$

where $NO_{2_{2020}}$ represents the monthly average NO_2 concentration during the first lockdown period in year 2020. $NO_{2_{2017-2019}}$ represents the average of NO_2 concentration same period before pandemic in years 2017– 2019.

In this study, Pearson's correlation coefficient was used to investigate the relationship between measures of human activities and various air pollutants for monthly data of generally from 2017–2020. Specifically, we intended to identify which air pollutants have a stronger correlation with human activities, providing insights into the potential links between human activity and pollutants in the BMR. The estimation equation for Pearson's correlation coefficient was calculated using the following formula (2.2):

$$r = \frac{n(\sum x_t y_t) - (\sum x_t)(\sum y_t)}{\sqrt{[n\Sigma {x_t}^2 - (\sum x_t)^2][n\Sigma {y_t}^2 - (\sum y_t)^2]}} \quad (2.2)$$

In equation (2.2), n represents the number of observations. x_t represents the monthly values of measures of human activity being examined of month t. y_t represents the

monthly values of the air pollutant being examined of month *t*. $\sum x_t y_t$ is the sum of the product of each paired observation of human activities and the air pollutant being examined. $\sum x_t$ and $\sum y_t$ represent the sums of the human activities values and the air pollutant values, respectively. $\Sigma {x_t}^2$ and $\Sigma {y_t}^2$ denote the sums of the squared x_t and y_t values, respectively.

In addition, we intended to look into how sensitive the measures of human activities, specifically expressway traffic volume, public transportation ridership and NTL, are to changes in air pollutants, specifically NO_2, SO_2, CO, O_3, PM_{10} and $PM_{2.5}$ levels during the lockdown period in the BMR. We used multiple regression analysis to understand the associations between these variables from general 2017–2020. To account for the impact of the lockdown period on the relationship between human activities and air pollutants levels, we included an indicator variable, which took a value of 1 during the lockdown period and 0 otherwise. This allowed us to compare the sensitivity of human activities to air pollutants during the lockdown to non-lockdown periods. The estimation equation for Multiple regression was calculated using the following formula (2.3):

$$y_t = b_0 + b_1 x_t + c I_t + \varepsilon_t \tag{2.3}$$

$$I_t = \begin{cases} 1, & t\ is\ in\ period\ of\ lockdown \\ 0, & other\ wise \end{cases}$$

where y_t and x_t are the dependent (air pollutants) and independent (human activities) variables of month *t*, respectively. b_0 represents the intercept term, capturing the baseline air pollutants. The coefficients b_1 and c quantify the impact of human activities and the lockdown effect that is not explained by human activity change on air pollutants levels during the lockdown period, respectively. The term ε_t represents the error term, accounting for unexplained variability in the model. I_t is an indicator variable that represents whether a specific period corresponds to the lockdown period or not. During the lockdown period, I_t takes a value of 1 while outside of the lockdown period, I_t takes a value of 0.

2.3 Results

2.3.1 Air pollution assessment during COVID-19

Data from hourly ground-based observations of air pollutants were aggregated and transformed into monthly averages from 2017– 2020. Similarly, data on air pollutants, expressway traffic volume, public transportation ridership, and NTL were averaged for the years 2017 to 2019 as a baseline to compare with the corresponding data from 2020, specifically during the COVID-19 lockdown period from March to June, 2020. The findings of this investigation will be discussed in the following sections.

Table 2.2 *Descriptive statistics of air pollutant concentrations, expressway traffic volume and public transport ridership data across the Bangkok Metropolitan Region in year 2017 to 2020*

	Year 2017-2019			Year 2020		
	Mean	Min	Max	Mean	Min	Max
NO_2 (ppb)	15.85	10.29	24.04	15.78	8.73	21.01
SO_2 (ppb)	3.80	2.52	5.92	3.99	2.62	4.72
CO (ppm)	0.62	0.45	0.78	0.44	0.33	0.49
O_3 (ppb)	18.12	11.04	24.77	22.26	13.41	24.30
PM_{10} (µg./m^3)	41.72	29.32	63.69	41.63	28.48	68.53
$PM_{2.5}$ (µg./m^3)	24.61	13.89	44.24	21.46	12.11	40.98
Expressway traffic volume	1227.33	1160.70	1270.99	1049.18	589.86	1216.97
Public transport ridership	314.53	280.33	359.33	260.58	78.00	312.00
Nighttime light	19.49	10.143	23.17	19.42	5.03	23.91

Table 2.3 *Average air pollutant concentrations and human activities during the first lockdown and same period in 2017 to 2019 in the Bangkok Metropolitan Region*

Pollutant	Year 2017-2019 (Before pandemic)	Year 2020 (During lockdown)	%Change
NO_2 (ppb)	15.36	10.55	-34.87
SO_2 (ppb)	2.94	2.94	-0.08
CO (ppm)	0.55	0.37	-32.86
O_3 (ppb)	17.63	23.17	31.45
PM_{10} (µg./m^3)	34.49	31.69	-8.12
$PM_{2.5}$ (µg./m^3)	24.60	21.46	-12.77
Expressway traffic volume	1227.33	1049.18	-31.02
Public transport ridership	314.53	260.58	-47.11
Nighttime light	19.69	18.83	-4.40

2.3.1.1 Nitrogen Dioxide (NO_2)

The comparison of monthly NO_2 values (ppb) was of special interest for determining the overall change in the NO_2 levels between the first lockdown in 2020, compared to the same period from 2017–2019 (Fig. 2.4). Results revealed that the NO_2 levels decreased by 34.87% during the first lockdown in 2020 (March to June, 2020) compared with those of the same period in 2017– 2019 as shown in Table 2.3. The minimum, maximum, and average NO_2 levels in 2017–2019 were 10.29, 24.04, and 15.85 ppb, respectively, while those in 2020 were 8.73, 21.01 and 15.78 ppb, respectively (Table 2.2).

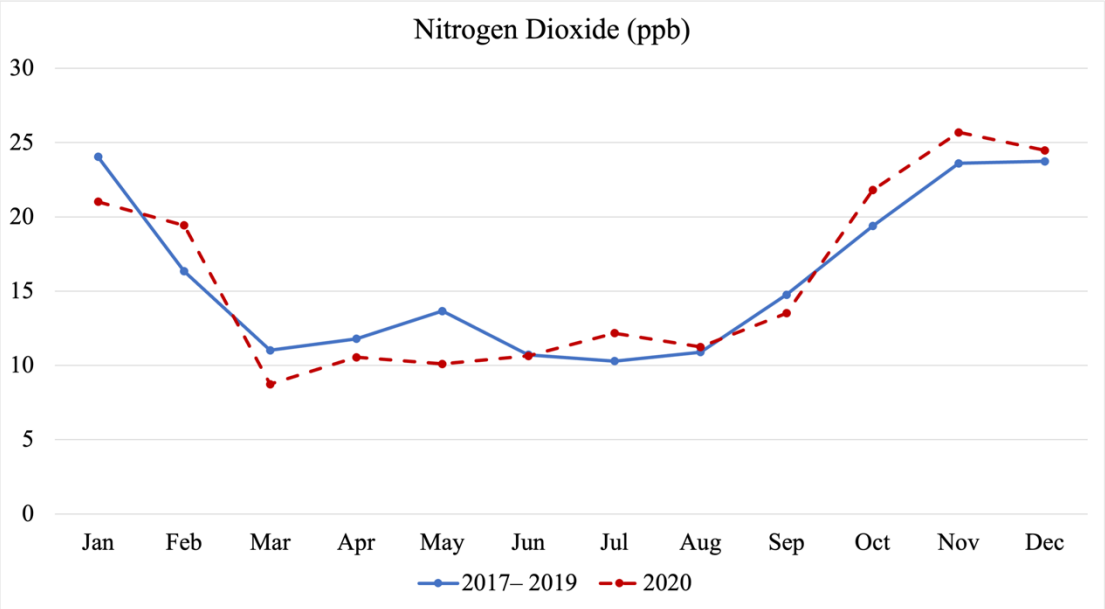

Figure 5.4 *Time-trends of monthly averaged of NO_2 concentration between 2017 to 2020*

2.3.1.2 Sulphur dioxide (SO_2)

Figure 2.5 depicts the monthly SO_2 values (ppb) levels observed during the lockdown periods in 2017 and 2020. When compared to the corresponding period from 2017–2019, SO_2 levels decreased by 0.08% in during the initial lockdown period in 2020 (Table 2.3). Between 2017– 2019, the minimum, maximum, and average SO_2 levels were 2.52, 5.92, and 3.80 ppb, respectively (Table 2.2), while in 2020, these values were 2.62, 4.72, and 3.99 ppb, respectively.

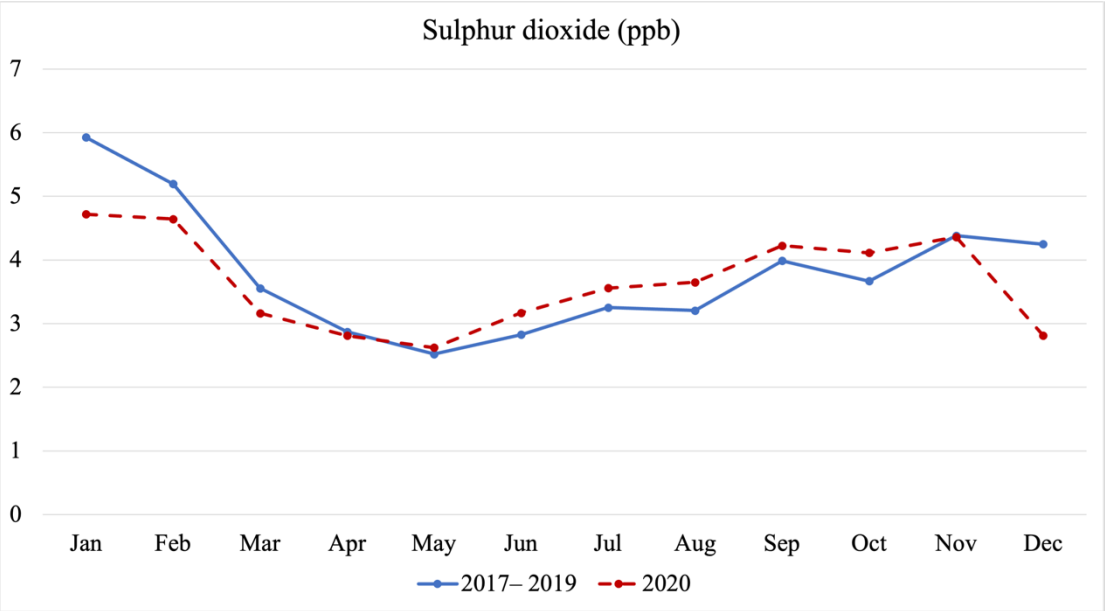

Figure 6.5 *Time-trends of monthly averaged of SO_2 concentration between 2017 to 2020*

2.3.1.3 Carbon monoxide (CO)

The comparison of monthly CO levels (ppm) during the lockdown periods of 2020 compared to the same period from 2017– 2019 (Fig.2.6) revealed a 32.86% decrease in CO levels during the first lockdown in 2020 when compared to the corresponding period from 2017–2019 (Table 2.3). The minimum, maximum, and average concentrations of CO from 2017–2019 were 0.45, 0.78, and 0.62 ppm, respectively (Table 2.2), while in 2020; these values were 0.33, 0.49, and 0.44 ppm, respectively.

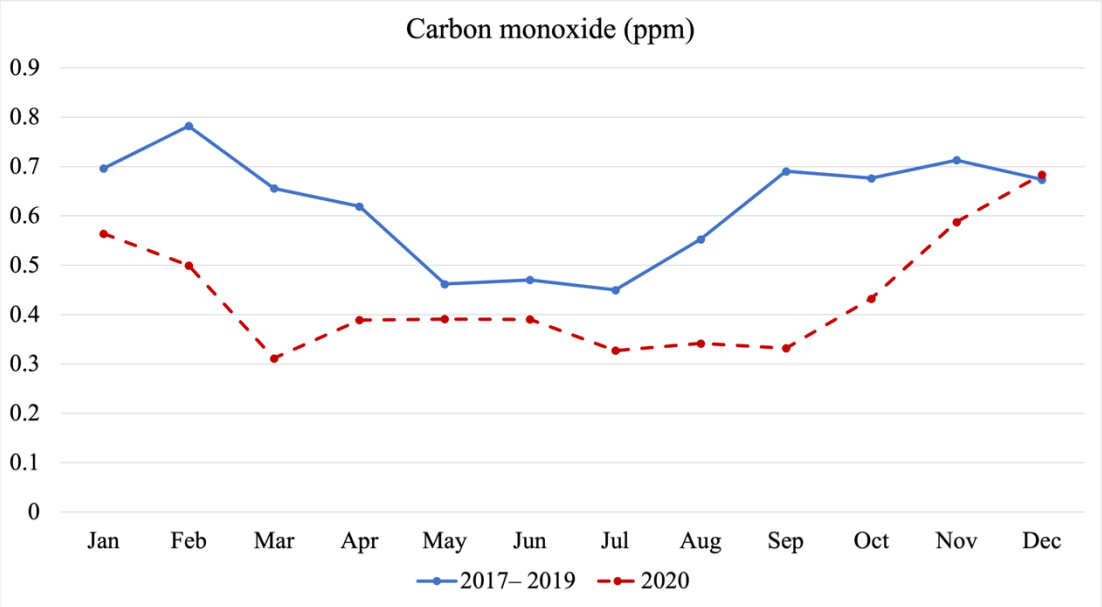

Figure 7.6 *Time-trends of monthly averaged of CO concentration between 2017 to 2020*

2.3.1.4 Ozone (O_3)

A comparison of monthly O_3 levels (ppb) during the lockdown periods 2020 and the same period from 2017–2019 (Fig. 2.7) revealed 31.45% increase in O_3 levels during the first lockdown in 2020 compared to the period before lockdown from 2017 –2019 (Table 2.3). The minimum, maximum, and average O_3 concentrations from 2017 to 2019 were 11.04, 24.77, and 18.12 ppb, respectively (Table 2.2), while in 2020, were 13.41, 24.30, and 22.26 ppb, respectively.

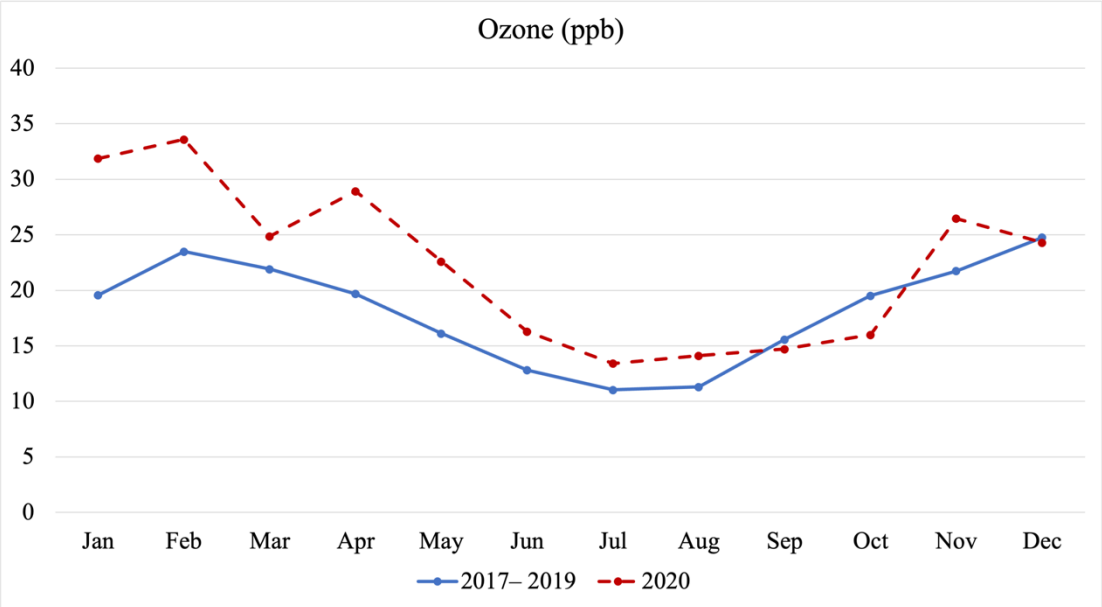

Figure 8.7 *Time-trends of monthly averaged of O_3 concentration between 2017 to 2020*

2.3.1.5 PM_{10} and $PM_{2.5}$

The examination of monthly PM_{10} values (µg./m^3) was assessing the overall fluctuation in PM_{10} levels during the 2020 lockdown period and the same period from 2017–2019 (Figure 2.8). The findings indicated an 8.12% reduction in PM_{10} levels during the first lockdown in 2020 when compared to the period preceding the lockdown between 2017 and 2019. Table 2.2 shows that the minimum, maximum, and average PM_{10} levels from 2017 to 2019 were 29.32, 63.69, and 41.72 µg./m^3, respectively. In 2020, these levels were 28.48, 68.53, and 41.63 µg./m^3, respectively.

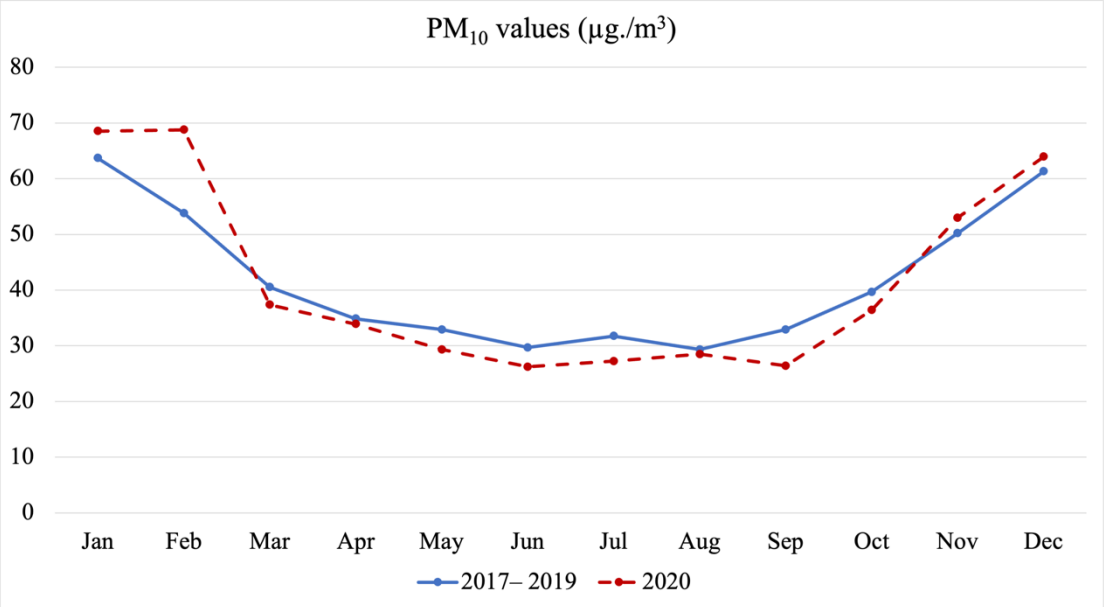

Figure 9.8 *Time-trends of monthly averaged of PM_{10} concentration between 2017 to 2020*

Figure 2.9 shows a comparison of monthly $PM_{2.5}$ values (µg./m^3) during the of 2020 lockdown period and the same period from 2017 to 2019 revealing a 12.77% reduction in $PM_{2.5}$ levels during the first lockdown in 2020 when compared to the corresponding period between 2017 and 2019. Table 2.2 shows that the minimum, maximum, and average $PM_{2.5}$ levels from 2017 to 2019 were 13.89, 44.24, and 24.61 µg./m^3. In 2020, these levels were observed as 12.11, 40.98, and 21.46 µg./m^3, respectively.

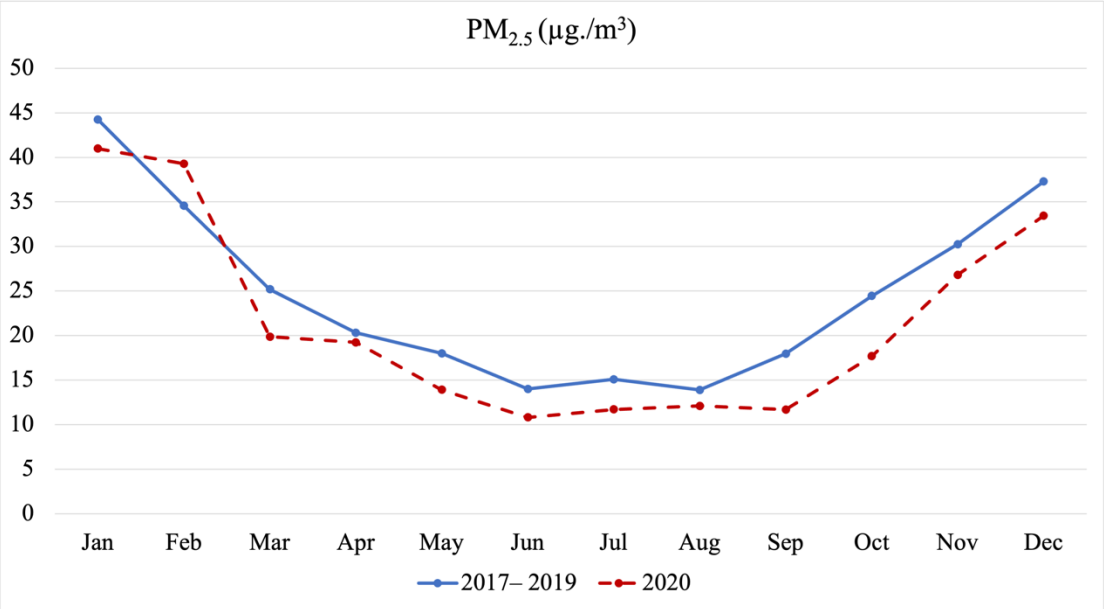

Figure 10.9 *Time-trends of monthly averaged of $PM_{2.5}$ concentration between 2017 to 2020*

2.3.1.1 Expressway Traffic Volume

The comparison of monthly expressway traffic volume data (thousand trips) was of particular interest for determining the overall change in the expressway traffic volume data between lockdown period in 2020 compared to the same period from 2017–2019 (Figure 2.10). The results showed that expressway traffic volume data decreased by 31.02 % during the first lockdown in 2020 when compared to the same period from 2017 to 2019. The minimum, maximum, and average expressway traffic volume data in 2017 to 2019 were 1160.70, 1270.99, and 1227.33 thousand trips, respectively, (Table 2.2) while those in 2020 were 589.86, 1216.97 and 1049.18 thousand trips, respectively.

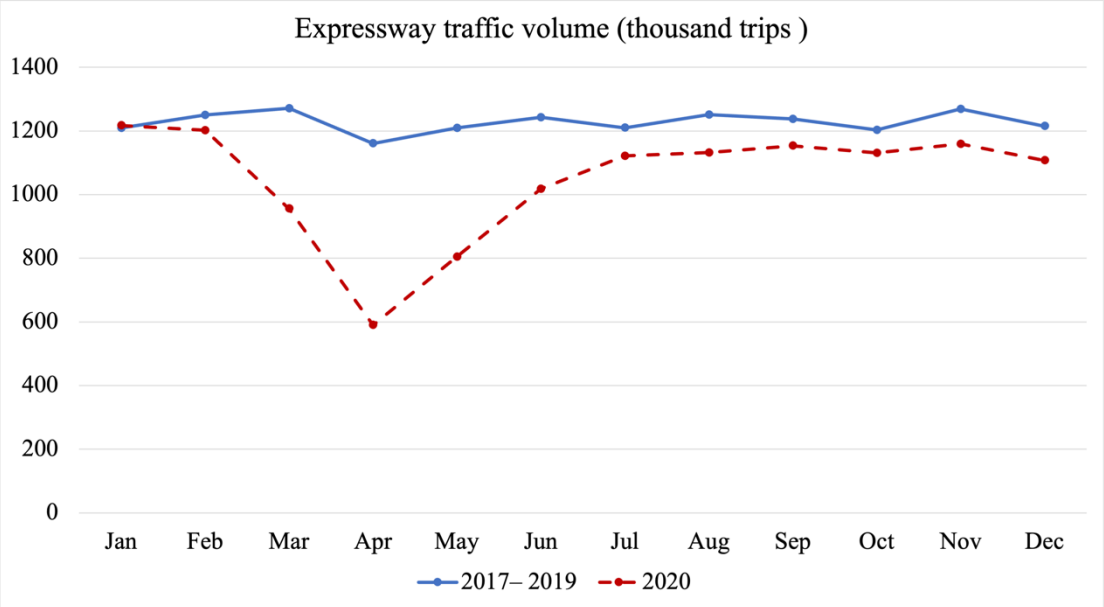

Figure 11.10 *Time-trends of monthly averaged of expressway traffic volume concentration between 2017 to 2020*

2.3.1.1 Public Transport Ridership

The monthly average public transportation ridership data in thousand trips were observed, with a specific focus on assessing the overall changes in the number of public transportation ridership data during the first lockdown in 2020, compared to the same period from 2017–2019 (Figure 2.11). The findings indicated a substantial decrease of 47.11% in the monthly average public transportation ridership data during the first lockdown in 2020 when compared to the same period in 2017–2019. Analysis of the data from 2017 –2019 revealed that the minimum, maximum, and average public transportation ridership per day figures were recorded as 280.33, 359.33, and 314.53 thousand trips, respectively (Table 2.2). In contrast, in 2020, these values were observed as 78, 312, and 260.58 thousand trips, respectively.

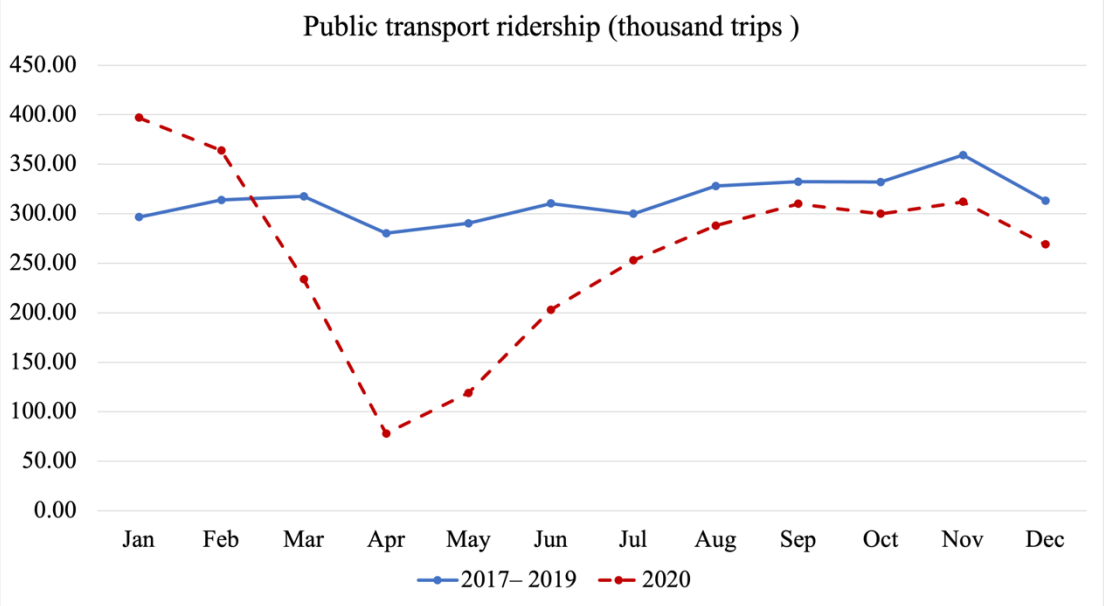

Figure 12.11 *Time-trends of monthly averaged of public transport ridership concentration between 2017 to 2020*

2.3.1.1 Nighttime light (NTL)

The comparison of monthly average NTL intensity (nanoWatts/cm^2/sr) between the first lockdown in 2020, compared to the same period from 2017– 2019 (Figure 2.12). The findings revealed a significant decrease of 4.40% in the monthly average of NTL during the first lockdown in 2020 when compared to the same period between 2017 and 2019. Examination of the data from 2017–2019 showed that the minimum, maximum, and average NTL figures were 10.43, 23.17 and 19.49 nanoWatts/cm^2/sr, respectively (Table 2.2). Conversely, in 2020, these values were 5.03, 23.91, and 23.91 nanoWatts/cm^2/sr, respectively.

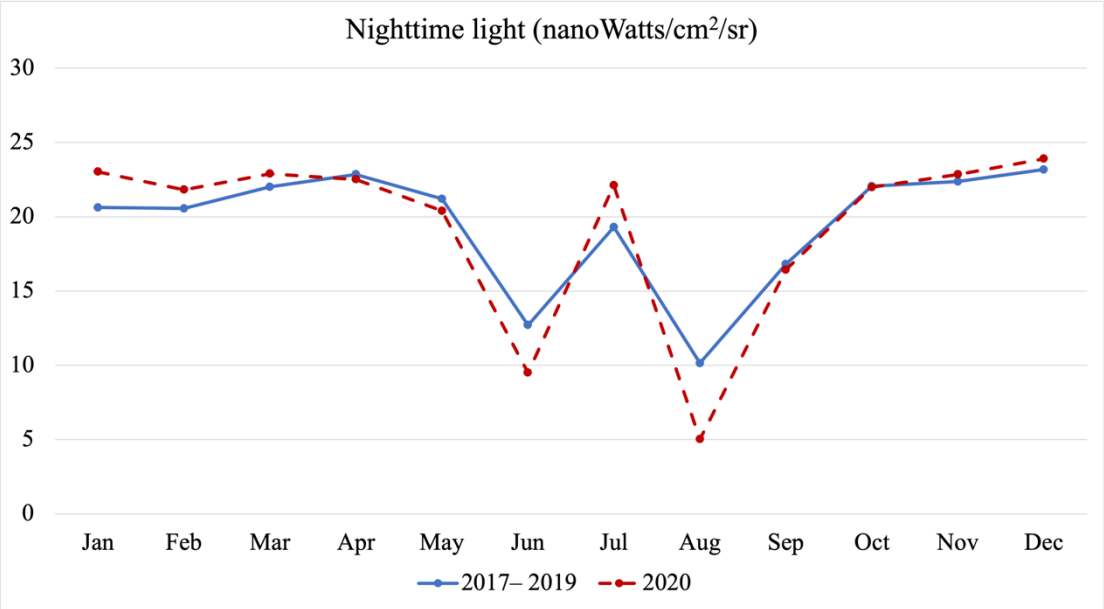

Figure 13.12 *Time-trends of monthly averaged of nighttime light concentration between 2017 to 2020*

2.3.2 Correlation between human activities and air pollutants in the Bangkok Metropolitan Region

Pearson's correlation coefficient was used to calculate the relationships between expressway traffic volume, public transportation ridership, NTL, and air pollutants. The correlation coefficients were calculated separately for each air pollutant, providing valuable insight into the magnitude and direction of the observed relationships.

The study examined the relationship between human activity and different air pollutants within the BMR region, specifically NO_2, SO_2, CO, O_3, PM_{10}, and $PM_{2.5}$. These correlations' characteristics were thoroughly investigated. The Pearson's correlation coefficients for the correlation between expressway traffic volume and air pollutants (Table 2.4) were NO_2 (0.227), SO_2 (0.195), CO (0.395), O_3 (-0.203), PM_{10} (0.199), and $PM_{2.5}$ (0.2168947). These coefficients show a positive relationship between traffic volume and NO_2, SO_2, CO, PM_{10}, and $PM_{2.5}$, indicating that as expressway traffic volume increases, so do the concentrations of these air pollutants. However, there was a negative correlation found between traffic volume and O_3, implying that higher expressway traffic volume is associated with lower levels of O_3.

Table 2.4 *Descriptive of correlation between expressway traffic volume and air pollutants in the Bangkok Metropolitan Region*

Air pollutants	Expressway traffic volume	
	r	p-value
NO_2	0.227	> 0.05
SO_2	0.195	> 0.05
CO	0.395	< 0.01
O_3	-0.203	> 0.05
PM_{10}	0.199	> 0.05
$PM_{2.5}$	0.217	> 0.05

Regarding the correlation between public transportation ridership and air pollutants (Table 2.5), the Pearson's correlation coefficients were as follows: NO_2 (0.405), SO_2 (0.355), CO (0.299), O_3 (0.072), PM_{10} (0.359), and $PM_{2.5}$ (0.315). These coefficients show a positive correlation between ridership and NO_2, SO_2, CO, PM_{10}, and $PM_{2.5}$, implying that as ridership increases, so do the concentrations of these air pollutants.

However, the correlation between ridership and O_3 was relatively weak (0.072), implying a less pronounced relationship between ridership and O_3 levels.

Table 2.5 *Descriptive of correlation between public transportation and air pollutants in the Bangkok Metropolitan Region*

Air pollutants	Public transportation ridership	
	r	p-value
NO_2	0.405	< 0.01
SO_2	0.355	< 0.01
CO	0.299	< 0.05
O_3	0.072	> 0.05
PM_{10}	0.359	< 0.01
$PM_{2.5}$	0.315	< 0.05

Furthermore, the relationship between NTL and various air pollutants was investigated as shown in Table 2.6. The Pearson's correlation coefficients for this analysis were: NO_2 (0.553), SO_2 (0.226), CO (0.239), O_3 (0.417), PM_{10} (0.424), and $PM_{2.5}$ (0.443). These coefficients show a significant positive correlation between NTL and NO_2, O_3, PM_{10}, and $PM_{2.5}$, implying that higher levels of NTL concentrations are associated with higher concentrations of these air pollutants. However, the correlation between NTL and SO_2 was relatively weaker (0.226), indicating a less pronounced relationship between nighttime light and SO_2 levels. Notably, the largest correlation observed in this study was between NTL and NO_2, with a Pearson's correlation coefficient of 0.553. This finding suggests a strong positive relationship between NTL and NO_2 levels, indicating that areas with higher NTL intensity tend to exhibit elevated concentrations of NO_2.

Table 2.6 *Descriptive of correlation between nighttime light and air pollutants in the Bangkok Metropolitan Region*

Air pollutants	Nighttime light intensity	
	r	p-value
NO_2	0.553	< 0.001
SO_2	0.226	> 0.05
CO	0.239	> 0.05
O_3	0.417	< 0.01
PM_{10}	0.424	< 0.01
$PM_{2.5}$	0.443	< 0.001

2.3.3 Multiple regression analysis between human activities and air pollution changes in the Bangkok Metropolitan Region

Multiple regression analysis revealed important insights into the sensitivity of human activities (expressway traffic volume, public transportation ridership and NTL) to changes in air pollutant levels, specifically NO_2, SO_2, CO, O_3, PM_{10}, $PM_{2.5}$, while considering the lockdown period into account. The model included the lockdown indicator as an indicator variable, with set 1 representing the lockdown period and set 0 representing the no lockdown period. Table 2.7 presents the multiple R-squared values for each regression model.

For the analysis of NO_2 levels, the model found an R^2 of 0.29 for NTL, 0.09 for expressway traffic volume, and 0.16 for public transportation ridership, indicating that NTL is the human activity most sensitive to NO_2. Regarding the analysis of SO_2 levels, the R^2 value was 0.10 for NTL, 0.04 for expressway traffic volume, and 0.14 for public transportation ridership. These findings indicated that public transportation ridership is

a human activity that is more sensitive to SO_2 levels. For CO, the model achieved an R^2 of 0.23 with NTL, 0.16 with expressway traffic volume, and 0.13 with public transportation ridership with NTL being the most sensitive measure of human activity to NO_2. R^2 was 0.34 with NTL, 0.04 with expressway traffic volume, and 0.15 with public transportation ridership for analysis of O_3. These findings demonstrated that NTL is a measure of human activity that is more sensitive to O_3. In terms of PM_{10}, the model achieved an R^2 of 0.25 with NTL, 0.05 with expressway traffic volume, and 0.13 with public transportation ridership, indicating that NTL is a more sensitive human activity to NO_2 than expressway traffic volume. The R^2 values for NTL, expressway traffic volume, and public transportation ridership in the $PM_{2.5}$ analysis were 0.28, 0.05, and 0.10, respectively. These findings demonstrated that NTL is a human activity that is more sensitive to O_3.

These results indicate that NTL is a more sensitive measure of human activity to NO_2, SO_2, CO, O_3, PM_{10} and $PM_{2.5}$ levels, whereas expressway traffic volume and public transportation ridership have no significant impact on these pollutants in the BMR. On the other hand, the number of riders appears to affect SO_2 levels.

Thus, these results revealed that NTL is the most sensitive measure of human activities to changes in air pollutants is. We will use NTL as human indicator to the effect of human activity on air pollution change caused by the COVID-19 lockdown in the subsequent chapters.

Table 2.7 *Multiple regression analysis between air pollutants and measure of human activities in the Bangkok Metropolitan Region during the lockdown period*

	Nighttime light			**Expressway traffic volume**			**Public transportation ridership**		
	b_1	**c**	**R^2**	**b_1**	**c**	**R^2**	**b_1**	**c**	**R^2**
NO_2	0.426***	-6.128**	0.255	-0.004	-7.838	0.088	0.046*	0.795	0.164
SO_2	0.052.	-0.965	0.090	0.001	-0.652	0.043	0.0116*	0.817	0.138
CO	0.007*	-0.219**	0.183	0.0004	-0.057	0.158	0.0002	-0.195	0.131
O_3	0.611**	4.706	0.349	-0.007	1.691	0.043	0.059*	13.559**	0.153
PM_{10}	1.047***	-10.342*	0.220	0.009	-7.612	0.046	0.122*	7.998	0.139
$PM_{2.5}$	0.797***	-8.143*	0.243	0.008	-5.766	0.054	0.064	1.305	0.099

*Note. P-value '***' 0.001 '**' 0.01 '*' 0.05 '.' 0.1*

2.4 Discussion

During Thailand's lockdown period, NO_2, SO_2, O_3, PM_{10}, and $PM_{2.5}$ concentration decreased significantly, with reductions of 34.87%, 0.08%, 32.86%, 8.12%, and 12.77% respectively, compared to baseline levels between 2017– 2019. These reductions can be attributed to the restrictions imposed on movement and commuting, which resulted in a substantial decrease in vehicular traffic within the BMR due to the implementation of the lockdown measures. It is worth noting that the BMR encompasses wide range of economic sectors, including urban, industrial, agricultural, and tourism activities, with Bangkok serving as a vital hub for the national economy. Nonetheless, the COVID-19 lockdown measures effectively halted human mobility by necessitating remote work and stay-at-home orders, resulting in a decrease in inter-province traffic. In contrast, a substantial increase of approximately 31.45% was observed in O_3 levels. This finding can be explained by the fact that O_3 is classified as a secondary pollutant, which is dependent on the presence of its precursors, namely NOx and VOCs. It is possible that the reduction in emissions of these precursors during the lockdown period contributed to an elevation in O_3 concentration in the atmosphere. A reduction in NOx emissions, which are involved in both O_3 formation and removal, can decrease the removal of O_3 from the atmosphere, potentially leading to an increase in O_3 concentration. Furthermore, in areas where O_3 formation is limited by the availability of VOCs rather than NOx, a decrease in NOx emissions can shift the system to being VOC-limited, allowing more VOCs to react and produce O_3, resulting in an increase in O_3 concentration (Lu et al., 2020).

In addition, Pearson's correlation coefficient was used to examine the monthly correlation between human activities and various air pollutants. The result suggests that expressway traffic volume, public transportation use and NTL are associated with variations in air pollutant concentrations. The strongest correlation was observed between NTL and NO_2, suggesting that nighttime activities contribute significantly to NO_2 emissions. NO_2 is emitted primarily from the combustion of fossil fuels, particularly in urban areas with residential and commercial heating, industrial processes and road transportation. NTL are typically higher in urban areas, making them more visible in satellite imagery. Therefore, the strong spatial correlation between urban areas, where artificial lighting is prevalent, and NO_2 emissions contributes to the

correlation between NTL intensity and NO_2 levels. (Bechle et al., 2015). Furthermore, For the other two measures of human activity, data on public transportation ridership only cover a portion of transportation. NTL may encompass a broader range of human activities, such as other traffic modes, industrial, electric power consumption (Elvidge et al., 2001) and economic activity (Ghosh et al., 2010; Chen and Nordhaus, 2011).

This study employed the multiple regression analysis to investigate the sensitivity of human activities to changes in air pollution levels during a lockdown period. This approach enabled us to gain insights into the relationships between air pollution and specific human activities, thereby contributing to our understanding of the impact of human activities and the efficacy of lockdown measures in reducing air pollution. The findings indicate that NTL is a more sensitive human activity to NO_2, CO, O_3, PM_{10}, and $PM_{2.5}$ levels than expressway traffic volume and public transportation ridership in the BMR. Alternatively, the number of riders appears to have an effect on SO_2 levels. Thus, these results revealed that NTL is the human activity most sensitive to variations in air pollutants. NTL data can provide spatial information regarding the distribution of human activities and emissions. It measures the intensity of artificial lighting, which can be used as a proxy for urbanization, population density, and economic activity (Liu et al., 2021a). The Thai government's announcement of the first lockdown, resulted in strict restrictions on people's movement, resulting in the closure of public transportation, educational institutions, and non-essential local businesses (WHO, 2020). This decrease in human activity has the potential to reduce air pollution emissions. As a reliable indicator of human activities, NTL can exhibit a significant decrease during the lockdown period, making it appear more sensitive to variations in air pollution levels than other variables.

The study's findings indicate that when compared to other measures of human activity in the BMR, NTL has the highest sensitivity to air pollutants. This suggests that changes in NTL intensity are more sensitive to variations in regional air pollution levels. The parameter 'c' estimates the deviation of lockdown periods from other "normal" periods. The impact of the lockdown on NO_2 levels is clear in this case, as there is a substantial reduction in NO_2 levels during this period. Although, the changes in NTL intensity alone cannot fully account for the observed decrease in NO_2 concentrations during the lockdown. This implies that although NTL is generally correlated with NO_2,

the reduction in NO_2 during the lockdown may be influenced by a variety of other regional factors, a concept known as "contextuality". In other words, there are factors other than NTL intensity that contribute to the observed reduction in NO_2 levels during the lockdown. Furthermore, in the following chapter, we will use NTL as an indicator of human activity and expand area from the BMR to the entire country of Thailand, with a focus on the lockdown period, to investigate the contextuality of the association between the changes in human activity and air pollution.

2.5 Conclusion

This study aims to investigate variations in air pollution by using ground-based air pollutants such as NO_2, SO_2, CO, O_3, $PM_{2.5}$, and PM_{10}. The study compared changes in air pollutant levels during Thailand's first lockdown in 2020 to the baseline period of 2017– 2019 in the BMR area. The monthly NO_2, SO_2, PM_{10}, and $PM_{2.5}$ concentrations decreased significantly during the lockdown period. The primary cause for the decrease in air pollutant concentrations is the cessation of anthropogenic activities such as transportation, travel, industrial activities, which are the primary source of such pollutants (Sharma et al., 2020).

NTL showed a strong positive monthly temporal correlation with NO_2 levels in the BMR. NO_2 is primarily emitted from the combustion of fossil fuels, particularly in congested urban areas. The strong spatial correlation between urban areas, with high levels of artificial lighting and NO_2 emissions contributes to the relationship between NTL intensity and NO_2 levels (Bechle et al., 2015).

However, multiple regression analysis showed that the NTL reduction cannot fully explain the reduction of NO_2 during the lockdown period. In the following chapter, a more detailed geographical analysis could reveal the contextual association between human activities and air pollution to explore the changes in human activities and air pollution during COVID-19 lockdown period.

CHAPTER 3

The Impact of Changes in Anthropogenic Activity Caused by COVID-19 Lockdown on Reducing Nitrogen Dioxide Levels in Thailand Using Nighttime Light Intensity

The previous chapter examined the changes and correlations in the Bangkok Metropolitan Region air pollutants during the lockdown versus the baseline. Moreover, we investigated how sensitive human activities are to changes in air pollution levels. This chapter will look at the regionally varying relationship between changes in human activity and Thailand's air pollution levels. Noted that the content of this chapter was published as a journal article in *Sustainability* (Thongrueang et al., 2023).

3.1 Introduction

In mid-March 2020, the Thai government announced the implementation of the first lockdown and administration zoning, which commenced at midnight and affected approximately 68 million citizens (Figures 3.1 and 3.2). The lockdown imposed strict restrictions on the movement of people, resulting in the closure of public transport, schools, colleges, universities, and non-essential local businesses. To enforce the lockdown effectively, the government imposed maximum controls and additional restrictions on movement (Figure 3.2), including a ban on leaving homes between 22:00 and 04:00 local time (WHO, 2020). As a result, anthropogenic, industrial, vehicular, and commercial energy-consuming activities in Thailand were substantially reduced due to COVID-19 lockdowns (Jain and Sharma, 2020), leading to a reduction in air pollution. The Pollution Control Department (2021) reported that environmental quality had improved in all aspects after the first lockdown, as transportation and economic activities were temporarily halted. Furthermore, the implementation of restrictions caused Thailand's air quality index resulted to improve overall by 30% (Kaewrat et al., 2022).

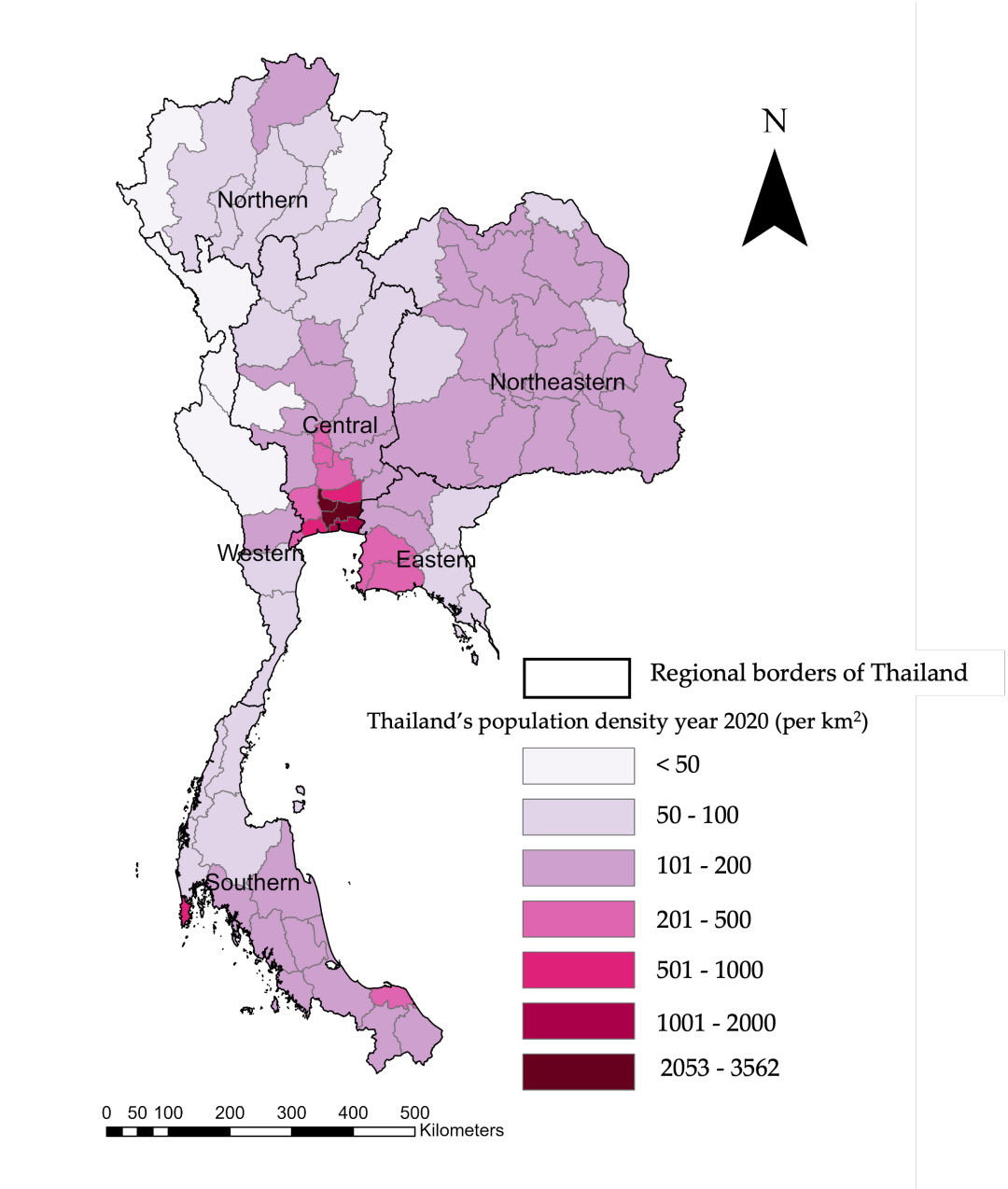

Figure 3.1 *Population density of Thailand*

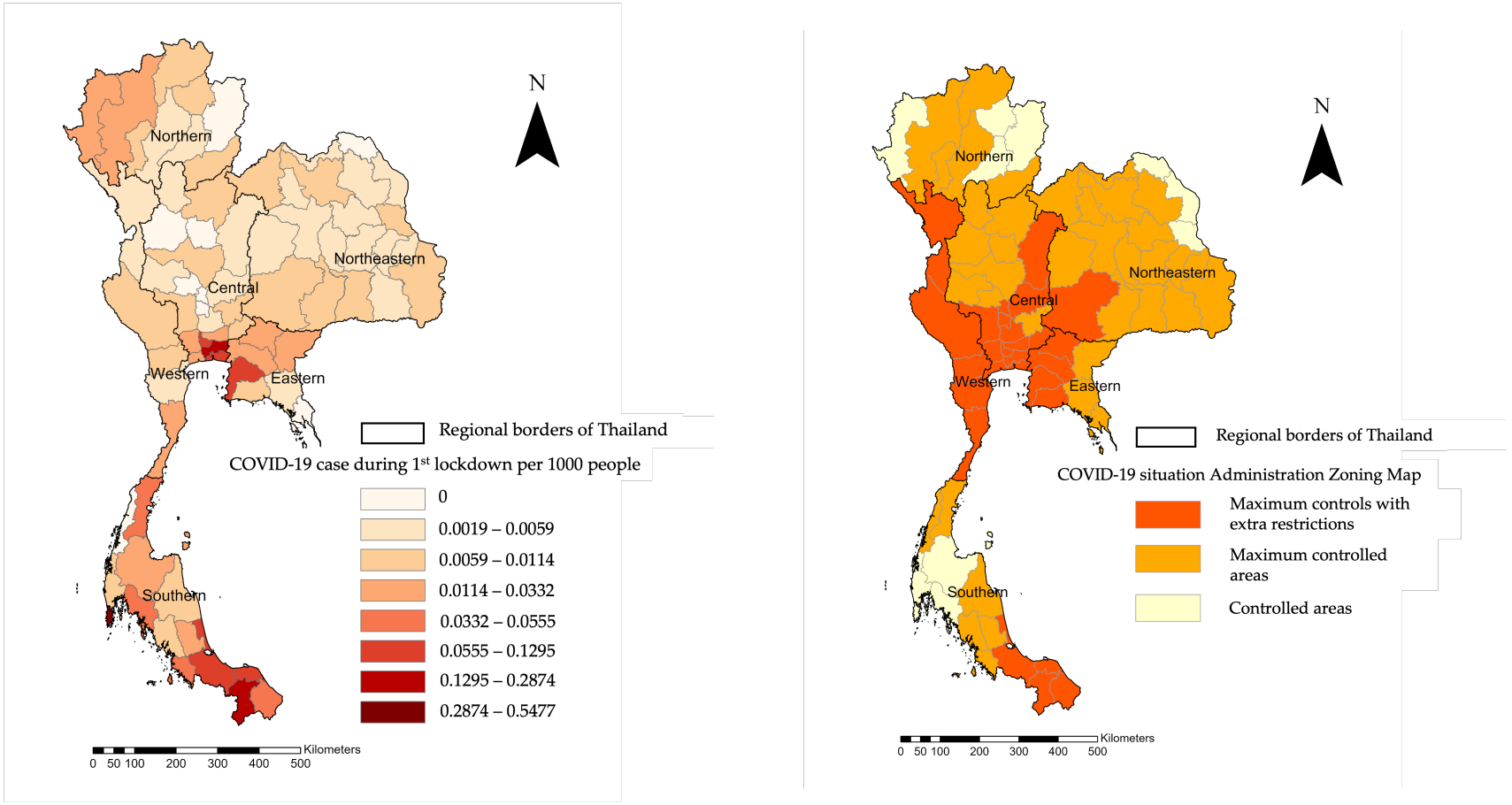

Figure 3.2 *COVID-19 cases per 1000 people during the first lockdown and COVID-19 situation administration zoning map (March 18 to June 30, 2020).*

However, the extent to which the COVID-19 pandemic-induced reduction in anthropogenic activity has resulted in a decrease in air pollution on a geographic scale remains unclear due to the challenges associated with identifying changes in anthropogenic activity at a high geographical resolution. To overcome this difficulty, one potential solution is to employ nighttime light (NTL) imagery indicators, which are the most sensitive human activity observed from Chapter 2. Moreover, NTL can be correlated with economic indicators, such as gross regional product, at different spatial scales (Doll et al., 2006). Kovács (2022) found a relationship between past emissions of NTL intensity and the relative change in NO_2 concentration in metropolitan France. Observations during the lockdown in Spain demonstrated a significant reduction in urban light emissions, NO_2, and aerosols (Bustamante-Calabria et al., 2021). Xu et al. (2021) demonstrated that NTL radiation in Asia decreased following COVID-19 lockdowns in cities, indicating a decrease in anthropogenic activity levels, particularly in commercial and residential areas (Shao et al., 2021). Despite the widespread use of NTL in studies of economic activity and natural disasters (Doll et al., 2006; Zhao et al., 2018), limited research has been conducted to examine the relationship between air pollution and NTL during the COVID-19 lockdown period.

The NO_2 concentration in the air was chosen as the measure of air pollution in this study due to its strong association with anthropogenic activities, such as emissions from transportation. Liu et al. (2020b) demonstrated that air quality improved as a result of reduced vehicle usage and industrial production during the COVID-19 pandemic. Significant reductions in NO_2 emissions were observed as a result of reduced reliance on fossil fuels, including transportation and industrialization (Jechow and Hölker, 2020). The intensity of light emitted at night and its contribution to atmospheric NO_2 concentrations can vary depending on the type of anthropogenic activity. In Thailand, transportation, power generation, industrial activities, and biomass burning are the primary sources of NO_2 emissions. In urban areas, transportation, specifically cars and motorcycles, is the primary contributor to NO_2 emissions, while in rural areas, agricultural waste burning and forest fires are the primary contributors to poor air quality (Stockholm Environment Institute, 2021; World Bank, 2002). Therefore, the relationship between changes in NTL and air pollution is likely to vary geographically. In this study, we used GWR to investigate the regionally varying association between changes in NTL and air pollution in Thailand. Specifically, we examined the

relationships between observations of NTL and NO_2 in the air prior to the 2019 lockdown (pre-lockdown) and during Thailand's COVID-19 control lockdown in 2020.

3.2 Materials and Methods

3.2.1 Data Sources and Preparation

The NO_2 data used in this study were obtained from the Sentinel-5 Precursor (S5P) satellite, which is a component of the Global Monitoring for Environment and Security (Copernicus) program launched by the European Space Agency to monitor air pollution (Veefkind et al., 2012). The Tropospheric Monitoring Instrument (TROPOMI), a multispectral imaging spectrometer with a wide field of view, is utilized to record the measurements. This instrument allows for global daily coverage and has a high spatial resolution of 7×7 km^2, enabling the sampling of small-scale variabilities, especially in the lower troposphere. Consequently, TROPOMI is suitable for monitoring emissions sources and holds potential for air quality research (Ialongo et al., 2020). The S5P level 3 Near Real Time was used in this study, sourced from the Google Earth Engine (GEE). Other researchers, such as Liu et al. (2020a), have used TROPOMI data to demonstrate that NO_2 concentrations in urban areas of China and India were significantly higher than previously estimated. Furthermore, TROPOMI data have indicated that high levels of NO_2 in Africa were caused by numerous fires, particularly in the savannah and rainforest (Van Der Velde et al., 2021).

The NTL intensity data were gathered through Suomi-NPP satellite observations. The Suomi-NPP satellite, operated by NASA and the National Oceanic and Atmospheric Administration, possesses the Visible Infrared Imaging Radiometer Suite (VIIRS) that includes a day/night band (DNB). This DNB enables the acquisition of multitemporal NTL data and facilitates near-real-time monitoring due to its high repetition frequency (Elvidge et al., 2013). The VIIRS sensor captures data while in a polar orbit, during the appropriate time for observing Thailand, typically around 00.00–00.30. We used the VIIRS Nighttime Day/Night Band Composites Version 1 in this study, which contains monthly averaged radiance composite images. We acquired stable composite data from the VIIRS-DNB data of 2019 and 2020 by applying the median reducer in the GEE to eliminate the maximum value of NTL. The average DNB radiance value was selected from the composite VIIRS-DNB data. To upscale NO_2 and

NTL to 7 × 7 km^2 grid cells, we employed the nearest neighbor resampling technique in the GEE.

The land cover data used in this study were acquired from the land-cover portal website, which is maintained by SERVIR-Mekong. This website offers high-quality land cover information, which is sourced from multiple quality control sources. The processing of NO_2 concentrations, NTL intensity, and land cover was conducted using 7 × 7 km^2 grid cells.

3.2.2 Estimation of Air Pollution Emission and Its Relationship with Anthropogenic Activities

To conduct a comparative analysis, the satellite-based NO_2 concentrations and NTL measurements were determined by considering the median from 18th March to 30th June for both 2019 (before the implementation of lockdown measures) and 2020 (during the first lockdown period). The calculations were performed using the GEE platform, and the results were reported at the level of 7 × 7 km^2 grid cells. Specifically, the changes in the NO_2 concentrations during the lockdown period in 2020 were computed by comparing them to the pre-lockdown period in 2019.

Furthermore, the present study investigated the relationship between the changes in NO_2 and NTL data using a local spatial regression model known as Geographically Weighted Regression (GWR) model (Equations (3.1)– (3.3)). The objective was to estimate the geographically varying coefficients and determine the effects of the reduction in anthropogenic activities on air pollutant concentrations across different regions of Thailand during the pandemic outbreak phase. To handle large datasets, we employed a scalable variant of GWR (Murakami et al., 2020), which is available in the R package of the GWmodel (Lu et al., 2014). To account for the nonlinearity between NTL and NO_2, we applied a logarithmic transformation. Equation (3.1) expresses the GWR model:

$$y_i = \beta_0(u_i, v_i) + \beta_1(u_i, v_i)x_i + \varepsilon_i \quad (3.1)$$

In Equation (3.1), (u_i, v_i) represents the coordinates (easting, northing) of point i. The dependent variable y_i and the independent variable x_i are defined in Equations (3.2) and (3.2) as follows:

$$y_i = logNO_{2_{i,2020}} - logNO_{2_{i,2019}} \quad (3.2)$$

$$x_i = logNTL_{i,2020} - logNTL_{i,2019} \quad (3.3)$$

In Equation (3.2), $logNO_{2_{i,2019}}$ and $logNO_{2_{i,2020}}$ represent the log-transformed NO_2 concentrations for the pre-lockdown period in 2019 and during the lockdown period in 2020, respectively. In Equation (3.3), $logNTL_{i,2019}$ and $logNTL_{i,2020}$ denote the log-transformed average NTL intensity for the pre-lockdown period in 2019 and during the lockdown period in 2020, respectively.

3.2 Results

3.2.1 NO_2 Level and NTL Intensity Change in Thailand

The study examined the changes in monthly NO_2 values (mol/m^2 × 10^5) to determine the overall variations in NO_2 levels between 2019 and 2020 (Figure 3.3). The national monthly changes in NO_2 and NTL, as shown in Figure 3.3, did not exhibit any visible lockdown-induced changes. This could be due to differing degrees of lockdown restrictions, with some locations being less affected by the initial lockdown and an overall increase in NTL due to economic growth. In contrast, the geographical distributions of the comparative changes in NO_2 and NTL during the lockdown period (Figures 3.4 and 3.5) are more pronounced, suggesting that the impact of the lockdown on NTL and NO_2 cannot be captured by the national monthly changes. The results showed a 10.36% reduction in NO_2 levels during the first lockdown in 2020 (March 18, 2020 –June 30, 2020) compared to the same period in 2019. In 2019, the minimum, maximum, and average NO_2 levels were 4.06, 16.20, and 6.74 mol/m^2 × 10^5, respectively (Figure 3.4a), while those in 2020 were 3.83, 13.49, and 6.04 mol/m^2 ×

10^5, respectively (Figure 3.4b). While there was a decrease in NO_2 levels observed in the mountainous regions of the northern and northeastern parts of Thailand, where there are dense forests, the most substantial reduction proportions of NO_2 were observed in the central part of Bangkok, which includes the primary shopping, dining, and nightlife areas (Figure 3.4c). Additionally, a comparison of NO_2 levels before and during the lockdown periods revealed that NO_2 levels decreased in various regions, including the northern, northeastern, central, western, eastern, and southern during the lockdown period when compared to the same period in 2019.

Figure 3.3 depicts the comparison of monthly trends to determine the overall change in NTL intensity between 2019 and 2020. The analysis of the minimum, maximum, and average NTL intensities before and during the lockdown period revealed that in 2019, the values were 0.001, 51.19, and 1.04 $nW/cm^2/sr$, respectively (Figure 3.5a), while in 2020, the values were 0.12, 49.40, and 1.09 $nW/cm^2/sr$, respectively (Figure 3.5b). The central part of Bangkok experienced a substantial decrease in NTL intensity, while the eastern and northern regions experienced a slight decrease and other regions experienced an increase (Figure 3.5c).

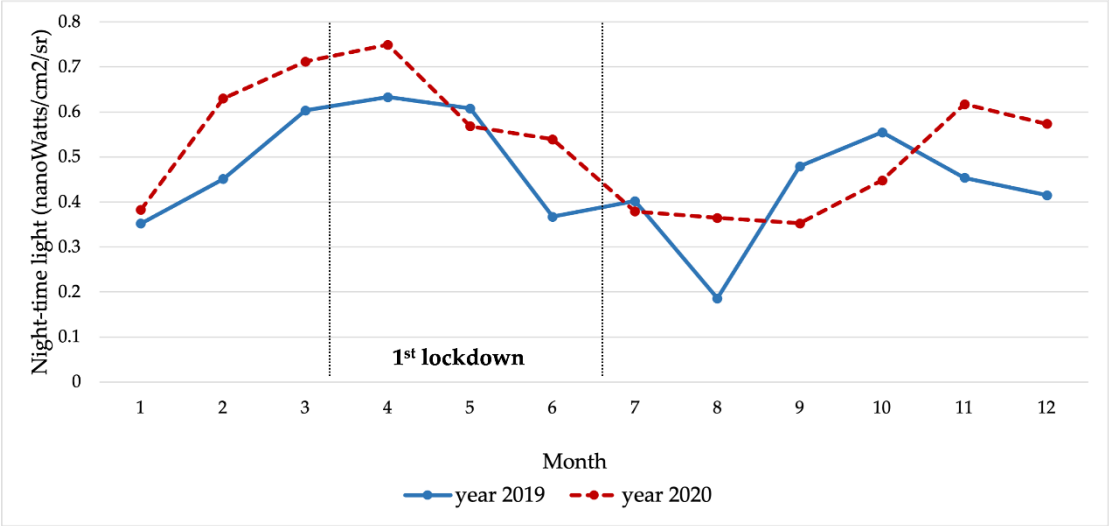

(a)

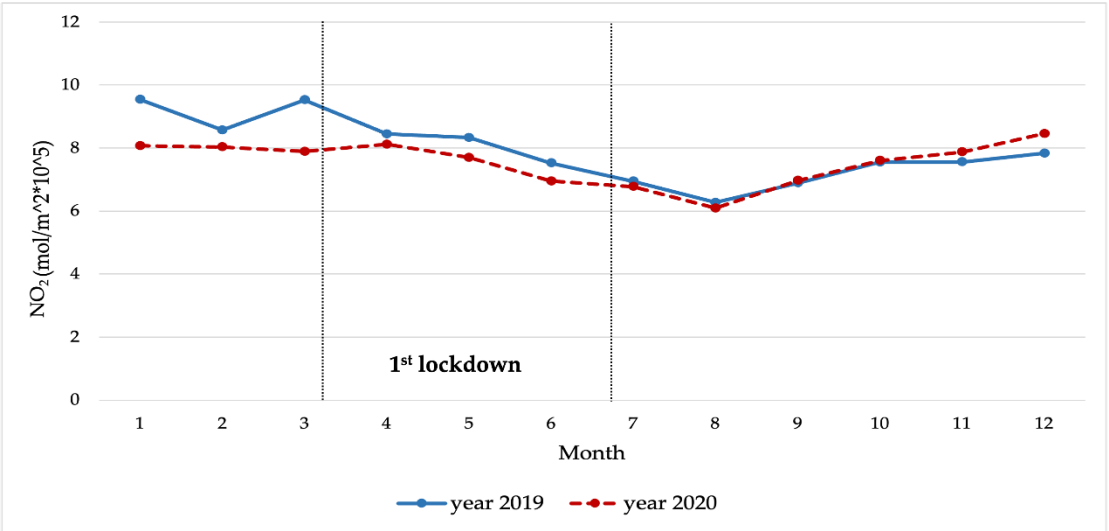

(b)

Figure 3.3 *Monthly trends of nighttime light (a) and NO_2 (b) in 2019 and 2020 in Thailand.*

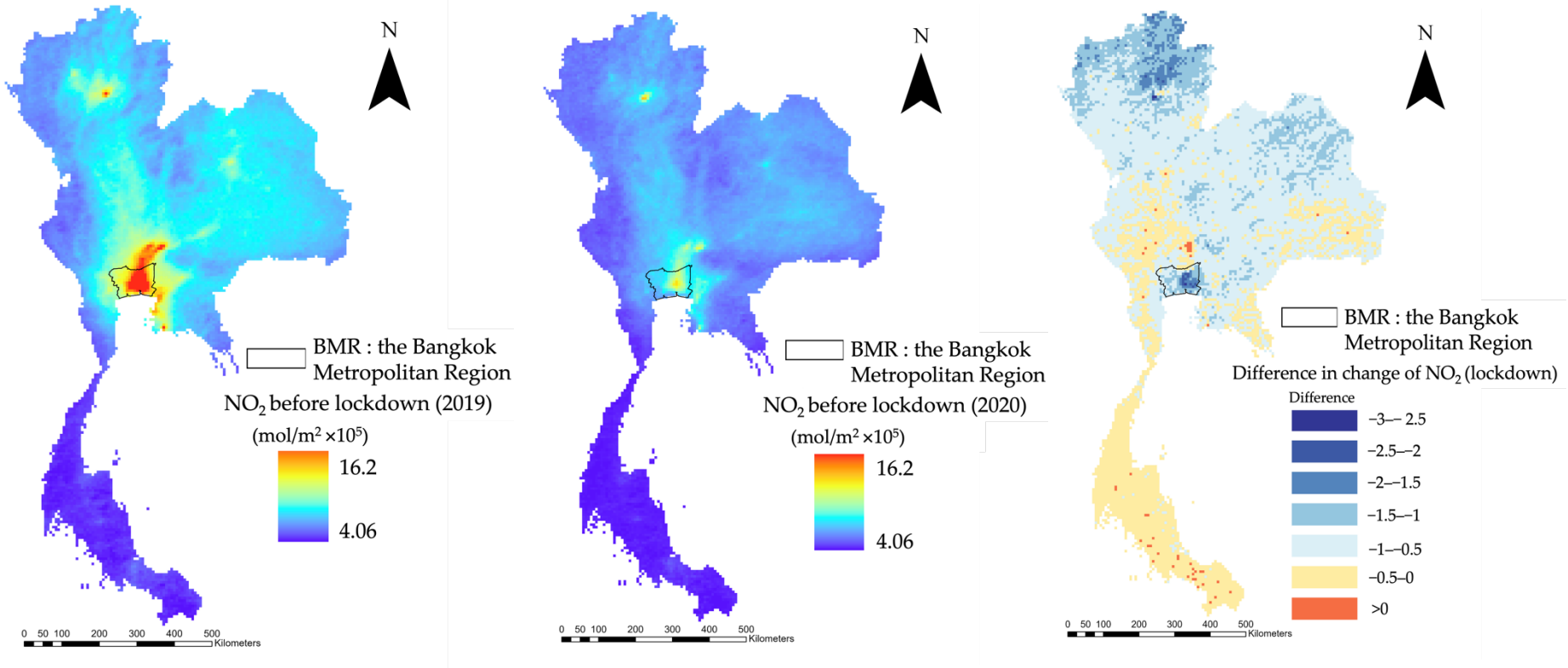

(a) **(b)** **(c)**

Figure 3.4 *Spatial distribution of the change in NO_2 levels during the first lockdown period in 2020 compared to the same period in 2019.*

Note. The figures provide visual insights into the spatial patterns of changes in NO_2 levels across Thailand during the COVID-19 pandemic outbreak. The map presents three sub-figures: (a) NO_2 levels before the lockdown period in 2019, ranging from 18 March 2019 to 30 June 2019; (b) NO_2 levels during the lockdown period in 2020, ranging from 18 March 2020 to 30 June 2020; and (c) the difference in the change of NO_2 levels between the two period.

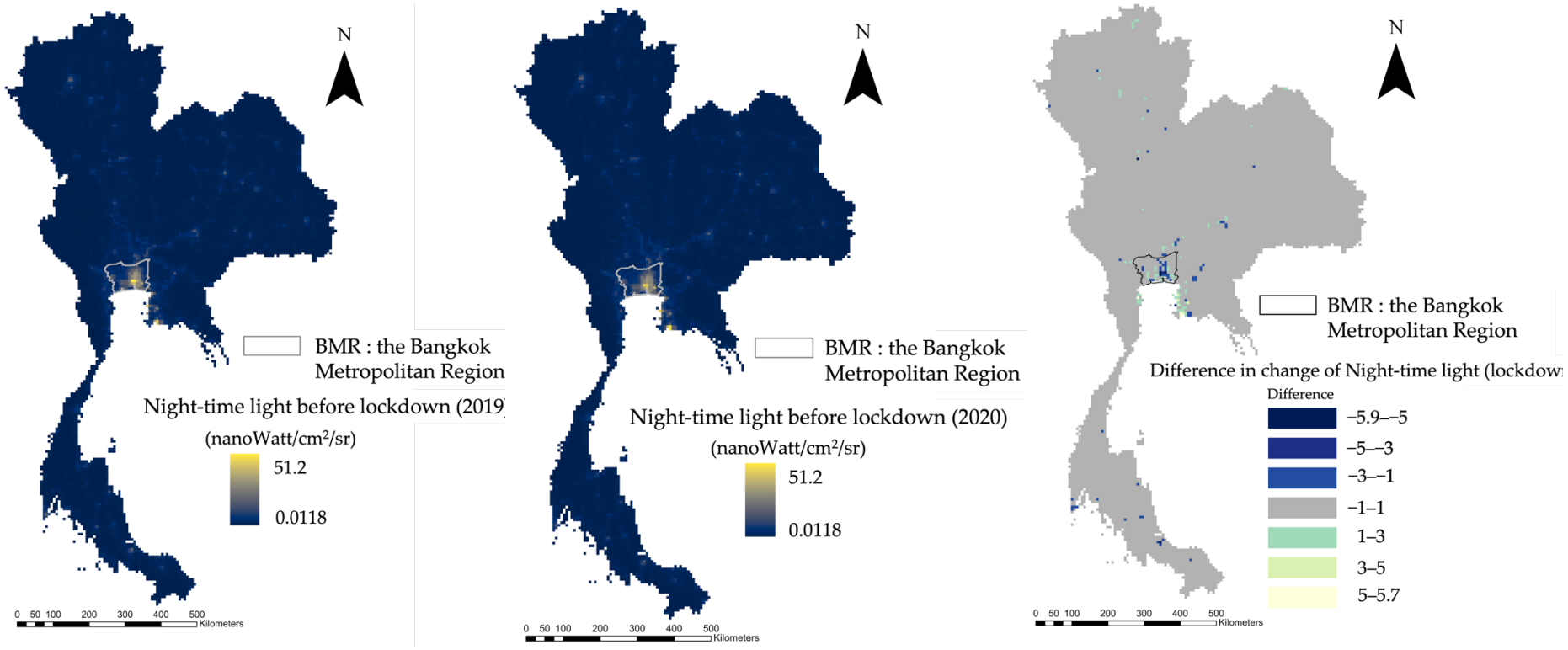

(a) **(b)** **(c)**

Figure 3.5 *Spatial distribution of the difference in nighttime light intensity between the first lockdown period in 2020 and the same period in 2019.*

Note. The figure consists of three subfigures: (a) shows the NTL intensity before the lockdown period in 2019 (from 18 March 2019 to 30 June 2019), (b) shows the NTL intensity during the lockdown period in 2020 (from March 18, 2020 –June 30, 2020), and (c) shows the difference in NTL change between the two periods.

Figure 3.6 depicts the areas where reductions in NO_2 and NTL intensity occurred across different land cover categories in Thailand. These areas consist of grid cells where the NO_2 and NTL levels decreased during the same period in 2019 and 2020, indicating a negative change. Table 3.1 reveals that a substantial reduction in NO_2 levels was observed in cropland, forest and mixed forest, as well as urban and built-up areas. Meanwhile, the reduction in NTL intensity was mostly observed in urban and built-up areas. The land cover category of urban and built-up areas comprises approximately 31.66% of Thailand, whereas orchards or plantation forests and croplands cover 17.59% and 16.58% of the country, respectively.

Table 3.1 *Land cover types in NO_2 and nighttime light intensity reduction areas*

Land Cover Types	Nighttime Light (Decreased)		NO_2 (Decreased)	
	Count	Percentage (%)	Count	Percentage (%)
Surface Water	2	1.01	12	0.96
Mangroves	0	0.00	0	0.00
Flooded Forest	0	0.00	0	0.00
Forest	17	8.54	334	26.85
Orchard or Plantation Forest	35	17.59	62	4.98
Evergreen Broadleaf	8	4.02	69	5.55
Mixed Forest	16	8.04	251	20.18
Urban and Built-Up	63	31.66	96	7.72
Cropland	33	16.58	369	29.66
Rice	19	9.55	25	2.01
Mining	0	0.00	1	0.08
Barren	0	0.00	0	0.00
Wetlands	1	0.50	2	0.16
Grassland	1	0.50	15	1.21
Shrubland	0	0.00	2	0.16
Aquaculture	4	2.01	6	0.48

Note. Count is the number of 7×7 km^2 grid cells

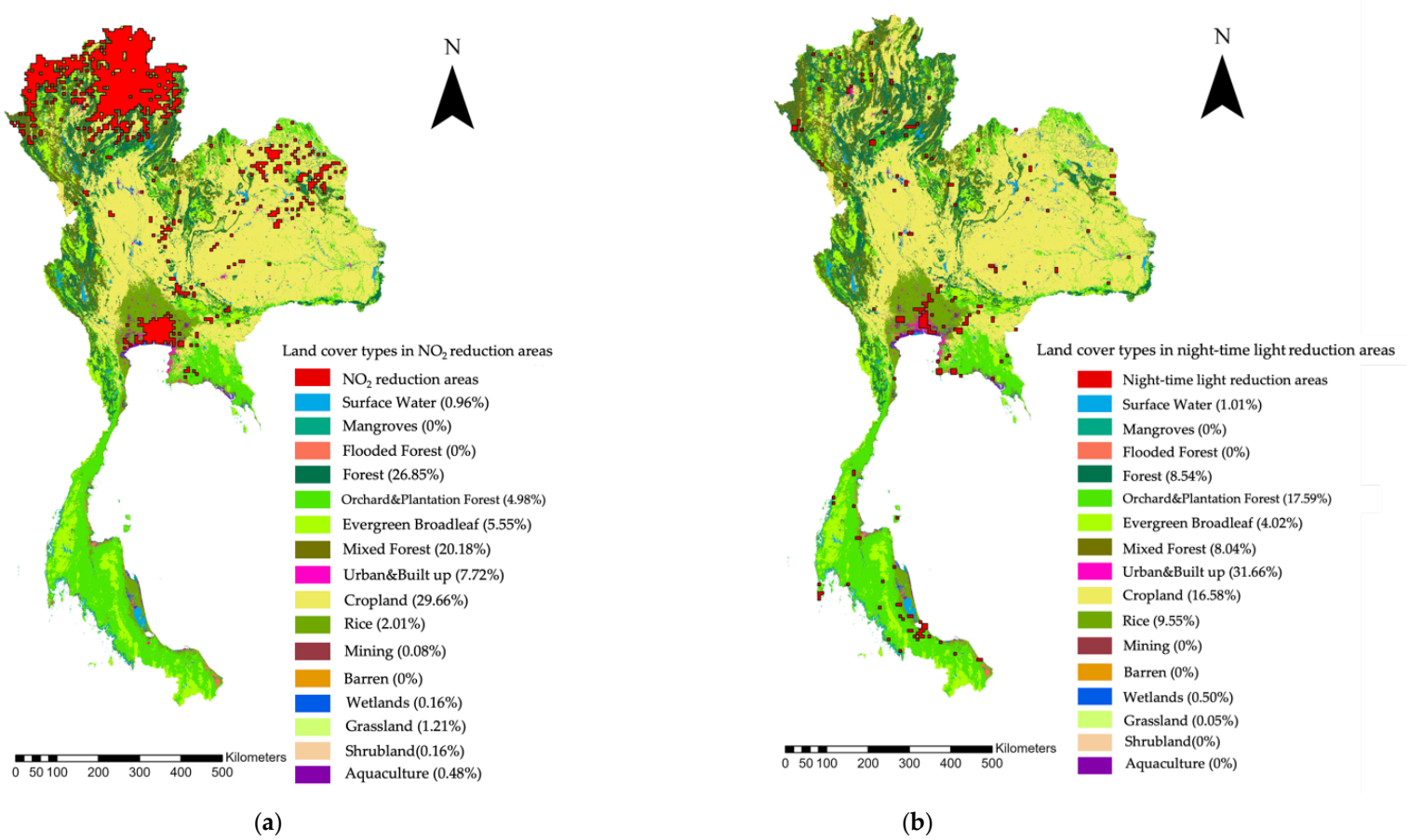

Figure 3.6 *Land cover types in reduction areas*

Note. The figure consists of two sub-figures: (a) NO_2 and (b) nighttime light intensity reduction areas.

3.2.2 Association between the NTL and NO_2 Levels

The study found that there were positive correlations between the log-transformed NTL and NO_2 levels. Pearson correlation coefficients were calculated and revealed that for the period preceding the lockdown in 2019, the coefficient was r = 0.33, while for the lockdown period in 2020, it was r = 0.38. In order to investigate this relationship further, we used the annual change in the log-transformed NO_2 level as the dependent variable and the log-transformed NTL as the independent variable. To analyze the data, a GWR model was fitted.

The estimated coefficient of NTL (β_1) in the GWR model fitted to the data revealed that there were widespread positive correlations between the changes in NTL and NO_2 levels in the central, western, and northern regions of the country, while negative correlations were observed in the peripheral areas (Figure 3.7). The positive correlation indicates that when NTL intensity decreased, NO_2 levels also decreased. A higher slope coefficient suggests that a more substantial reduction in air pollution resulted from a decrease in NTL intensity. The R-squared value of the fitted GWR model was 0.592, indicating a moderate level of fit.

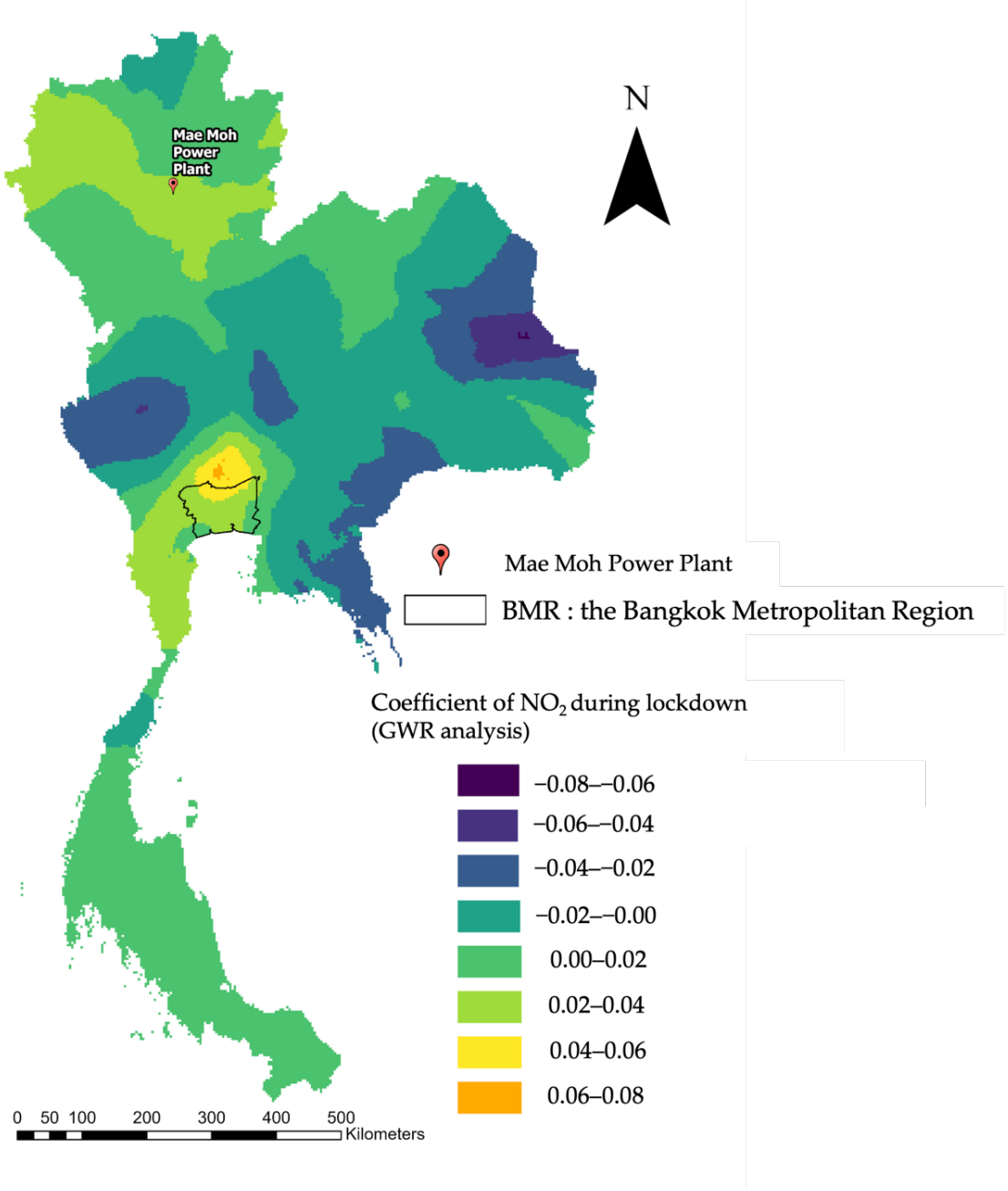

Figure 3.7 *Geographically weighted regression (GWR) estimates of the slope coefficient.*

3.3 Discussion

During the period of lockdown in Thailand, there was a reduction in the NO_2 levels by 10.36% compared to the same period in 2019. Additionally, there was a notable reduction in NTL intensity around Bangkok and its surrounding areas during the lockdown period. GWR analysis revealed a positive correlation between the changes in NTL and NO_2 levels, particularly in urbanized areas, especially the BMR. The central region of Thailand includes diverse economic sectors, such as urban, industrial, agricultural, and tourism, with Bangkok serving as the country's major economic sector. Additionally, provinces in central Thailand that are connected to Bangkok through a road network have higher traffic. During Thailand's dry season (November-February), the concentration of air pollutants exceeds the country's air quality standards. However, the implementation of COVID-19 lockdowns effectively halted human mobility by requiring people to work remotely and stay at home, reducing inter-province traffic. This resulted in a substantial decrease in the concentration of NO_2 and the intensity of NTL in the region. The findings indicate that the reduction in anthropogenic activities in cities, as reflected by the NTL changes, substantially decreased the NO_2 concentrations in the air surrounding the cities.

However, it is crucial to exercise caution when examining the geographic context of the relationship between NTL intensity and NO_2 emissions. NTL intensity decreased across land use categories, including urban and built-up areas (31.66%), orchards and plantation forests (17.59%), and croplands (16.58%). The NO_2 reduction process in orchards, planted forests, and cropland areas is most likely an unintended consequence. The primary factor contributing to the decline in NO_2 during lockdown measures can be attributed to reduced transportation and industrial activities, resulting from restrictions on international mobility and business operations, particularly in the BMR and adjacent regions encompassing agricultural land covers. Reduced human activity in urbanized areas may result in a lower NO_2 emission, resulting in lower NO_2 in agricultural land covers near the BMR. Agriculture employs approximately 30% of Thailand's labor force (Musikawong et al., 2021). A portion of the agricultural workforce also resides on their farmland. The NTL sources in plantation forests and cropland might have been produced by inhabitants' daily activities. Consequently, the results demonstrated that the decrease in NTL in agricultural land-use categories across

Thailand was smaller than in urban and built-up areas, while NO_2 decreased in most cropland (29.66%), forest (26.85%), and mixed forest (20.18%) areas. Specifically, NO_2 reduction was observed in northern Thailand, a non-urban region dominated by forests and cropland. This reduction may be attributed to the decline in agricultural combustion, such as burn farming, which is characteristic of this region (Yin et al., 2019), due to the lockdown. However, further study is necessary to comprehensively understand this process.

While NO_2 concentrations are associated with emissions produced by transportation and are frequently employed as indicators of local air pollution exposure at various scales (Levy et al., 2014), some NO_2 emission sources are not produced by transportation or daily human activities. In northern Thailand, forest fires and power plants contribute to NO_2 emissions (Xu et al., 2021). For instance, severe air pollution from the Mae Moh Power Plant in Lampang Province, Thailand, in 1992 and 1997 (Pollution Control Department, 2000) had negative impact on human health, property, animals, and vegetation in the surrounding areas. According to the GWR findings, the correlations between alterations in NO_2 concentrations and NTL data were estimated to be approximately zero or negative, with NTL increasing as NO_2 levels decreased in 2020 compared to 2019 in the northern and northeastern areas of Thailand. This phenomenon could be attributed to temporally activated emission sources with non-urban light, such as agricultural residue burning and forest fires, generating relatively minor NO_2 emissions in comparison to coal power plants and vehicle exhaust, which are Thailand's primary sources of NO_2 emissions (Greenpeace, 2015).

The effects of lockdown measures have been observed in recent global studies (Menut et al., 2020). Incorporating data from the second and third waves of the pandemic could lead to a more comprehensive understanding of the air pollution impacts resulting from lockdowns. However, the general population has started to adapt to the pandemic, incorporating various countermeasures into their daily routines and becoming less fearful of the pandemic than during the initial lockdowns. Consequently, the first wave of lockdowns was the most severe in its approach to the pandemic. The implementation of non-pharmaceutical interventions led to heightened caution among individuals when venturing outside or engaging in public outdoor activities. During this period, there was a substantial reduction in air pollution due to a reduction in human

movement and activities, effectively serving as a natural experiment. Additionally, it may be beneficial to examine longer time periods prior to 2019 to better understand the natural fluctuations in atmospheric NO_2. As Thailand is a developing country, pollutant levels can fluctuate. Thus, in order to gain a more comprehensive understanding of such changes, this study focused on changes in NO_2 concentrations during the 2020 lockdown period compared to same timeframe in 2019, particularly in urban areas, to attain a more comprehensive understanding of such alterations.

Using geographically detailed mobility data in future studies could potentially reveal a more robust association between human activities and air pollution. However, in Thailand and other developing countries, such data can be costly and may not cover the entire region. Thus, while mobility data could serve as a viable metric for assessing human activity levels, it is currently unavailable. As a result, we used NTL data, which can be used in other countries with similar methodologies. Nonetheless, the scope of this study was limited to Thailand. Subsequent research could broaden the study area by using satellite data, which could easily encompass other regions or the entirety of Southeast Asia. Additionally, addressing several challenging issues necessitates a more detailed analysis and understanding of meteorological influences over extended time periods.

3.4 Conclusion

This study aims to examine the correlation between NO_2 and NTL in Thailand during the initial lockdown period in 2020. The study reveals a substantial decline in NO_2 and NTL levels in most urban and built-up areas when compared to the same period in 2019. We used GWR to examine the regionally varying association between changes in NTL and air pollution in Thailand. It was observed that there is a positive correlation between the changes in NO_2 and NTL in the Bangkok Metropolitan Region. These findings suggest that reductions in anthropogenic activities in urban areas, as reflected by the NTL in cities, have a substantial impact on reducing atmospheric NO_2 concentrations. As a result, the study suggests that NTL observations can be used to monitor changes in air pollution caused by anthropogenic activities in urban areas.

CHAPTER 4

The Effect of Anthropogenic Activity Caused by COVID-19 Lockdown Resulting in Changes in Nitrogen Dioxide Levels Using Nighttime Light Intensity in South and Southeast Asia

In chapter 3, the observation of the regionally varying association between the changes in human activities and air pollution during the lockdown period in Thailand has been discussed. This chapter will investigate the changes in NO_2 and NTL during the COVID-19 lockdown in 18 cities across SA and SEA regions to explore how the changes are regulated by different situations in the cities with different lockdown policies.

4.1 Introduction

As discussed in previous chapters, the implementation of lockdown measures and the subsequent disruption of human and industrial activities have resulted in a substantial decrease in air pollution levels, particularly in the concentration of NO_2. The emergence of the Coronavirus outbreak in the SA and SEA region was officially confirmed in mid-January 2020. Following this confirmation, the number of confirmed cases in SEA countries began to rapidly increase. In addition to the standard preventive measures, many countries in SA and SEA implemented lockdown measures ranging from community-specific to nationwide restrictions. Many studies have examined the changes in air quality during periods of lockdown in SA and SEA countries. Kanniah et al. (2020) observed a large reduction of 27%–34% in tropospheric NO_2 column density within urban agglomerations in SEA during the COVID-19 period of 2020. Additionally, there was a substantial decrease in the levels of PM_{10}, $PM_{2.5}$, CO, and SO_2 in Malaysian urban areas when compared to the mean levels recorded from 2015–2019. Dhaka, Kathmandu, Jakarta, and Hanoi experienced the highest NO_2 concentration reductions by approximately 40% –47% during the lockdown period in 2020 compared to the corresponding period in 2019 among 19 Southeast Asia cities (Roy et al., 2021).

The findings presented in Chapter 2 showed a monthly positive correlation between the intensity of NTL and NO_2 concentrations in the BMR. In Chapter 3, we confirmed that such positive correlation was mainly observed in major urban areas like the BMR.

This chapter highlights a wider contextuality regulating the relations between the changes in NTL and NO_2 in major cities in SA and SEA by broadening the study area from Thailand to the international extent. Considering the large differences in the conditions in SA and SEA's major cities, this chapter examines the impact of human activity caused by COVID-19 lockdown on NO_2 concentrations in 18 major cities in SA and SEA.

4.2 Materials and Methods

4.2.1 Study area

We selected seven cities in SA, namely Dhaka (Bangladesh), Islamabad (Pakistan), Kabul (Afghanistan), Kathmandu (Nepal), New Delhi (India), Colombo (Sri Lanka) and Thimphu (Bhutan), as shown in Table 4.1. We also selected 11 cities in SEA countries, namely Jakarta (Indonesia), Yangon (Myanmar), Bangkok (Thailand), Bandar Seri Begawan (Brunei), Kuala Lumpur (Malaysia), Manila (Philippines), Phnom Penh (Cambodia), Singapore, Dili (East Timor), Vientiane (Laos), and Ho Chi Minh city (Vietnam), as presented in Table 4.1. According to GADM (2018), SA is located between the latitudes 23° N and 55° N and the longitudes 60° E and 130° E (Figure 4.1), while SEA is geographically located between 29° N and 11° S and 92° E and 141° E (Figure 4.2). In this study, the administrative boundaries of each nation's main cities were used to define its borders. The city boundaries used in this study were obtained from the Global Administrative Areas (GADM) version 3.6 database, which was released in 2018 and can be accessed at www.diva-gis.org.

Table 4.1*The study area description*

Country	City	Estimated Population (City)	GDP per capita USD	Started date
Indonesia	Jakarta	33,756,000	15,855	10th April 2020
Myanmar	Yangon	6,874,000	5,131	23rd March 2020
Thailand	Bangkok	18,007,000	22,675	18th March 2020
Brunei	Bandar Seri Begawan	100,700	75,583	24th March 2020
Malaysia	Kuala Lumpur	8,911,000	36,846	18th March 2020
Philippines	Manila	24,922,000	11,420	15th March 2020
Cambodia	Phnom Penh	2,463,000	6,092	9th April 2020
Singapore	Singapore	5,983,000	133,894	7th April 2020
East Timor	Dili	222,323	2,741.39	28th March 2020
Laos	Vientiane	1,001,477	9,800	1st April 2020
Vietnam	Ho Chi Minh City	15,136,000	14,458	1st April 2020
Bangladesh	Dhaka	21,741,000	7,985	26th March 2020
Pakistan	Islamabad	1,015,000	6,662	23rd March 2020
Afghanistan	Kabul	4,435,000	2,456	28th March 2020
Nepal	Kathmandu	1,442,000	4,677	24th March 2020

Country	City	Estimated Population (City)	GDP per capita USD	Started date
India	New Delhi	29,617,000	8,293	25th March 2020
Sri Lanka	Colombo	5,648,000	14,230	20th March 2020
Bhutan	Thimphu	114,551	13,077	11th August 2020

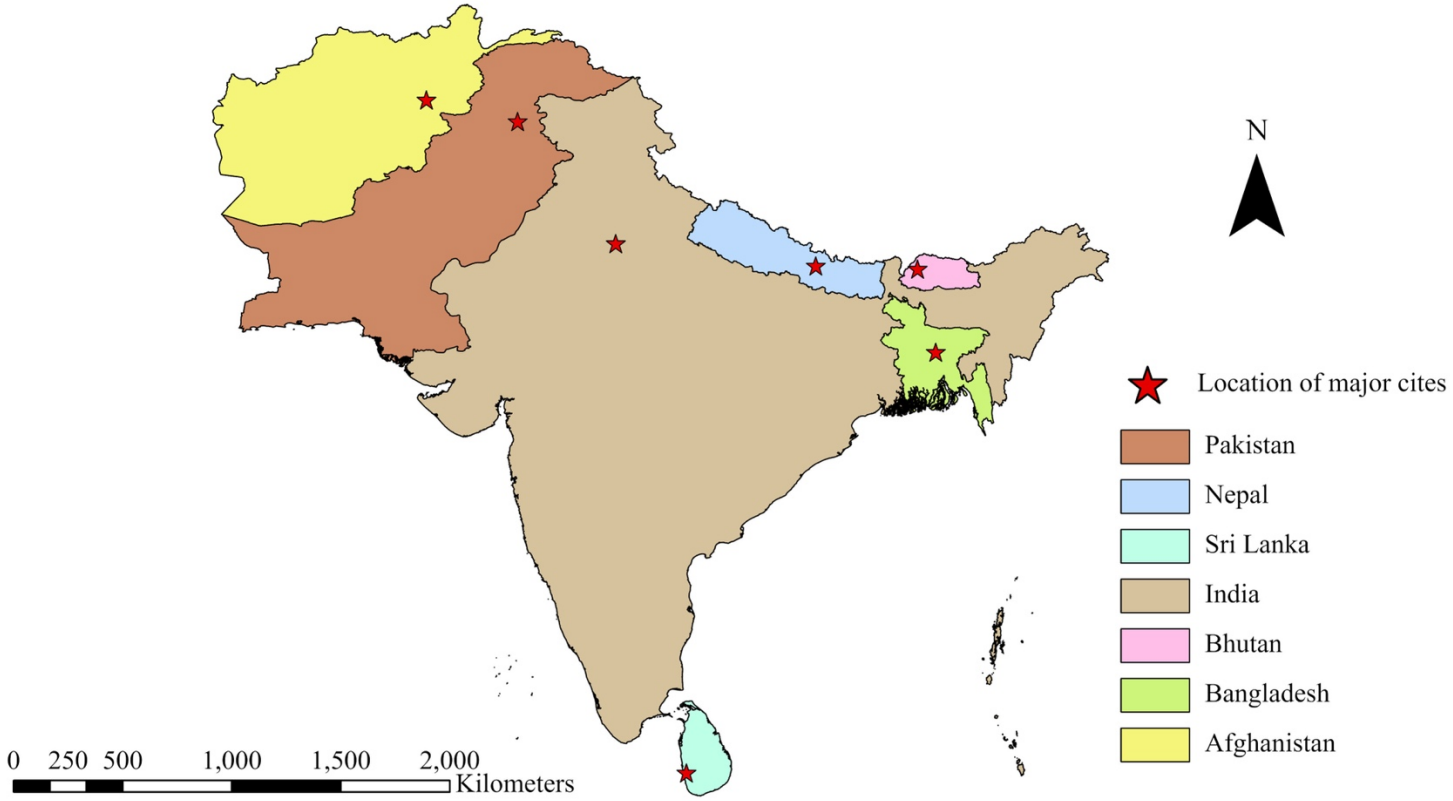

Figure 4.1 *South Asia region map*

Note. The red star is the location of 7 cities.

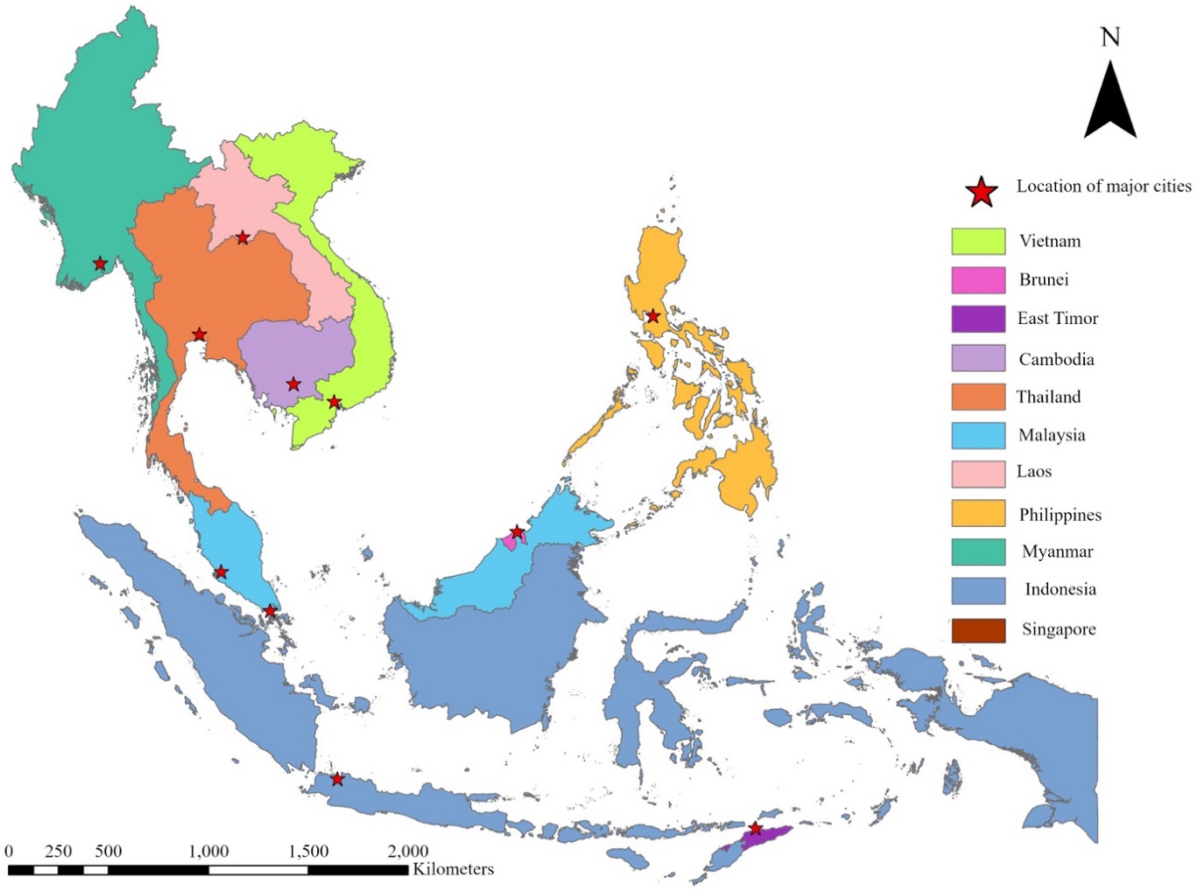

Figure 4.2 *Southeast Asia region map*

Note. The red star is the location of 11 cities.

4.2.2 Data collection

The data utilized in this chapter corresponds to the NO_2 data discussed in Chapter 3. The NO_2 data were obtained from observations made by the S5P (Sentinel-5 Precursor) satellite, which is part of the Copernicus program initiated by the European Space Agency for the purpose of monitoring air pollution (Veefkind et al., 2012). The measurements were conducted using the TROPOMI payload, which is a multispectral imaging spectrometer mounted on the satellite. S5P level 3 Near Real Time data from the GEE were used for the selected 18 cities. NO_2 data calculated mean of values for each month base on the shapefile of city extent.

The NTL intensity data were gathered from observations conducted by the Suomi-NPP satellite, specifically, the Visible Infrared Imaging Radiometer Suite Day/Night Band (VIIRS-DNB) instrument, located on the Suomi-NPP satellite operated jointly by NASA and the National Oceanic and Atmospheric Administration. The VIIRS-DNB instrument provides multitemporal NTL data, enabling near-real-time monitoring due to its high repetition frequency (Elvidge et al., 2013). For this study, we used the VIIRS Stray Light Corrected Nighttime Day/Night Band Composites Version 1. These composites consist of monthly averaged radiance composite images derived from nighttime data obtained from the VIIRS Day/Night Band (DNB). To ensure the stability of the composite data, we used the GEE's median reducer to eliminate the maximum NTL values. To examine the relationship between NO_2 levels and NTL, the 'avg_rad' band from the VIIRS Nighttime Day/Night Band Composites Version 1 dataset is used. The monthly NTL intensity value for each city was calculated as the mean of the monthly NTL values within each city's shapefile boundary.

4.2.3 Statistical Analysis

In order to examine the impact of the COVID-19 lockdown on air pollution, specifically NO_2, and human activity, represented by NTL, we intended a comparative study among the 18 cities in SA and SEA. To facilitate this comparison, the monthly median values of satellite-based NO_2 concentrations and NTL measurements were computed using data from 2019– 2020. Following the previous chapters analyzing the first lockdown period, we again focus on the same periods: "before-lockdown period" from March to July, 2019 and "during-lockdown period" from March to July, 2020. To

determine the change in NO_2 concentration and NTL intensity between the two periods, a percentage change was summarized. The percentage change in NO_2 concentrations was calculated using the following formula (4.1):

$$PC_{NO_2} = \left(\left(NO_{2_{2020}} - NO_{2_{2019}}\right) \div NO_{2_{2019}}\right) \times 100 \quad (4.1)$$

where $NO_{2_{2019}}$ represents the monthly average NO_2 concentration for the before-lockdown period in 2019, and $NO_{2_{2020}}$ represents the monthly average NO_2 concentration for the during-lockdown period in 2020.

The percentage change in NTL intensity was calculated using the following formula (4.2):

$$PC_{NTL} = \left((NTL_{2020} - NTL_{2019}) \div NTL_{2019}\right) \times 100 \quad (4.2)$$

where NTL_{2019} represents the monthly average NTL concentration for the year 2019, and NTL_{2020} represents the monthly average NTL concentration for the year 2020.

In addition, to investigate the different experiences in NO_2 and NTL percentage change among the study cities during the first lockdown period, hierarchical agglomerative cluster analysis was employed to uncover groupings of cities, characterized by similar NO_2 and NTL percentage changes during that period. Ward method was applied as the linkage criterion for the clustering. This algorithm begins by treating each data point as an individual cluster and then progressively merges the pair of clusters that minimally contributes to the overall increase in the within-cluster variance. This process continues iteratively until a specified number of clusters are formed.

Using the result of the clustering of cities, a scatter diagram was generated to visually illustrate the characteristics of the city groups. This graphical representation plotted the NTL percentage change on the x-axis and the NO_2 percentage change on the y-axis, with each dot symbolizing a specific city. The position of each dot reflects the city's NO_2 and NTL percentage changes.

Furthermore, this study employed descriptive statistical techniques using boxplots and another type of graphs to summarize the city's attribute variables by cluster to facilitate understanding of what city characteristics underlie the changes in NTL and NO_2. The variables includes GDP per capita, area size, estimated population, and levels of policy restrictions for each of the 18 cities.

4.3 Results

4.3.1 NO_2 Level and NTL Intensity Change in the 7 Cities in Southeast Asia

The variations in monthly NO_2 concentrations ($mol/m^2 \times 10^5$) in the study periods were shown in (Figure 4.3) for seven SA cities. NO_2 levels decreased in all seven SA cities during the initial lockdown in 2020, including Dhaka, Islamabad, Kabul, Kathmandu, New Delhi, Colombo, and Thimphu, compared to the same period in 2019. The greatest drop was in New Delhi (20.93%), followed by Kathmandu (12.72%) and Kabul (12.14%). The remaining capitals saw declines ranging from 10.14% to 6.42%. Islamabad (10.14%), Dhaka (9.95%), Thimphu (7.53%), and Colombo (6.42%) are listed in detail.

In addition, the monthly trends were compared to ascertain the overall change in NTL intensity, measured in $nanoWatts/cm^2/sr$, between 2019 and 2020 (Figure 4.4). Colombo experienced the largest decrease of NTL (18.81%), while Islamabad did the second largest decrease of (10.45%). Other cities whose NTL intensities changed during the lockdown were New Delhi (10.02%), Dhaka (2.52%), and Thimphu (0.60%). Kathmandu and Kabul, on the other hand, experienced large increases of 28.90% and 4.17 %, respectively.

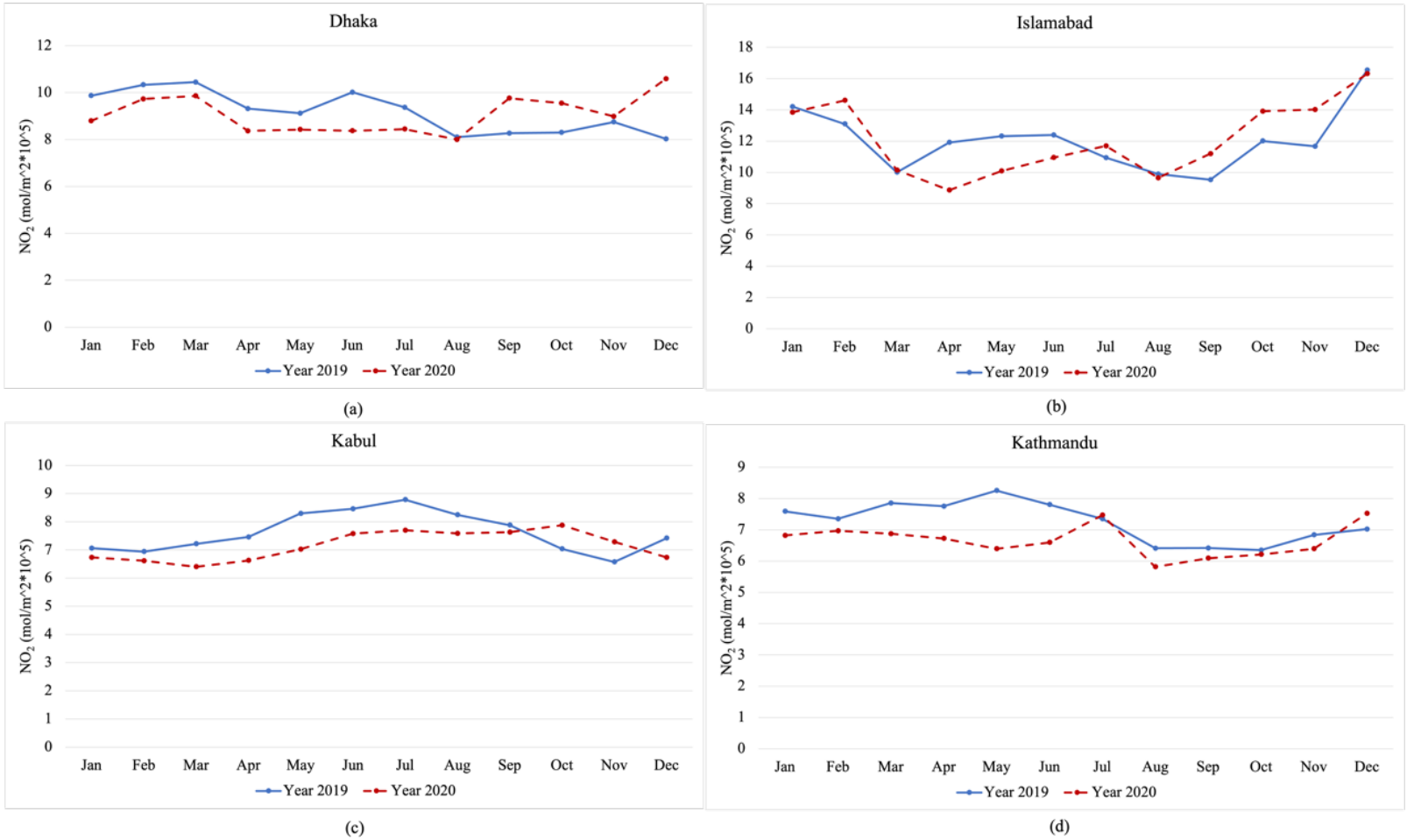

Figure 4.3 *Monthly trends of NO_2 of 7 cities in South Asia in 2019 and 2020*

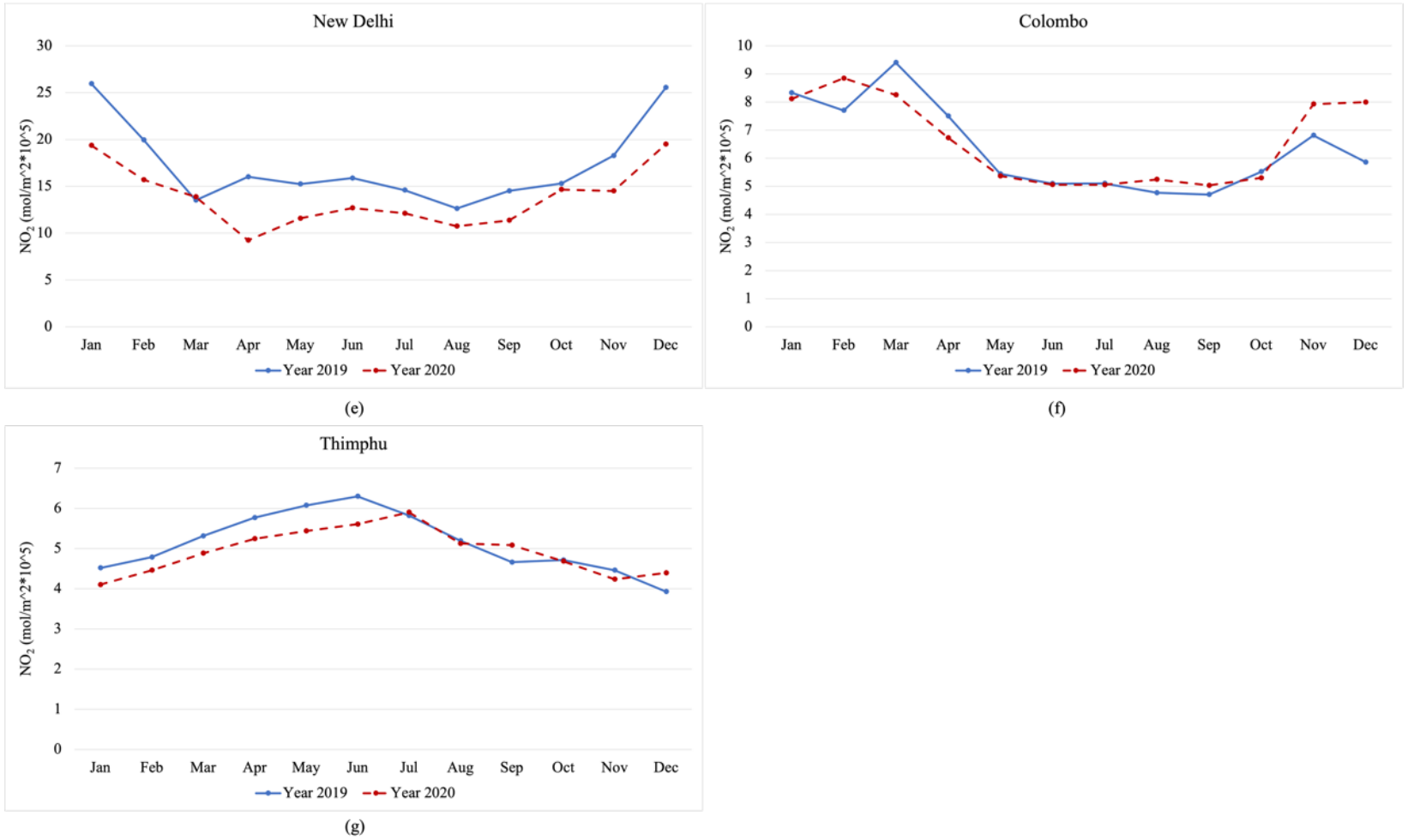

Figure 4.3 *Monthly trends of NO_2 of 11 cities in Southeast Asia in 2019 and 2020 (continue)*

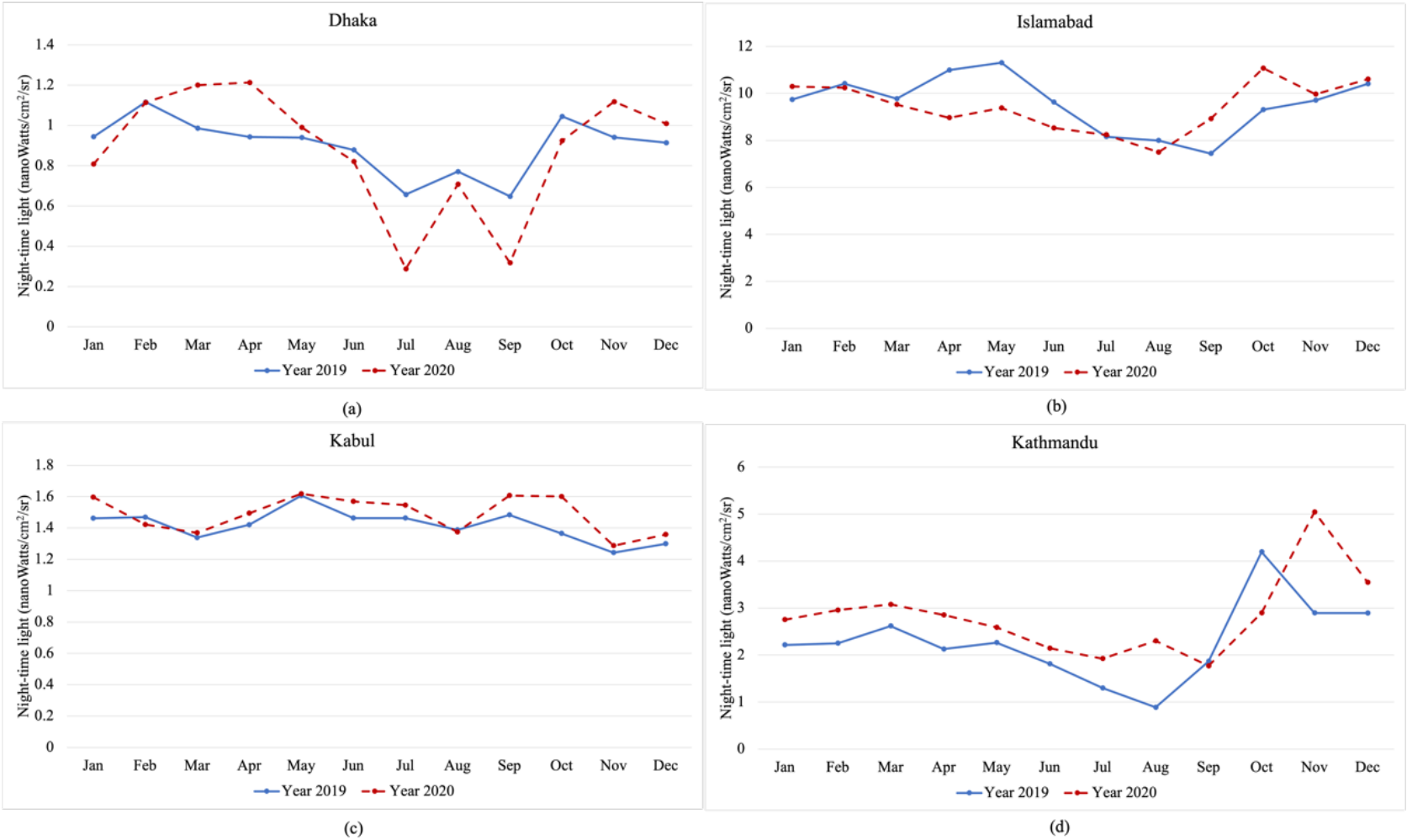

Figure 4.4 *Monthly trends of Nighttime light of 7 cities in South Asia in 2019 and 2020*

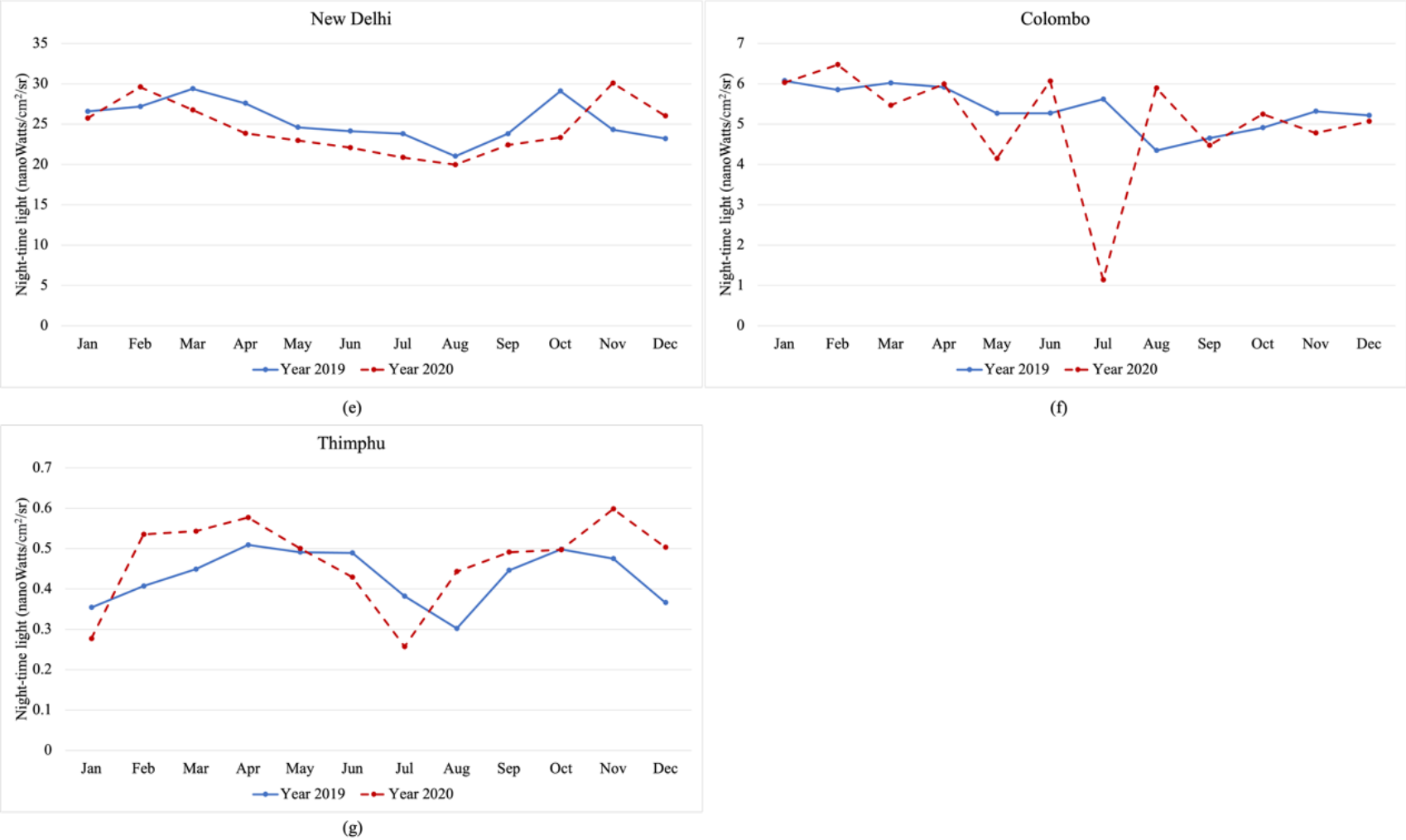

Figure 4.4 *Monthly trends of Nighttime light of 7 cities in South Asia in 2019 and 2020 (continue)*

4.3.2 NO_2 Level and NTL Intensity Change in the 11 Cities in Southeast Asia

The variations in monthly NO_2 concentrations ($mol/m^2 \times 10^5$) in the study periods were shown in (Fig. 4.5) for the 11 cities in SEA. The figure showed a reduction in NO_2 levels in all capital cities of SEA during the initial lockdown in 2020, as compared to the same period in 2019. Most large decreases were observed in Jakarta (30.43%), Singapore (22.83%), and Manila (22.56%). The remaining capitals saw drops ranging from 19.89% to 0.37%. The detailed breakdown is as follows: Kuala Lumpur (19.89%), Vientiane (12.22%), Yangon (11.58%), Bangkok (10.54%), Phnom Penh (7.96%), Ho Chi Minh city (3%), Bandar Seri Begawan (1.06%), and Dili (0.37%).

The monthly trends of NTL intensity, measured in $nanoWatts/cm^2/sr$, between 2019 and 2020 were shown in Figure 4.6 for the SEA cities. Among the cities, Bandar Seri Begawan (18% decrease) and Bangkok (12% decrease) exhibited the most substantial drop in NTL intensities during the lockdown period. Other cities recorded the following changes in NTL intensities during the lockdown: Manila (11.62% decrease), Singapore (8.14% decrease), Jakarta (7.66% decrease), Ho Chi Minh city (5.48% decrease), and Phnom Penh (0.86% decrease) while Vientiane, Dili, Yangon and Kuala Lumpur exhibited clear increases of 18.69%, 10.32%, 1.82%, and 1.25%, respectively.

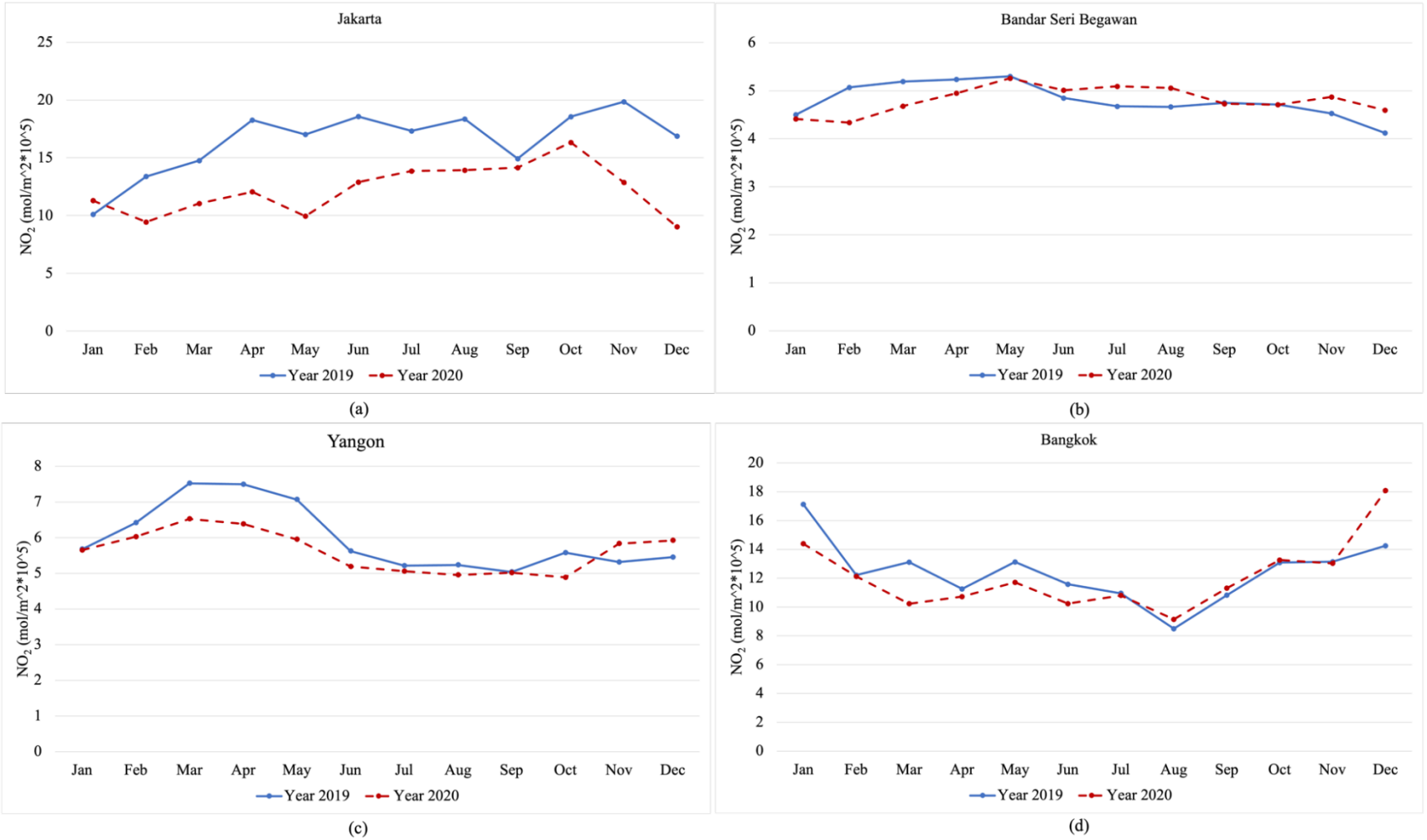

Figure 4.5 *Monthly trends of NO_2 of 11 cities in Southeast Asia in 2019 and 2020*

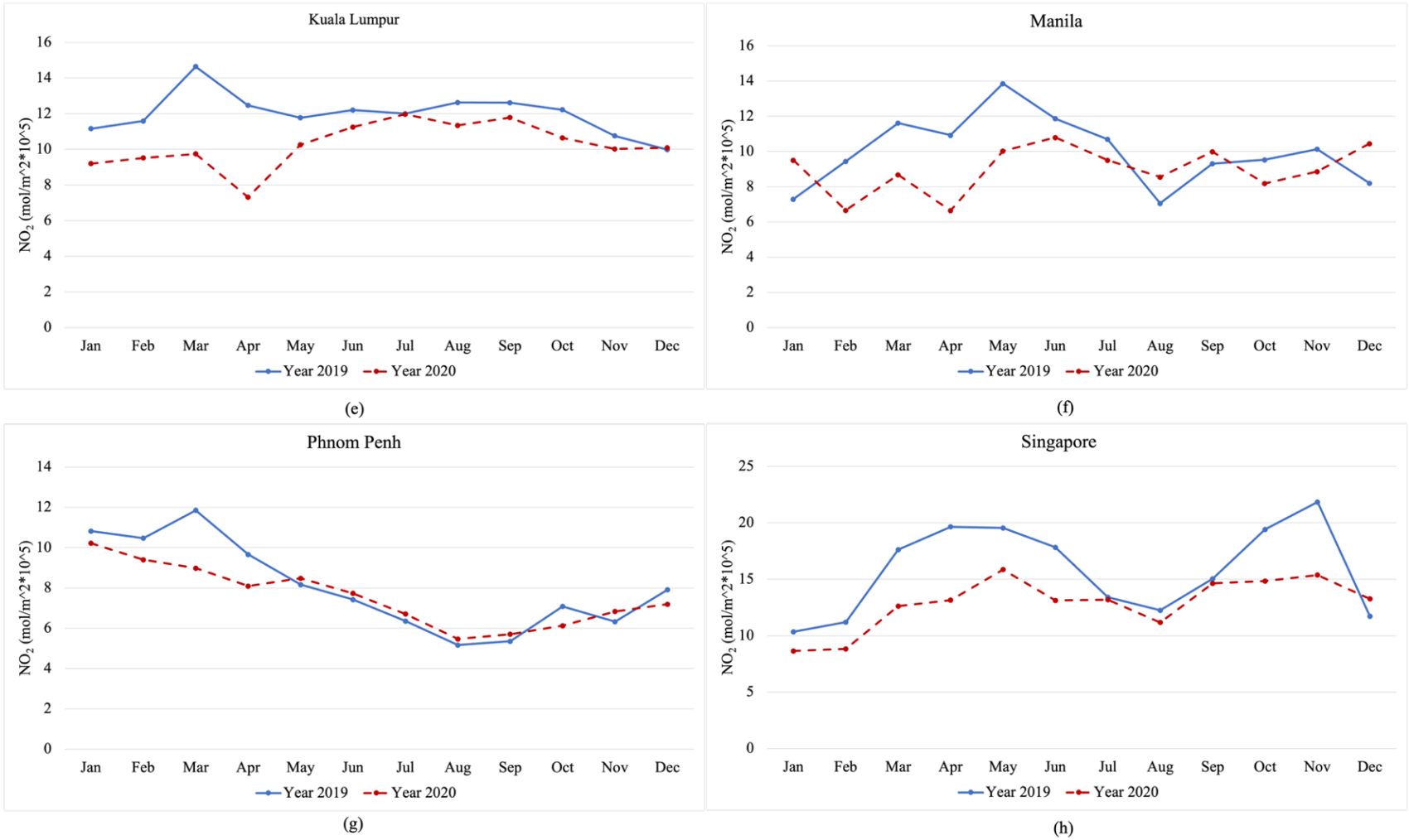

Figure 4.5 *Monthly trends of NO_2 of 11 cities in Southeast Asia in 2019 and 2020 (continue)*

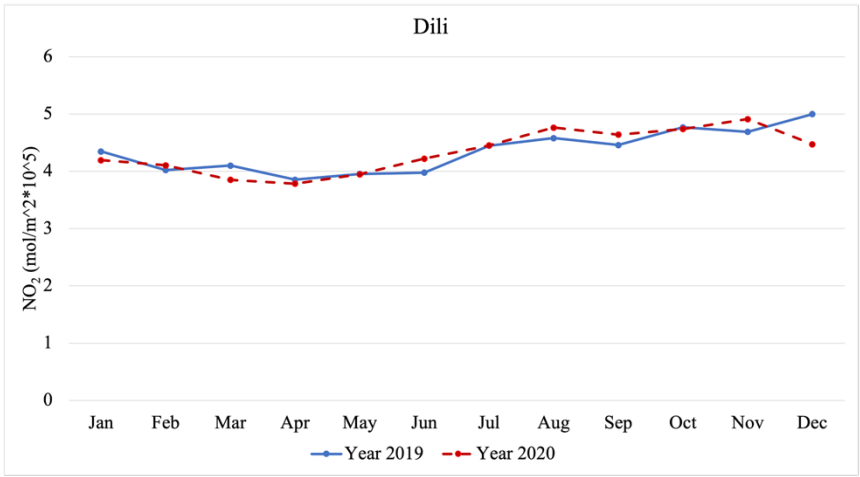

(i)

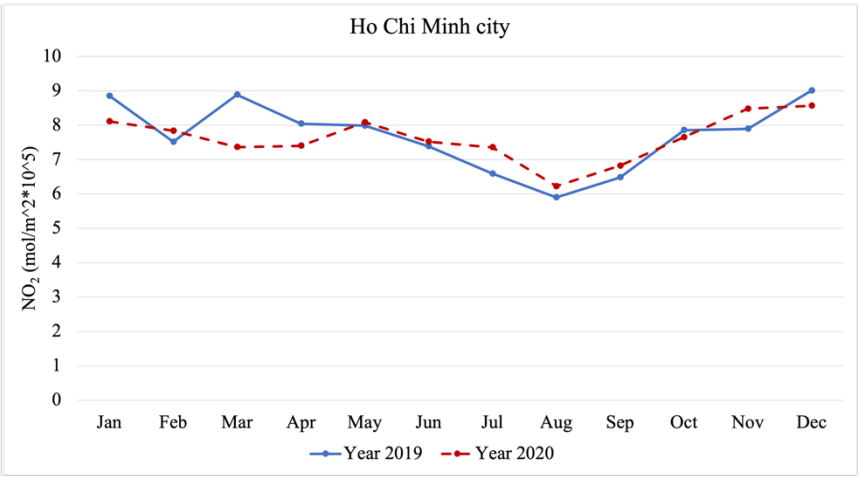

(j)

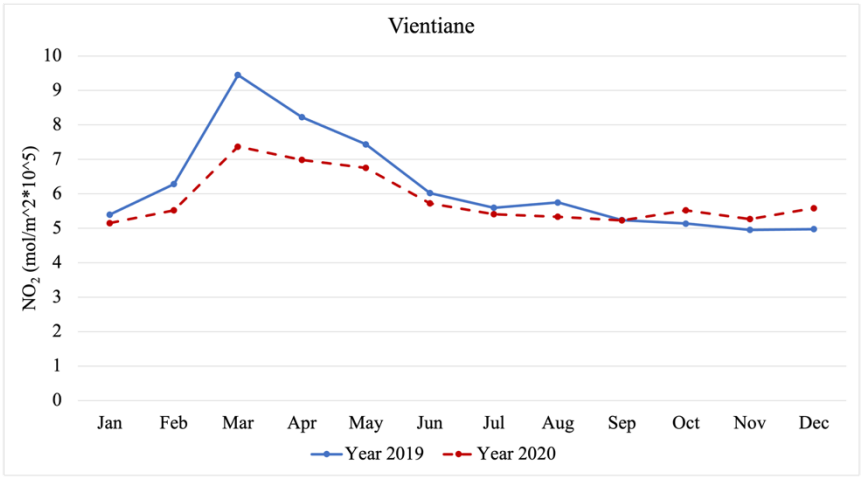

(k)

Figure 4.5 *Monthly trends of NO_2 of 11 cities in Southeast Asia in 2019 and 2020 (continue)*

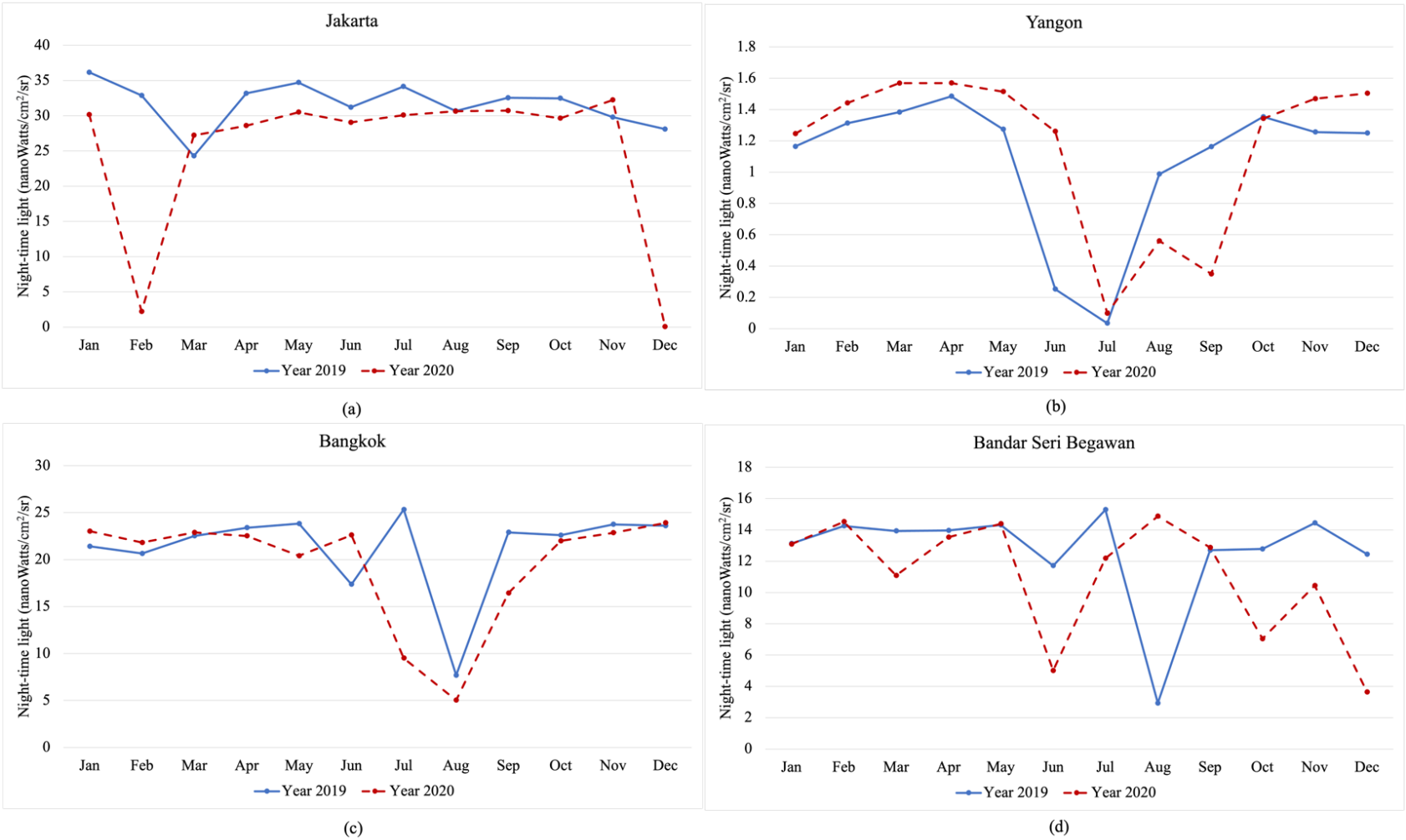

Figure 4.6 *Monthly trends of nighttime light of 11 cities in Southeast Asia in 2019 and 2020*

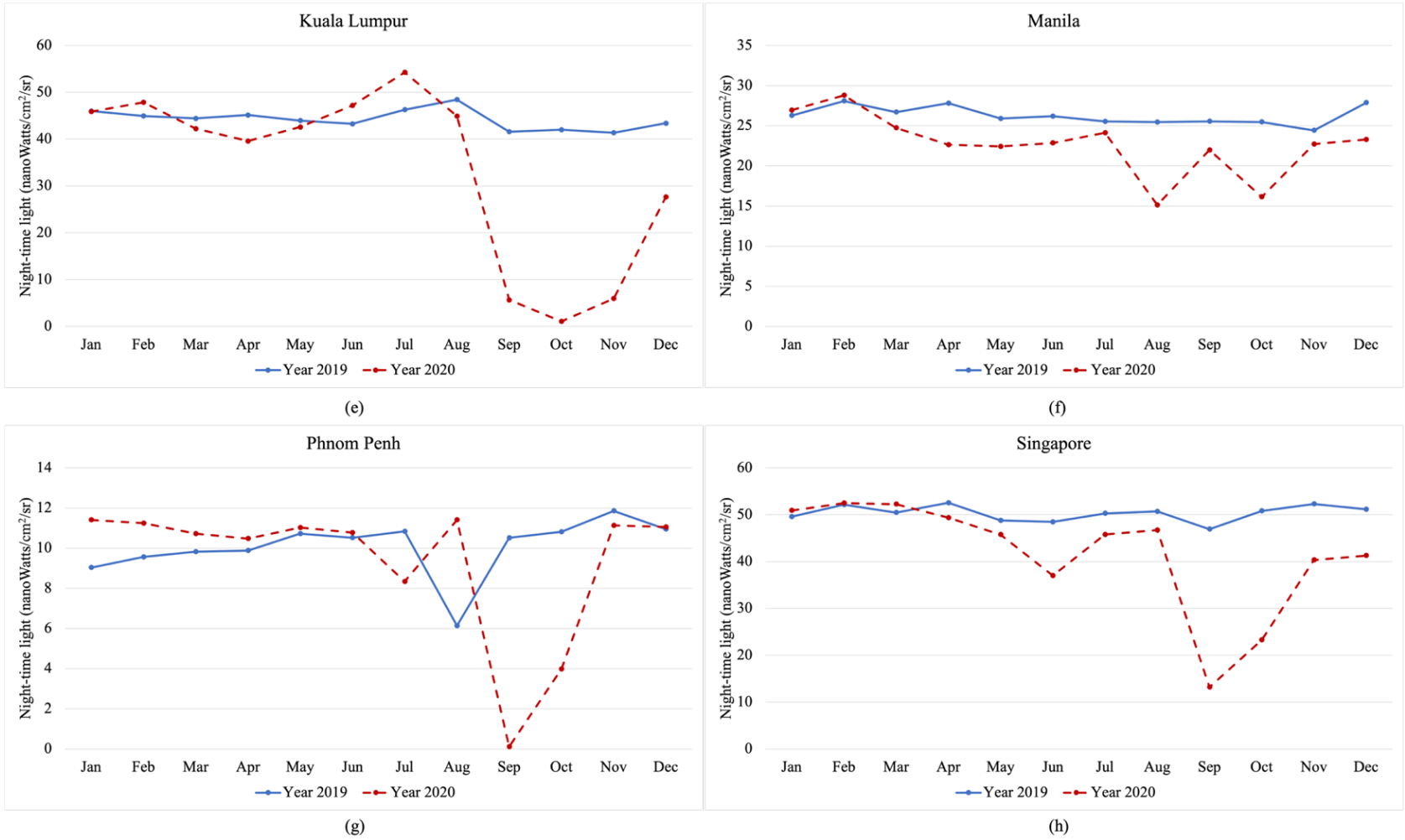

Figure 4.6 *Monthly trends of nighttime light of 11 cities in Southeast Asia in 2019 and 2020 (continue)*

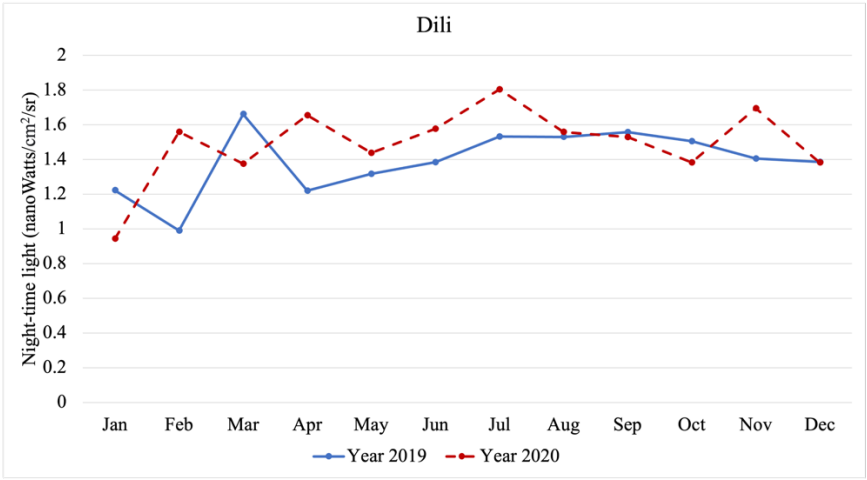

(i)

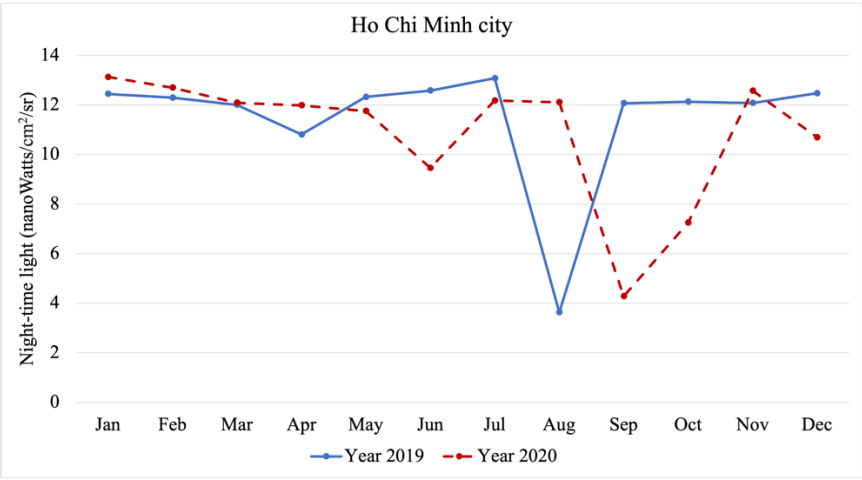

(j)

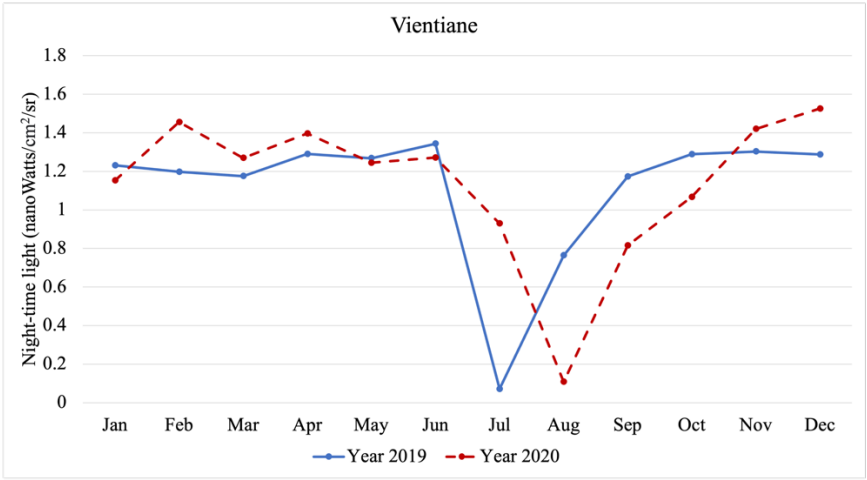

(k)

Figure 4.6 *Monthly trends of nighttime light of 11 cities in Southeast Asia in 2019 and 2020 (continue)*

Table 4.2 *Description of study cities*

Country	City	Estimated Population (City)	Area (km^2)	GDP per capita USD	Started date of lockdown	% reduction of NO_2	% reduction of NTL	Stay-at-home	Internal movement	Cancellation of public events
Sri Lanka	Colombo	5,648,000	37.31	14,230	2020/03/20	6.42	18.81	2	1	2
Brunei	Bandar Seri Begawan	100,700	100.36	75,583	2020/03/24	1.06	18.79	0	0	1
Thailand	Bangkok	18,007,000	1,568.70	22,675	2020/03/18	10.54	12.91	2	2	2
Philippines	Manila	24,922,000	633.00	11,420	2020/03/15	22.56	11.62	1	0	2
Pakistan	Islamabad	1,015,000	906.50	6,662	2020/03/23	10.14	10.45	2	2	2
India	New Delhi	29,617,000	42.70	8,293	2020/03/25	20.93	10.02	2	2	2
Singapore	Singapore	5,983,000	719.20	133,894	2020/04/07	22.83	8.14	1	2	2
Indonesia	Jakarta	33,756,000	661.50	15,855	2020/04/10	30.43	7.66	2	1	2
Vietnam	Ho Chi Minh City	15,136,000	2,095.00	14,458	2020/04/01	3.00	5.48	2	1	2
Cambodia	Phnom Penh	2,463,000	679.00	6,092	2020/04/09	7.96	0.86	0	0	0
Bhutan	Thimphu	114,551	26.10	13,077	2020/04/11	7.53	0.60	1	1	1
Malaysia	Kuala Lumpur	8,911,000	243.00	36,846	2020/03/18	19.89	-1.25	0	0	1
Bangladesh	Dhaka	21,741,000	306.40	7,985	2020/03/26	9.95	-2.45	2	2	2
Afghanistan	Kabul	4,435,000	1,028.00	2,456	2020/03/28	12.14	-4.17	1	2	2
East Timor	Dili	222,323	178.60	2,741	2020/03/28	0.37	-10.32	0	0	0
Laos	Vientiane	1,001,477	3,920	9,800	2020/04/01	12.22	-18.69	0	0	0
Nepal	Kathmandu	1,442,000	50.70	4,677	2020/03/24	12.72	-24.35	2	1	1
Myanmar	Yangon	6,874,000	598.80	5,131	2020/03/23	11.58	-35.77	2	2	2

Note. The specific policy and response categories are coded as follows: 0 – No measures, 1 – Recommend and 2 – Restrict

4.3.3 The different experiences among the study cities during the lockdown period

The study involved conducting hierarchical agglomerative clustering analysis, specifically utilizing Ward method, to classify the18 cities in SA and SEA. The classification was based on the standardized percentage changes observed in NO_2 and NTL intensity during the first lockdown period in 2020. The dendrogram of the analysis indicated four distinct clusters, as represented in Figure 4.7.

The scatter diagram generated to visualize these clusters exhibited a distinct differentiation among the four groups. Each data point on the scatter diagram corresponds to a city, where its location is determined by the percentage change in NTL on the x-axis and NO_2 on the y-axis. The color-coding of points was determined according to their cluster assignments, as shown in Figure 4.8.

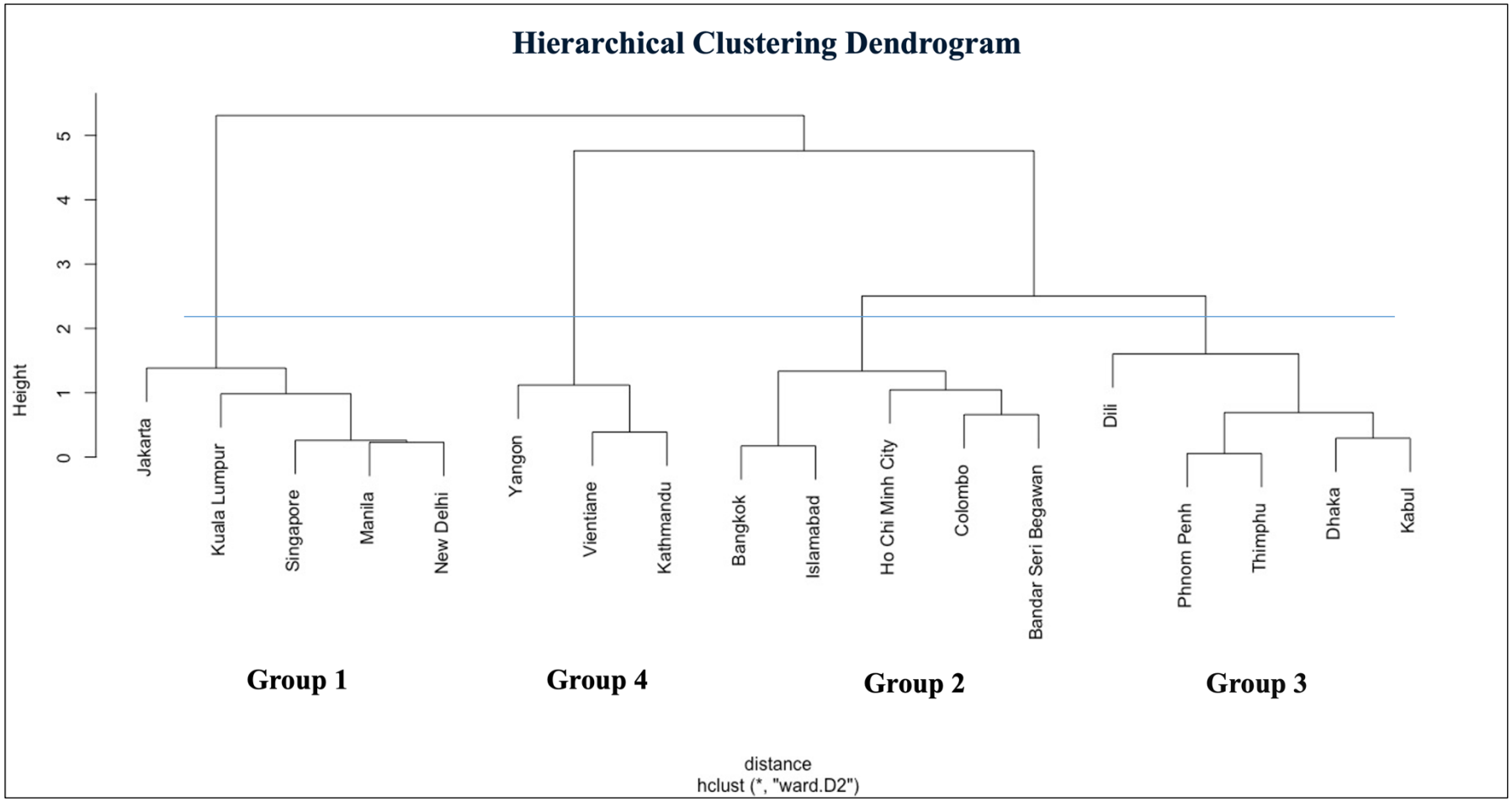

Figure 4.7 *Hierarchical Clustering Dendrogram of percentage reduction of nighttime light and percentage reduction of NO_2 during the lockdown period in 18 cities*

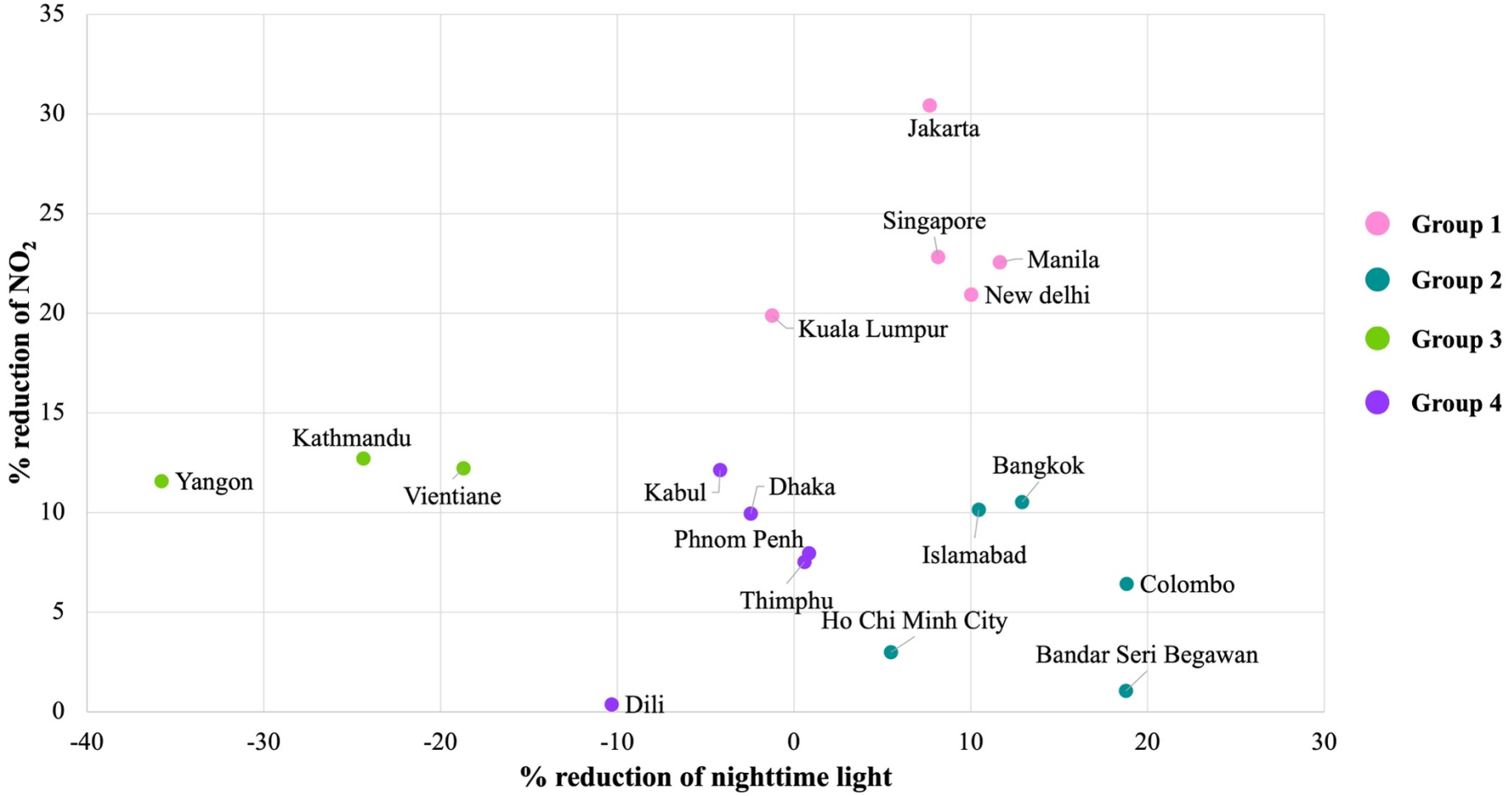

Figure 4.8 *Scatter diagram of percentage reduction of nighttime light and percentage reduction of NO_2 during the lockdown period in 18 cities*

The first group consists of cities with large NTL and NO_2 reductions, particularly in Jakarta, Singapore, Manila, and New Delhi. However, Kuala Lumpur presents substantial decreases in NO_2 levels, while also observing an increase in NTL emissions. The large decrease in NTL and NO_2 can be attributed to a decrease in overall economic activity and human movement during the lockdown period (Liu et al., 2020a). Factors such as urbanization, industrial emissions, transportation patterns, and local regulations may contribute to these variations. When people were confined to their homes during the lockdown, the reduction in commuting and industrial activity would have had a localized impact on pollution levels. This targeted reduction in emissions may have resulted in a clearer between changes in NTL and NO_2. Moreover, the cities in this group have nearly identical levels of lockdown. As show in Table 4.2 and Figure 4.12– 4.14, the cities have implemented the recommend and restrict response levels in accordance with lockdown restrictions, including stay-at-home, internal movement, and cancellation of public events.

The second group including Bandar Seri Begawan, Colombo, Bangkok, Islamabad, and Ho Chi Minh City had high reduction in NTL and low reduction in NO_2. For Bangkok and Islamabad, the level of lockdown measures implemented was restrict across all policy aspects of the lockdown as shown in Table 4.2 and Figure 4.12– 4.14. This may have contributed to a higher reduction in NTL. However, the reduction in NO_2 levels was relatively lower than that observed in the first group. The varying degrees of lockdown policy restrictions implemented within each city could be a determining factor influencing NO_2 reduction.

The third group including Yangon, Kathmandu, and Vientiane displayed a pattern with substantial increase of NTL but high reduction in NO_2. For Vientiane, government implemented “no measures” for all aspects of the lockdown policies as shown in Table 4.2 and Figure 4.12– 4.14. The citizen could continue their daily routines unhindered by any specific restrictions. Furthermore, cities in this group are in less developed countries (Fan et al., 2022; Mali et al., 2022; Wang et al., 2019) with lower GPD per capita and smaller population than the cities in groups 1 and 2 as shown Figure 4.9 and 4.11. This could result in a rapid growth of economic activity in these cities from years before the COVID-19 lockdown leading to the substantial increase of NTL. The Government of Nepal prioritized the reconstruction and recovery of damaged

infrastructure, including the electricity infrastructure following the 2015 earthquake near Kathmandu, (Chaulagain et al., 2016). This might lead to the increase of NTL during lockdown period compared to the same period before. Regarding the large reduction in NO_2, in Yangon, the level of lockdown measures implemented "restrict" across all policy aspects of the lockdown as shown in Table 4.2. The substantial decrease in NO_2 during the lockdown period can be attributed to the decrease in economic activity and human movement due to the lockdown implementation. In case of Kathmandu and Vientiane, the reduction of human activities from the lockdown measures in neighboring countries (such as India, Myanmar, and China) can cause the reduction in these cities. This may result in NO_2 reductions in these cities.

The fourth group is composed of the cities in which NO_2 was moderately reduced while NTL increased or was almost unchanged during the lockdown period. The group includes Dili, Dhaka, Kabul, Thimphu, and Phnom Penh. Specifically, Phnom Penh, and Dili implemented "no measures" for all aspects of the lockdown policies as shown in Table 4.2 and Figure 4.12– 4.14. This is due to different lengths of lockdown periods in each country but the study primarily focused on the period from March through July in 2020. During this specific lockdown period, although Phnom Penh and Dili did announce some form of lockdown measures, they were less severe in terms of intensity when compared to other cities. Furthermore, this group's cities have lower GDP per capita and smaller population than cities in other groups as shown in Figure 4.9 and Figure 4.11. Low GPD per capita cities typically have low level of urbanization, transportation demand, and infrastructure, including well-lit streets, commercial districts, and residential areas. This might lead to lower levels of NO_2 emission in these cities. Moreover, this group has a smaller population and a lower GDP per capita; as a result, NTL may not be able to effectively monitor human activities related to air pollution fluctuation.

4.3.4 Description of boxplots and graphs analysis

Figures 4.9 is the boxplot giving a comparative view of the GDP per capita across four groups of cities obtained from the cluster analysis. Each boxplot presents the interquartile range, median, and potential outliers, providing a comprehensive visual summary of the data. Each box encapsulates the interquartile range, from the 25th to the 75th percentiles, indicating where the middle 50% of values fall.

Group 1 had the highest median GDP per capita of $15,855, indicating most extensive economic activity. Group 2 followed closely with a median GDP per capita of $14,458, reflecting slightly lower yet substantial economic performance. Group 3 showed a substantial drop in the median at $7,985. Group 4 exhibited a considerably lower median GDP per capita of $3,225, suggesting the lowest economic activity among the groups.

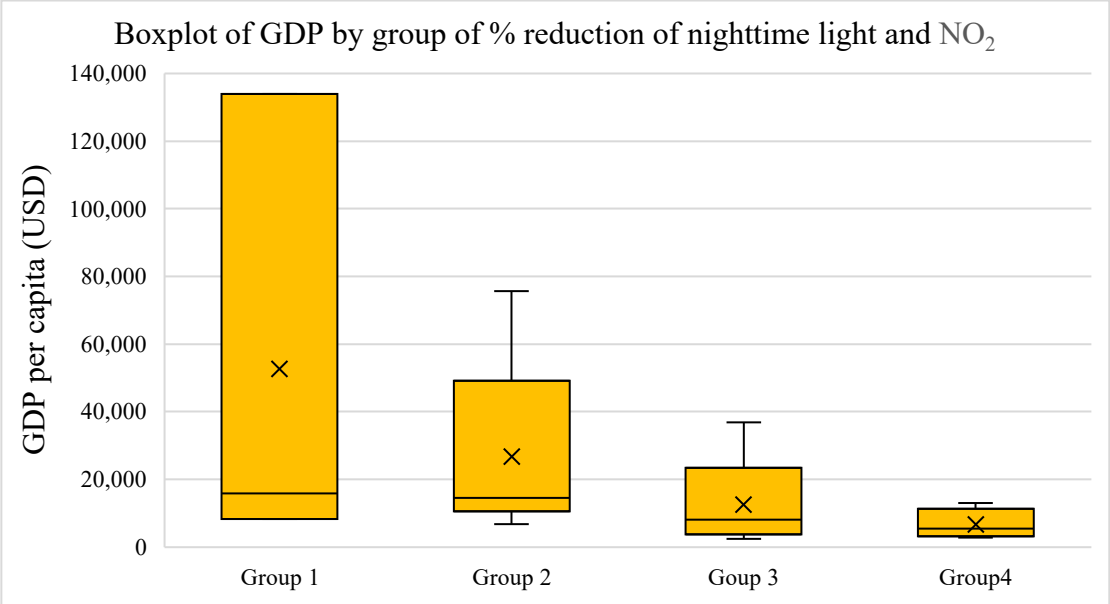

Figure 4.9 *Boxplot of GDP per capita by group of percentage of nighttime light and NO_2 reduction*

Figure 4.10 illustrates the distribution of area size (km^2) across the four groups. Group 1 has a median area size of 661.50 km^2. Group 2 tends to exhibit a larger area, as indicated by the largest median area of 906.50 km^2, while group 3 presents comparatively lower median of 598.80 km^2. Group 4 has the lowest median area of 114.65 km^2.

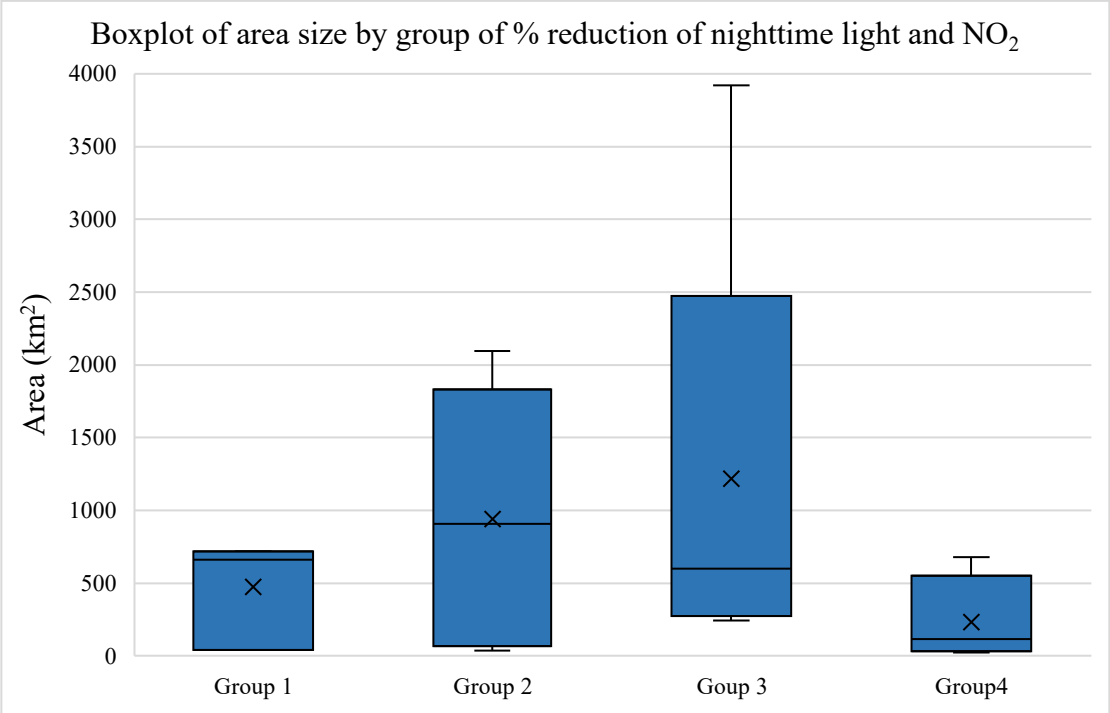

Figure 4.10 *Boxplot of area size by group of percentage of nighttime light and NO_2 reduction*

Figure 4.11 visualizes the estimated population distribution across the four groups. Group 1 has a median estimated population of 29,617,000. Group 2 and group 3 have median populations of 5,648,000 and 6,874,000, respectively, suggesting moderately populated areas with moderate changes in emissions and nighttime light. The lowest level of reduction is embodied by group 4, with a median population of 1,952,500, which may indicate that these areas are less populated or less urbanized.

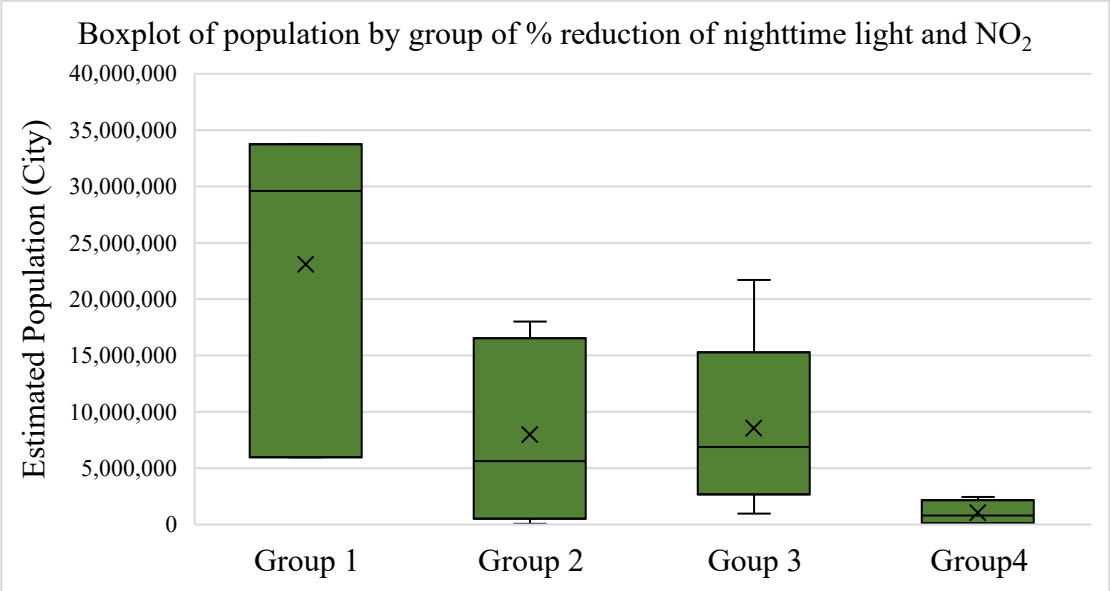

Figure 4.11 *Boxplot of estimated population by group of percentage of nighttime light and NO_2 reduction*

Figure 4.12 illustrates the effects of different levels of stay-at-home policies on the reduction of NTL and NO_2 across the four distinct groups. In the case of groups 1 and 2, it is observed that the level denoted as "restrict" is present in three cities, whereas the levels labeled as "recommend" and "no measures" are observed once. In contrast, group 3 exhibits a distinct pattern whereby the impact remains consistent despite the absence of measures (level 0) and restrictions (level 2). However, at the initial level (referred to as recommendation), the reduction observed is minimal, suggesting a possible reluctance towards adopting voluntary measures. Group 4 presents a pattern with twice as many cities at no measures and recommendations levels, reducing to just one at the restrict level. The bar plot captures a wide array of policy approaches to stay-at-home orders across cities, showcasing diversity in country response strategies.

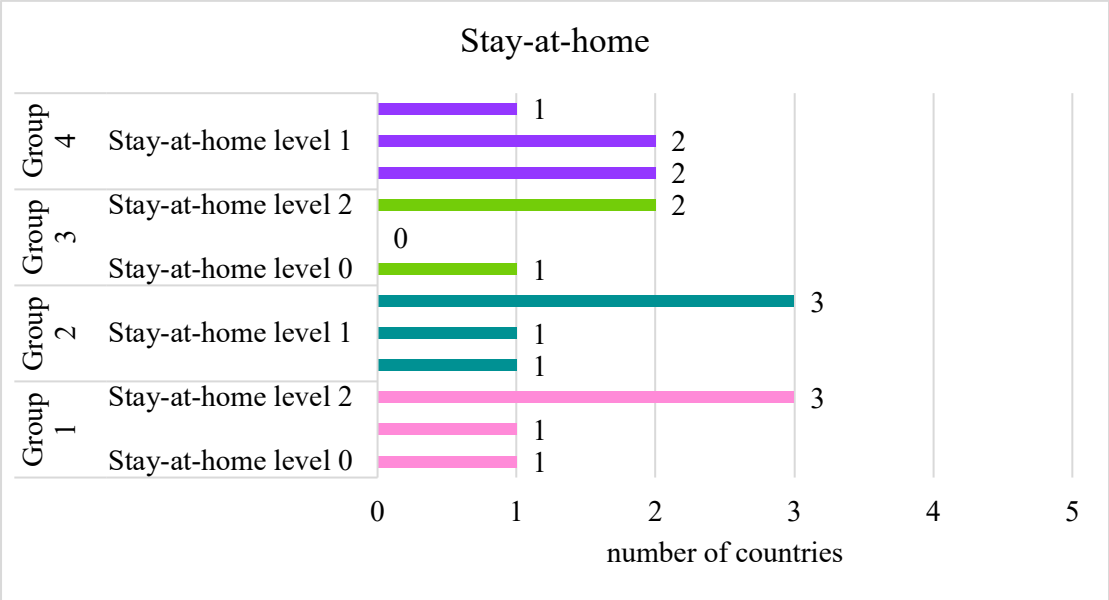

Figure 4.12 *Bar plot of stay-at-home policy restriction levels by group of percentage of nighttime light and NO_2 reduction*

Figure 4.13 illustrates the levels of internal movement policy restrictions across four distinct groups. Within group 1, it is observed that the level denoted as "no measures" is present once, whereas the levels labeled as "recommend" and "restrict" are observed twice. In group 2, the terms "no measures" and "restrict" are mentioned twice, while the term "recommend" is mentioned once. Group 3-reveals an equal distribution across all levels: “no measures,” “recommend,” and “restrict,” each appearing once. Group 4 exhibits a distribution that is in alignment with that of group 2, wherein the terms "no measures" and "restrict" are mentioned twice, while the term "recommend" is mentioned once.

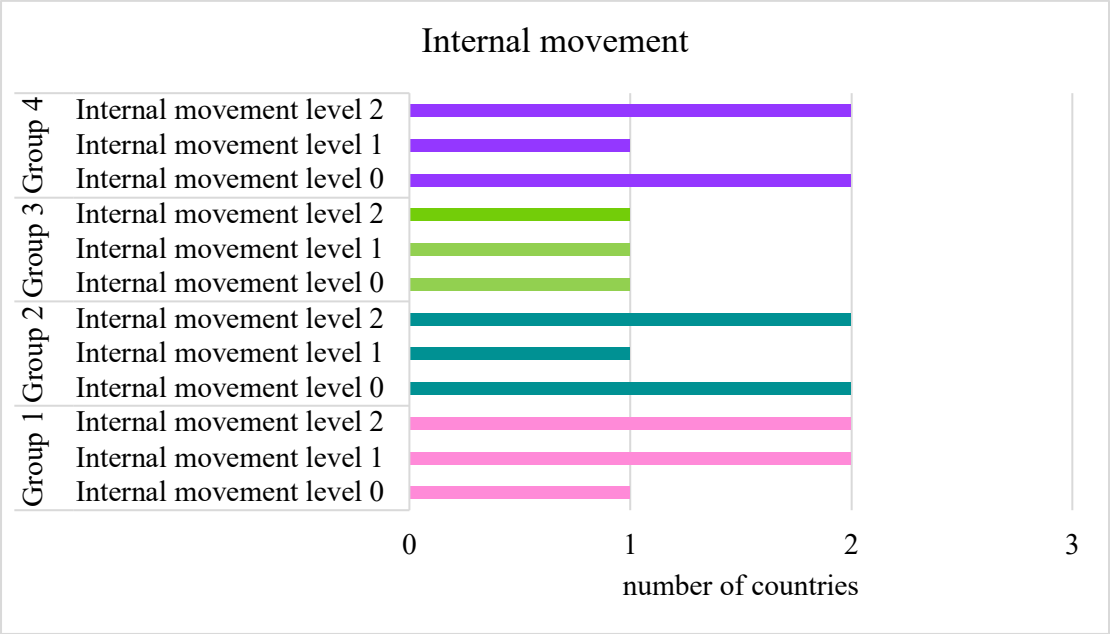

Figure 4.13 *Bar plot of internal movement policy restriction levels by group of percentage of nighttime light and NO_2 reduction*

Figure 4.14 presents the levels of policy restrictions on the cancellation of public events by the four groups. Groups 1 and 2 exhibit identical characteristics, demonstrating in the levels of policy restrictions ranging from 0 (no measures) to 4 (restrictions). Group 3 consistently maintains a policy level of 1 (recommended), regardless of any changes in the environment. In contrast, group 4 illustrates an initial policy restriction level of 2 (restrict), which subsequently decreases to 1 (recommend) at levels 1 and 2.

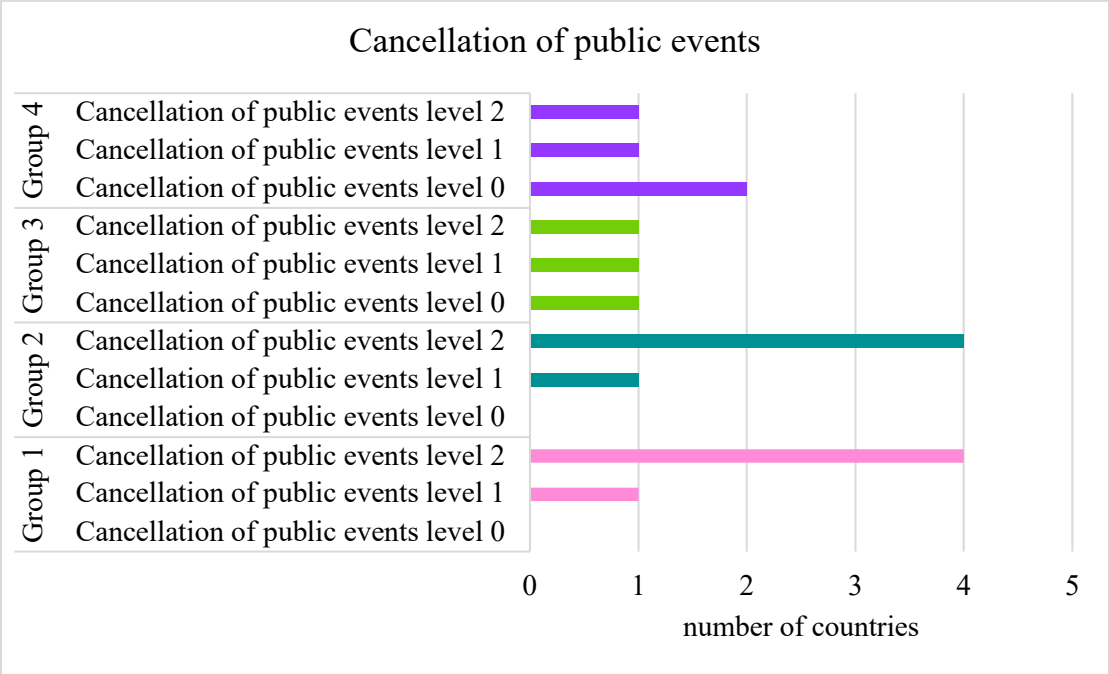

Figure 4.14 *Bar plot of cancelation of public events policy restriction levels by group of percentage of nighttime light and NO_2 reduction*

4.4 Discussion

Several major cities in SA and SEA experienced reductions in NO_2 concentrations during the COVID-19 lockdown period. The largest reductions were recorded in Jakarta, where NO_2 concentrations declined by 30.43%. Similarly, New Delhi, Singapore, Manila and Kuala Lumpur experienced a large reduction of 22.93%,22.83%, 22.56% and 19.89% respectively. Nitrogen Oxides (NOx) are primarily produced by combustion-related activities, including vehicle exhaust emissions, residential heating, power plants and industrial processes (Dumka et al., 2019). Initially released as nitrogen monoxide (NO), these compounds undergo rapid oxidation reactions, leading to the formation of NO_2. NO_2 is widely recognized as an indicator of anthropogenic combustion activities and acts as a precursor to the production of nitrate aerosols and ozone (Zhang et al., 2020). Strict restrictions resulted in large reductions in human activity, particularly in the transportation and industrial sectors. This reduction had a substantial impact on many aspects of society, including the transportation, industrial activities, commercial operations, institutions, and households (Venter et al., 2020). These sectors were identified as major contributors to air pollution in most countries prior to the COVID-19 pandemic (Klimont et al., 2017).

Cities such as Jakarta, Singapore, Manila, New Delhi, and Kuala Lumpur (group 1) exhibited large reductions in both NTL and NO_2 levels. During the lockdown, economic activities including industrial production, transportation, and commercial operations were substantially reduced. This decline in human activity likely led to a reduction in energy consumption, resulting in a decrease in NTL and emissions of pollutants like NO_2. The implementation of strict lockdown measures, including stay-at-home orders, internal movement restrictions, and cancellation of public events, likely contributed to these high reductions as shown in Figure 4.12– 4.14.

NTL reduction levels were also clear in Bandar Seri Begawan, Colombo, Bangkok, Islamabad, and Ho Chi Minh City (group 2), while NO_2 reduction levels were relatively smaller compared to group 1. Bangkok and Islamabad imposed restrictions on all aspects of the lockdown, which may have contributed to the higher reduction in NTL. Nevertheless, the decrease in NO_2 concentrations proved to be less substantial compared to the levels we observed in group 1. As shown in Figure 4.12– 4.14, the extent of NO_2 reduction may be influenced by the different levels of lockdown policies enforced in each city.

The third group, which included Yangon, Kathmandu, and Vientiane, exhibited distinct trends, with an increase in NTL and a substantial decrease in NO_2 levels. Despite Vientiane imposing "no measures" for all aspects of the lockdown policies (Table 4.2 and Figure 4.12– 4.14), allowing residents to maintain their usual activities. These cities are in developing countries, with smaller economies and populations than the cities in groups 1 and 2 (Figure 4.9 and 4.11). Rapid economic growth could be a reason for increased NTL intensity in these cities during the COVID-19 lockdown period compared to the same period in 2019. Yangon, the largest city in Myanmar, has undergone rapid urbanization due to its economic transition (Fan et al., 2022). After the 2015 earthquake reconstruction in Kathmandu, the government of Nepal prioritized the reconstruction of damaged infrastructure, which may have contributed to an increase in NTL during the lockdown period compared to the pre-lockdown period (Chaulagain et al., 2016). In contrast, the decrease in NO_2 in Yangon was due to strict lockdown measures reducing human movement and economic activities (Table 4.2 and Figure 4.12– 4.14). For Kathmandu and Vientiane, the reduction in human activities from lockdown measures in neighboring countries could have led to lower NO_2 levels.

Kathmandu's air pollution is influenced by factors such as vehicle emissions and long-range transportation of pollutants from India (Chen et al., 2015), which may contribute to NO_2 reductions in this city.

Cities such as Dili, Dhaka, Kabul, Phnom Penh, and Thimphu (group 4) experienced low reductions in NTL and NO_2 levels during the lockdown. The variations within this group are due to the severity and duration of lockdown measures. Phnom Penh and Dili, for example, implemented fewer and less intense lockdown measures compared to other cities during the specified period of analysis. Additionally, these cities have lower GDP per capita (Figure 4.9), limited urbanization, transportation demand, and infrastructure, which contribute to lower levels of NTL and NO_2 emissions. In the case of Chapter 3, NTL and NO_2 levels decreased substantially only in metropolitan cities like BMR. Similarly, in a broader international context, some countries may have the same situation. However, in less developed countries, the NTL capture could be compromised.

These findings indicate that the reduction in NTL intensity and NO_2 concentrations during the first wave of the pandemic is influenced by a number of factors, including the rigors of lockdown measures, city size, the diversity of emission sources, and the level of urbanization and infrastructure as shown in Figure 4.8– 4.10. Furthermore, NTL is also useful for monitoring human activity that related to NO_2 changes, which is only effective in more developed countries.

4.5 Conclusion

The analysis in this chapter focuses on the impact of city lockdowns on NO_2 and NTL changes in 18 cities in SA and SEA. Following the implementation of lockdown measures from March through July in 2020, NO_2 concentration generally decreased compared to the same period in 2019 in most of the cities. This indicated that the lockdown caused a substantial reduction in NO_2 in the 18 major cities in SA and SEA. Strict restrictions resulted in significant reductions in human activity, particularly in the transportation and industrial sectors. This reduction had a significant impact on various aspects of society, including transportation, industrial activities, commercial operations, institutions, and households (Venter et al., 2020). Moreover, reductions in NTL intensity were observed in some cities during the lockdown period, while some cities

experienced an increase in NTL. These variations can be attributed to differences in the duration and policies of the lockdown measures implemented, as well as economic activity in each country in the region.

Economic activities including industrial production, transportation, and commercial operations were significantly reduced in the cities studied during the lockdown. This decline in activity likely resulted in a decrease in energy consumption, resulting in decreased NTL and NO_2 emissions. However, the severity of lockdown policies, viz. degree of strictness and enforcement of measures, varied across the countries examined in this study.

In conclusion, the results of this study indicate a distinct and geographically diverse correlation between NO_2 emissions and NTL intensity in the South Asian and Southeast Asian cities examined during the COVID-19 lockdown. The implementation of lockdown measures resulted in a decrease in industrial, transportation, and commercial activities, which led to a general reduction in both NO_2 concentrations and NTL intensity. However, the variability in the strictness, enforcement of lockdown measures, and economic situations across the studied cities resulted in different levels of decrease and in some instances an increase in NTL intensity. In addition, NTL is beneficial for monitoring human activity related to air pollution (NO_2), which is only work well in more developed countries. However, further research is necessary to investigate the variations in this correlation across different contexts and under different policy enforcement conditions.

CHAPTER 5
Summary and Conclusion

The main objective of this thesis aims to investigate the influence of changes in NTL resulting from the COVID-19 lockdown on air pollution. The study focuses on various geographical scales of analysis, including the city-wide scale of the BMR, the national scale of Thailand, and an international scale consisting of a selection of 18 major cities within SA and SEA.

In Chapter 2, the study compares changes in air pollutants and human activities in the BMR during the COVID-19 lockdown and previous years. This analysis reveals a substantial reduction in air pollutant concentrations (NO_2, SO_2, PM_{10}, and $PM_{2.5}$), with a notable increase in O_3 levels during the lockdown period. The findings align with the existing literature, which also highlights the improvement of air quality worldwide during COVID-19 lockdowns (Liu et al., 2021b; Saha et al., 2022) However, this study extends these findings by demonstrating a strong positive monthly correlation between NO_2 levels and NTL intensity in the BMR, which suggests that urban areas with higher artificial lighting, indicative of human activity, were associated with elevated NO_2 emissions. This result supports the argument that NTL can be used as a sensitive indicator to monitor changes in air pollution caused by human activity.

In Chapter 3, the thesis employs Geographically Weighted Regression (GWR) to examine the local associations between changes in human activity (i.e., NTL) and air pollution (NO_2) around the first lockdown period in Thailand. This work helps to fill the research gap concerning the local association between NO_2 levels and human activity at a high geographical resolution. The results from this analysis indicate a positive relationship between changes in NTL and NO_2 levels, particularly in urbanized areas, which further affirms the usefulness of NTL observations for monitoring changes in air pollution caused by anthropogenic activities.

In Chapter 4, the study broadens its scope to examine major cities in SA and SEA, further reinforcing the general decrease in NO_2 concentrations during the lockdown period, consistent with previous studies (Liu et al., 2021b; Saha et al., 2022). Additionally, it illustrates how NTL intensity varies among cities, affected by factors such as lockdown measures' duration and policies, and economic activity. This finding

indicates that the NTL is beneficial for monitoring human activity related to air pollution (NO_2) especially in more developed countries with larger populations, contributing to the understanding of the differential impacts of lockdown policies on air pollution in a broader international context (Schneider et al., 2022).

The findings presented in this thesis contribute to our understanding of the intricate relationship between human activities and air pollution during the COVID-19 period. The reduction in anthropogenic activities has resulted in lower concentration of air pollutants, specifically NO_2, highlighting the substantial influence of human activities on air pollution. The positive correlations between NO_2 and NTL highlight the utility of NTL as a proxy for human activities contributing to air pollution. The study also highlights the potential of using NTL as an indicator to monitor changes in air pollution caused by human activities in urban areas. NTL is beneficial for monitoring human activities related to air pollution, but only under certain conditions. NTL is quite useful for monitoring air pollution when there is a sudden change in human activities, which is causing air pollution in cities with large populations and more developed economic activities. However, in regions with less development and smaller populations, NTL does not function well.

Implications

The findings from this study have important insights for understanding the relationship between human activities and air pollution during the COVID-19 pandemic. This study revealed a substantial reduction in NO_2 emissions as a result of decreased human activity due to the COVID-19 lockdown. This decrease in air pollution had positive effects on human health, including fewer cases of respiratory and cardiovascular diseases, reducing healthcare costs and potentially saving lives (He et al., 2020; Saadat et al., 2020). Additionally, the lockdowns caused substantial economic losses due to business closures, unemployment, and decreased consumer spending (BBC, 2020; Cutler and Summers, 2020). However, the economic value of the air quality improvement can be calculated in terms of healthcare cost savings and increased productivity due to fewer ill days. In addition, the monetary valuation of health benefits, such as the value of statistical life or years of life spared, may demonstrate that the health benefits outweigh some of the economic losses. However, the beneficial

improvements in air quality were temporary and came at the cost of massive societal disruption.

Although the current environmental changes are temporary, this short improvement in air quality during lockdown may be an encouraging sign for governing authorities and policymakers seeking to improve air quality through planned and strict limitations on emission sources. To control pollution levels in their regions with minimal economic impact, governments may implement a strategic lockdown at pollution focuses for a period of time.

Furthermore, broadening the study to include multiple cities in SA and SEA contributes to a better understanding of the regional variations in air pollution and the impact of lockdown measures. The variations observed in NTL changes across different countries highlight the need for tailored approaches to address specific socio-economic contexts and implement effective policies. The findings can contribute to informed decision-making processes and aid in the development of targeted strategies to improve air quality and public health in urban areas, both during and after crisis.

Future studies

This thesis investigates the influence of changes in NTL resulting from COVID-19 lockdown on air pollution., acknowledging that NTL may not be a precise indicator of air pollution (NO_2). There has been a notable increase in the availability of datasets regarding human mobility in developed countries. Using geographically detailed mobility data in future research could potentially reveal a stronger link between human activities and air pollution. However, Chapter 2 provided the discussion about the notion of mobility. In Thailand and other developing nations, such data can be expensive and may not cover the entire region. Thus, despite the fact that mobility data could be used to measure human activity levels, it is currently unavailable. Consequently, we utilized NTL data, which can be applied to comparable methodologies in other countries. However, the scope of this investigation was limited to 18 cities in SA and SEA. Future research could broaden the scope of the current study by utilizing satellite data, which can easily encompass additional regions or the entire world. Additionally, addressing several challenging issues necessitates a more

detailed analysis and understanding of meteorological influences over extended time periods.

List of Publication

Original paper

1. Thongrueang, N., Tsutsumida, N., & Nakaya, T. (2023). The Impact of Changes in Anthropogenic Activity Caused by COVID-19 Lockdown on Reducing Nitrogen Dioxide Levels in Thailand Using Nighttime Light Intensity. *Sustainability*, *15*(5), 4296. https://doi.org/10.3390/su15054296

Conferences Proceedings

1. Thongrueang, N and Nakaya,T. (2021) The impact on air pollution due to COVID-19 lockdown in Thailand. In Proceedings of the 62nd Annual Meeting for the Japanese Society of Tropical Medicine Global Health Issues during/after COVID-19 (JSTM2021), Japan

2. Thongrueang,N., Nakaya,T., and Tsutsumida,N. (2021) The Impact of COVID-19 Outbreak on Air Quality in Thailand. In Proceedings of the 30th Annual Meeting of the Geographic Information Systems Conference (GISA2021), Japan

REFERENCES

Agarwal, A., Kaushik, A., Kumar, S., & Mishra, R.K. (2020). Comparative study on air quality status in Indian and Chinese cities before and during the COVID-19 lockdown period. Air Quality, Atmosphere & Health, 13, 1167-1178. https://doi.org/10.1007/s11869-020-00881-z

Agnew, J., Gillespie, T. W., Gonzalez, J., & Min, B. (2008). Baghdad nights: Evaluating the US military 'surge' using nighttime light signatures. Environment and Planning A, 40(10), 2285-2295. https://doi.org/10.1068/a41200

Amaral, S., Monteiro, A. M., Câmara, G., & Quintanilha, J. A. (2006). DMSP/OLS night-time light imagery for urban population estimates in the Brazilian Amazon. International Journal of Remote Sensing, 27(05), 855-870. https://doi.org/10.1080/01431160500181861

Asian Development Bank (ADB). (n.d.). Developing Asia Growth to Fall in 2020 on COVID-19 Impact [News Release]. Retrieved from https://www.adb.org/news/

Badia, A., Langemeyer, J., Codina, X., Gilabert, J., Guilera, N., Vidal, V., Segura, R., Vives, M., & Villalba, G. (2021). A Take-Home Message from COVID-19 on Urban Air Pollution Reduction through Mobility Limitations and Teleworking. npj Urban Sustainability, 1, 35. https://doi.org/10.1038/s42949-021-00037-7

Bao, R., & Zhang, A. (2020). Does lockdown reduce air pollution? Evidence from 44 cities in northern China. Science of The Total Environment, 731, 139052. https://doi.org/10.1016/j.scitotenv.2020.139052

BBC. (2020). Corona: a visual guide to the economic impact. Retrieved July 18, 2023, from https://www.bbc.com/news/business-51706225

Beig, G., Bano, S., Sahu, S. K., Anand, V., Korhale, N., Rathod, A., Yadav, R., Mangaraj, P., Murthy, B. S., Singh, S., & Latha, R. (2020). COVID-19 and environmental-weather markers: Unfolding baseline levels and veracity of linkages in tropical India. Environmental Research, 191, 110121. https://doi.org/10.1016/j.envres.2020.110121

Butt, M. J. (2012). Estimation of light pollution using satellite remote sensing and geographic information system techniques. GIScience & Remote Sensing, 49(4), 609-621. https://doi.org/10.2747/1548-1603.49.4.609

Bustamante-Calabria, M., Sánchez de Miguel, A., Martín-Ruiz, S., Ortiz, J.-L., Vílchez, J. M., Pelegrina, A., García, A., Zamorano, J., Bennie, J., & Gaston, K. J. (2021). Effects of the COVID-19 Lockdown on Urban Light Emissions: Ground and Satellite Comparison. Remote Sensing, 13, 258. https://doi.org/10.3390/rs13020258

Chauhan, A., & Singh, R. P. (2020). Decline in PM2.5 concentrations over major cities around the world associated with COVID-19. Environmental Research, 187, 109634. https://doi.org/10.1016/j.envres.2020.109634

Chaulagain, H., Rodrigues, H., Silva, V., Spacone, E., & Varum, H. (2016). Earthquake loss estimation for the Kathmandu Valley. Bulletin of Earthquake Engineering, 14, 59-88. https://doi.org/10.1007/s10518-015-9811-5

Chen, P., Kang, S., Li, C., Rupakheti, M., Yan, F., Li, Q., Ji, Z., Zhang, Q., Luo, W., & Sillanpää, M. (2015). Characteristics and sources of polycyclic aromatic hydrocarbons in atmospheric aerosols in the Kathmandu Valley, Nepal. Science of the Total Environment, 538, 86-92. https://doi.org/10.1016/j.scitotenv.2015.08.049

Chen, T. M., Gokhale, J., Shofer, S., & Kuschner, W. G. (2007). Outdoor air pollution: Nitrogen dioxide, sulfur dioxide, and carbon monoxide health effects. American Journal of Medical Sciences, 333(4), 249-256. https://doi.org/10.1097/MAJ.0b013e31803b900f

Chen, X., & Nordhaus, W. D. (2011). Using luminosity data as a proxy for economic statistics. Proceedings of the National Academy of Sciences, 108(21), 8589-8594. https://doi.org/10.1073/pnas.1017031108

Chuersuwan, N., Nimrat, S., Lekphet, S., & Kerdkumrai, T. (2008). Levels and major sources of $PM_{2.5}$ and PM_{10} in Bangkok Metropolitan Region. Environmental International, 34, 671-677. https://doi.org/10.1016/j.envint.2007.12.018

Cohen, A.J., Brauer, M., Burnett, R., Anderson, H.R., Frostad, J., Estep, K., Balakrishnan, K., Brunekreef, B., Dandona, L., Dandona, R., and Feigin, V. (2017). Estimates and 25-year trends of the global burden of disease attributable to ambient air pollution: an analysis of data from the Global Burden of Diseases Study 2015. The Lancet, 389(10082), 1907-1918. https://doi.org/10.1016/S0140-6736(17)30505-6

Conticini, E., Frediani, B., & Caro, D. (2020). Can atmospheric pollution be considered a co-factor in extremely high level of SARS-CoV-2 lethality in Northern Italy? Environmental Pollution, 261, 114465. https://doi.org/10.1016/j.envpol.2020.114465

Cooper, M. J., Martin, R. V., Hammer, M. S., Levelt, P. F., Veefkind, P., Lamsal, L. N., Krotkov, N. A., Brook, J. R., & McLinden, C. A. (2022). Global fine-scale changes in ambient NO_2 during COVID-19 lockdowns. Nature, 601(7893), 380-387. https://doi.org/10.1038/s41586-021-04229-0

Cucinotta, D., & Vanelli, M. (2020). WHO declares COVID-19 a pandemic. Acta Biomedica: Atenei Parmensis, 91(1), 157. https://doi.org/10.23750/abm.v91i1.9397

Cutler, D. M., & Summers, L. H. (2020). The COVID-19 pandemic and the $16 trillion virus. Jama, 324(15), 1495-1496. https://doi.org/10.1001/jama.2020.19759

Doi, H., Osawa, T., & Tsutsumida, N. (2022). Assessing the potential repercussions of the COVID-19 pandemic on global SDG attainment. Discover Sustainability, 3(1), 1-11. https://doi.org/10.1007/s43621-021-00067-2

Doll, C. N., Muller, J. P., & Morley, J. G. (2006). Mapping regional economic activity from night-time light satellite imagery. Ecological Economics, 57(1), 75-92. https://doi.org/10.1016/j.ecolecon.2005.03.007

DOPA-Department of Provincial Administration. (2020). Statistic of Population by Province in 2020. Retrieved October 10, 2022, from https://stat.bora.dopa.go.th/stat/pk/pk_63.pdf

Dumka, U. C., Tiwari, S., Kaskaoutis, D. G., Soni, V. K., Safai, P. D., & Attri, S. D. (2019). Aerosol and pollutant characteristics in Delhi during a winter research campaign. Environmental Science and Pollution Research, 26, 3771-3794. https://doi.org/10.1007/s11356-018-3885-y

Dutheil, F., Baker, J. S., Navel, V., & Gomis, P. (2020). COVID-19 as a factor influencing air pollution? Environmental Pollution, 263, 114466. https://doi.org/10.1016/j.envpol.2020.114466

Elvidge, C. D., Cinzano, P., Pettit, D. R., Arvesen, J., Sutton, P., Small, C., Nemani, R., Longcore, T., Rich, C., Safran, J., & Weeks, J. (2007). The Nightsat mission concept. International Journal of Remote Sensing, 28(12), 2645-2670. https://doi.org/10.1080/01431160600981525

Elvidge, C. D., Baugh, K. E., Zhizhin, M., & Hsu, F. C. (2013). Why VIIRS data are superior to DMSP for mapping nighttime lights. In Proceedings of the Asia-Pacific Advanced Network, 35(0), 62. http://dx.doi.org/10.7125/APAN.35.7

Elvidge, C. D., Baugh, K., Zhizhin, M., Hsu, F. C., & Ghosh, T. (2017). VIIRS night-time lights. International Journal of Remote Sensing, 38(21), 5860-5879. https://doi.org/10.1080/01431161.2017.1342050

Fan, P., Chen, J., Fung, C., Naing, Z., Ouyang, Z., Nyunt, K. M., Myint, Z. N., et al. (2022). Urbanization, economic development, and environmental changes in transitional economies in the global south: A case of Yangon. Ecological Processes, 11(1), 65. https://doi.org/10.1186/s13717-022-00409-6

Fujisaka, S., et al. (1996). Slash-and-burn agriculture, conversion to pasture, and deforestation in two Brazilian Amazon colonies. Agriculture, Ecosystems & Environment, 59(1-2), 115-130. https://doi.org/10.1016/0167-8809(96)01015-8

GADM. (2018). GADM database of global Administration Areas. Retrieved February 5, 2023, from https://gadm.org/data.html

Ghosh, T., Powell, R. L., Elvidge, C. D., Baugh, K. E., Sutton, P. C., & Anderson, S. (2010). Shedding light on the global distribution of economic activity. The Open Geography Journal, 3(1). https://doi.org/10.2174/1874923201003010147

Greenpeace. (2015). Human cost of coal power. Retrieved February 15, 2022, from https://www.greenpeace.or.th/Thailand-human-cost-of-coal-power/en.pdf

Gu, Y., Zhang, W., Yang, Y., Wang, C., Streets, D. G., & Yim, S. H. L. (2020). Assessing outdoor air quality and public health impact attributable to residential black carbon emissions in rural China. Resources, Conservation and Recycling, 159, 104812. https://doi.org/10.1016/j.resconrec.2020.104812

Hamra, G. B., Laden, F., Cohen, A. J., Raaschou-Nielsen, O., Brauer, M., & Loomis, D. (2015). Lung cancer and exposure to nitrogen dioxide and traffic: A systematic review and meta-analysis. Environmental Health Perspectives, 123(11), 1107-1112. https://doi.org/10.1289/ehp.1408882

He, G., Pan, Y., & Tanaka, T. (2020). The short-term impacts of COVID-19 lockdown on urban air pollution in China. Nature sustainability, 3(12), 1005-1011.https://doi.org/10.1038/s41893-020-0581-y

Helin, J., & Weikard, H.-P. (2019). A model for estimating phosphorus requirements of world food production. Agricultural Systems, 176, 102666. https://doi.org/10.1016/j.agsy.2019.102666

Hong, S. H., Hwang, H., & Park, M. H. (2021). Effect of COVID-19 non-pharmaceutical interventions and the implications for human rights. International Journal of Environmental Research and Public Health, 18(1), 217. https://doi.org/10.3390/ijerph18010217

Hooke, R. L., & Martín-Duque, J. F. (2012). Land transformation by humans: A review. GSA Today, 12(12), 4-10. https://doi.org/10.1130/GSAT151A.1

Ialongo, I., Virta, H., Eskes, H., Hovila, J., & Douros, J. (2020). Comparison of TROPOMI/Sentinel-5 Precursor NO_2 observations with ground-based

measurements in Helsinki. Atmospheric Measurement Techniques, 13(1), 205-218. https://doi.org/10.5194/amt-13-205-2020

Iqbal, M. M., Shoaib, M., Agwanda, P., & Lee, J. L. (2018). Modeling approach for water-quality management to control pollution concentration: A case study of Ravi River, Punjab, Pakistan. Water, 10, 1068. https://doi.org/10.3390/w10081068

International Energy Agency. (2018). World Energy Statistics (Vol. 2018).

Installed Capacity, N. (2017). Central Electricity Authority, Ministry of Power, Government of India.

Jaenicke, J., Rieley, J.O., Mott, C., Kimman, P., & Siegert, F. (2008). Determination of the amount of carbon stored in Indonesian peatlands. Geoderma, 147(3-4), 151-158. https://doi.org/10.1016/j.geoderma.2008.08.008

Jain, S., & Sharma, T. (2020). Social and travel lockdown impact considering Coronavirus disease (COVID-19) on air quality in megacities of India: present benefits, future challenges and way forward. Aerosol and Air Quality Research, 20(6), 1222-1236. https://doi.org/10.4209/aaqr.2020.04.0171

Janssen, N. A., Brunekreef, B., van Vliet, P., Aarts, F., Meliefste, K., Harssema, H., & Fischer, P. (2003). The relationship between air pollution from heavy traffic and allergic sensitization, bronchial hyperresponsiveness, and respiratory symptoms in Dutch schoolchildren. Environmental Health Perspectives, 111(12), 1512-1518. https://doi.org/10.1289/ehp.6243

Jechow, A., & Hölker, F. (2020). Evidence That Reduced Air and Road Traffic Decreased Artificial Night-Time Skyglow during COVID-19 Lockdown in Berlin, Germany. Remote Sensing, 12, 3412. https://doi.org/10.3390/rs12203412

Kaewrat, J., Janta, R., Sichum, S., Rattikansukha, C., Tala, W., & Kanabkaew, T. (2022). Human Health Risks and Air Quality Changes Following Restrictions

for the Control of the COVID-19 Pandemic in Thailand. Toxics, 10(9), 520. https://doi.org/10.3390/toxics10090520

Kanniah, K. D., Zaman, N. A. F. K., Kaskaoutis, D. G., & Latif, M. T. (2020). COVID-19's impact on the atmospheric environment in the Southeast Asia region. Science of the Total Environment, 736, 139658. https://doi.org/10.1016/j.scitotenv.2020.139658

Khoder, M. I. (2002). Atmospheric conversion of sulfur dioxide to particulate sulfate and nitrogen dioxide to particulate nitrate and gaseous nitric acid in an urban area. Chemosphere, 49(6), 675-684. https://doi.org/10.1016/S0045-6535(02)00391-0

Kim, K.-H., Kabir, E., & Kabir, S. (2015). A review on the human health impact of airborne particulate matter. Environment International, 74, 136-143. https://doi.org/10.1016/j.envint.2014.10.005

Klimont, Z., Kupiainen, K., Heyes, C., Purohit, P., Cofala, J., Rafaj, P., Borken-Kleefeld, J., & Schöpp, W. (2017). Global anthropogenic emissions of particulate matter including black carbon. Atmospheric Chemistry and Physics, 17, 8681-8723. https://doi.org/10.5194/acp-17-8681-2017

Kovács, K. D. (2022). Nighttime light emissions explain the decline in NO_2 during a COVID-19-induced total lockdown in France. Geographia Technica, 17(1/2022), 104-115. https://doi.org/10.21163/gt_2022.171.08

Krecl, P., Targino, A.C., Oukawa, G.Y., & Junior, R.P.C. (2020). Drop in urban air pollution from COVID-19 pandemic: Policy implications for the megacity of São Paulo. Environmental Pollution, 265, 114883. https://doi.org/10.1016/j.envpol.2020.114883

Lelieveld, J., Evans, J. S., Fnais, M., Giannadaki, D., & Pozzer, A. (2015). The contribution of outdoor air pollution sources to premature mortality on a global scale. Nature, 525, 367-371. https://doi.org/10.1038/nature15371

Levy, I., Mihele, C., Lu, G., Narayan, J., & Brook, J. R. (2014). Evaluating multipollutant exposure and urban air quality: pollutant interrelationships, neighborhood variability, and nitrogen dioxide as a proxy pollutant. Environmental Health Perspectives, 122(1), 65-72. https://doi.org/10.1289/ehp.1306518

Lippmann, M., & Leikauf, G. D. (2020). Introduction and background. In Environmental Toxicants: Human Exposures and Their Health Effects (pp. 1-40). https://doi.org/10.1002/9781119438922.ch1

Liu, Q., Sha, D., Liu, W., Houser, P., Zhang, L., Hou, R., Lan, H., Flynn, C., Lu, M., Hu, T., & Yang, C. (2020a). Spatiotemporal Patterns of COVID-19 Impact on Human Activities and Environment in Mainland China Using Nighttime Light and Air Quality Data. Remote Sensing, 12, 1576. https://doi.org/10.3390/rs12101576

Liu, Z., Ciais, P., Deng, Z., Lei, R., Davis, S. J., Feng, S., Zheng, B., Cui, D., Dou, X., Zhu, B., et al. (2020b). Near-real-time monitoring of global CO_2 emissions reveals the effects of the COVID-19 pandemic. Nature Communications, 11(1), 5172. https://doi.org/10.1038/s41467-020-18922-7

Liu, B., Zhao, Q., Jin, Y., Shen, J., & Li, C. (2021a). Application of combined model of stepwise regression analysis and artificial neural network in data calibration of miniature air quality detector. Scientific Reports, 11(1), 3247. https://doi.org/10.1038/s41598-021-82871-4

Liu, F., Wang, M., & Zheng, M. (2021b). Effects of COVID-19 lockdown on global air quality and health. Science of the Total Environment, 755, 142533. https://doi.org/10.1016/j.scitotenv.2020.142533

Lokhandwala, S., & Gautam, P. (2020). Indirect impact of COVID-19 on the environment: A brief study in the Indian context. Environmental Research, 188, 109807. https://doi.org/10.1016/j.envres.2020.109807

Lu, B., Harris, P., Charlton, M., & Brunsdon, C. (2014). The GWmodel R package: further topics for exploring spatial heterogeneity using geographically weighted

models. Geo-Spatial Information Science, 17(2), 85-101. https://doi.org/10.1080/10095020.2014.917453

Lu, X., Zhang, L., Wang, X., Gao, M., Li, K., Zhang, Y., Yue, X., & Zhang, Y. (2020). Rapid increases in warm-season surface ozone and resulting health impact in China since 2013. Environmental Science & Technology Letters, 7(4), 240-247. https://doi.org/10.1021/acs.estlett.0c00171

Mahato, S., Pal, S., & Ghosh, K. G. (2020). Effect of lockdown amid COVID-19 pandemic on air quality of the megacity Delhi, India. The Science of the Total Environment, 730, 139086. https://doi.org/10.1016/j.scitotenv.2020.139086

Mali, B., Shrestha, A., Chapagain, A., Bishwokarma, R., Kumar, P., & Gonzalez-Longatt, F. (2022). Challenges in the penetration of electric vehicles in developing countries with a focus on Nepal. Renewable Energy Focus, 40, 1-12. https://doi.org/10.1016/j.ref.2021.11.003

Menut, L., Bessagnet, B., Siour, G., Mailler, S., Pennel, R., & Cholakian, A. (2020). Impact of lockdown measures to combat Covid-19 on air quality over western Europe. Science of The Total Environment, 741, 140426. https://doi.org/10.1016/j.scitotenv.2020.140426

Mesta, C., Cremen, G., & Galasso, C. (2022). Urban growth modelling and social vulnerability assessment for a hazardous Kathmandu Valley. Scientific Reports, 12(1), 6152. https://doi.org/10.1038/s41598-022-09347-x

Misra, P., Takigawa, M., Khatri, P., Dhaka, S. K., Dimri, A. P., Yamaji, K., Kajino, M., Takeuchi, W., Imasu, R., Nitta, K., & Patra, P. K. (2021). Nitrogen oxides concentration and emission change detection during COVID-19 restrictions in North India. Scientific Reports, 11(1), 9800. https://doi.org/10.1038/s41598-021-87673-2

Muhammad, S., Long, X., & Salman, M. (2020). COVID-19 pandemic and environmental pollution: a blessing in disguise? Science of The Total Environment, 138820. https://doi.org/10.1016/j.scitotenv.2020.138820

Murakami, D., Tsutsumida, N., Yoshida, T., Nakaya, T., & Lu, B. (2020). Scalable GWR: A linear-time algorithm for large-scale geographically weighted regression with polynomial kernels. Annals of the American Association of Geographers, 111(2), 459-480. https://doi.org/10.1080/24694452.2020.1774350

Musikawong, S., Jampaklay, A., Khamkhom, N., Tadee, R., Kerdmongkol, A., Buckles, L., Khachasin, S., & Engblom, A. (2021). Working and employment conditions in the agriculture sector in Thailand: A survey of migrants working on Thai sugarcane, rubber, oil palm and maize farms. International Labor Organization. Retrieved March 20, 2022, from https://www.ilo.org/asia/publications/WCMS_844317/lang--en/index.htm

Nakada, L. Y. K., & Urban, R. C. (2020). COVID-19 pandemic: Impacts on the air quality during the partial lockdown in São Paulo state, Brazil. Science of The Total Environment, 730, 139087. https://doi.org/10.1016/j.scitotenv.2020.139087

Ngarambe, J., Joen, S. J., Han, C. H., & Yun, G. Y. (2021). Exploring the relationship between particulate matter, CO, SO_2, NO_2, O_3 and urban heat island in Seoul, Korea. Journal of Hazardous Materials, 403, 123615. https://doi.org/10.1016/j.jhazmat.2020.123615

Pacheco, H., Díaz-López, S., Jarre, E., Pacheco, H., Méndez, W., & Zamora-Ledezma, E. (2020). NO_2 levels after the COVID-19 lockdown in Ecuador: A trade-off between environment and human health. Urban Climate, 34, 100674. https://doi.org/10.1016/j.uclim.2020.100674

Pata, U.K. (2020). How is COVID-19 affecting environmental pollution in US cities? Evidence from asymmetric Fourier causality test. Air Quality, Atmosphere & Health, 13(10), 1149-1155. https://doi.org/10.1007/s11869-020-00877-9

Patel, K. (n.d.). Airborne Nitrogen Dioxide Plummets Over China. Retrieved April 8, 2021, from https://www.earthobservatory.nasa.gov/images/146362/airborne-nitrogen-dioxide-plummets-over-china

Pei, Z., Han, G., Ma, X., Su, H., & Gong, W. (2020). Response of major air pollutants to COVID-19 lockdowns in China. Science of The Total Environment, 743, 140879. https://doi.org/10.1016/j.scitotenv.2020.140879

Pollution Control Department. (2000). Situation of Air Pollution in Decades on Thailand. Retrieved August 30, 2021, from http://www.pcd.go.th/public/Publications/print_report.cfm?task=report2543

Pollution Control Department. (2021). State of Thailand Environmental Quality 2020 (in Thai). Retrieved November 8, 2022, from https://www.pcd.go.th/pcd_news/11873

Rajput, H., Changotra, R., Rajput, P., Gautam, S., Gollakota, A. R., & Arora, A. S. (2020). A shock like no other: coronavirus rattles commodity markets. Environment, Development and Sustainability, 1-12. https://doi.org/10.1007/s10668-020-00934-4

Ramanathan, V., & Feng, Y. (2009). Air pollution, greenhouse gases and climate change: Global and regional perspectives. Atmospheric Environment, 43, 37-50. https://doi.org/10.1016/j.atmosenv.2008.09.063

Roy, S., Saha, M., Dhar, B., Pandit, S., & Nasrin, R. (2021). Geospatial analysis of COVID-19 lockdown effects on air quality in the South and Southeast Asian region. Science of the Total Environment, 756, 144009. https://doi.org/10.1016/j.scitotenv.2020.144009

Saadat, S., Rawtani, D., & Hussain, C. M. (2020). Environmental perspective of COVID-19. Science of the Total environment, 728, 138870. https://doi.org/10.1016/j.scitotenv.2020.138870

Saha, L., Kumar, A., Kumar, S., Korstad, J., Srivastava, S., & Bauddh, K. (2022). The impact of the COVID-19 lockdown on global air quality: A review. Environmental Sustainability, 5(1), 5-23. https://doi.org/10.1007/s42398-021-00213-6

Schneider, R., Masselot, P., Vicedo-Cabrera, A. M., Sera, F., Blangiardo, M., Forlani, C., & Gasparrini, A. (2022). Differential impact of government lockdown policies on reducing air pollution levels and related mortality in Europe. Scientific reports, 12(1), 726. https://doi.org/10.1038/s41598-021-04277-6

Seinfeld, J.H., & Pandis, S.N. (2016). Atmospheric chemistry and physics: from air pollution to climate change. John Wiley & Sons.

Sengupta, U., & Upadhyaya, V. B. (2016). Lost in transition? Emerging forms of residential architecture in Kathmandu. Cities, 52, 94-102. https://doi.org/10.1016/j.cities.2015.11.007

Shao, Z., Tang, Y., Huang, X., & Li, D. (2021). Monitoring work resumption of Wuhan in the COVID-19 epidemic using daily nighttime light. Photogrammetric Engineering & Remote Sensing, 87(3), 195-204. https://doi.org/10.14358/PERS.87.3.197

Sharma, S., Zhang, M., Gao, J., Zhang, H., & Kota, S.H. (2020). Effect of restricted emissions during COVID-19 on air quality in India. Science of The Total Environment, 728, 138878. https://doi.org/10.1016/j.scitotenv.2020.138878

Sicard, P., De Marco, A., Agathokleous, E., Feng, Z., Xu, X., Paoletti, E., Rodriguez, J.J.D., & Calatayud, V. (2020). Amplified ozone pollution in cities during the COVID-19 lockdown. Science of The Total Environment, 735, 139542. https://doi.org/10.1016/j.scitotenv.2020.139542

Stockholm Environment Institute. (n.d.). Air quality in Thailand. Retrieved January 12, 2023.

Subramaniam, Y., Masron, T. A., & Azman, N. H. N. (2020). Biofuels, environmental sustainability, and food security: A review of 51 countries. Energy Research & Social Science, 68, 101549. https://doi.org/10.1016/j.erss.2020.101549

Sutton, P. C. (2003). A scale-adjusted measure of "urban sprawl" using nighttime satellite imagery. Remote Sensing of Environment, 86(3), 353-369. https://doi.org/10.1016/S0034-4257(03)00078-6

Thongrueang, N., Tsutsumida, N., & Nakaya, T. (2023). The impact of changes in anthropogenic activity caused by COVID-19 lockdown on reducing nitrogen dioxide levels in Thailand using nighttime light intensity. Sustainability, 15, 4296. https://doi.org/10.3390/su15054296

Tobías, A., Carnerero, C., Reche, C., Massagué, J., Via, M., Minguillón, M. C., Alastuey, A., & Querol, X. (2020). Changes in air quality during the lockdown in Barcelona (Spain) one month into the SARS-CoV-2 epidemic. Science of The Total Environment, 726, 138540. https://doi.org/10.1016/j.scitotenv.2020.138540

Van Der Velde, I. R., Van Der Werf, G. R., Houweling, S., Eskes, H. J., Veefkind, J. P., Borsdorff, T., & Aben, I. (2021). Biomass burning combustion efficiency observed from space using measurements of CO and NO_2 by the TROPOspheric Monitoring Instrument (TROPOMI). Atmospheric Chemistry and Physics, 21(2), 597-616. https://doi.org/10.5194/acp-21-597-2021

Van Vliet, P., Knape, M., De Hartog, J., Janssen, N., Harssema, H., & Brunekreef, B. (1997). Motor vehicle exhaust and chronic respiratory symptoms in children living near freeways. Environmental Research, 74(2), 122-132. https://doi.org/10.1006/enrs.1997.3757

Veefkind, J. P., Aben, I., McMullan, K., Förster, H., De Vries, J., Otter, G., Claas, J., Eskes, H. J., De Haan, J. F., Kleipool, Q., & Van Weele, M. (2012). TROPOMI on the ESA Sentinel-5 Precursor: A GMES mission for global observations of the atmospheric composition for climate, air quality and ozone layer applications. Remote Sensing of Environment, 120, 70-83. https://doi.org/10.1016/j.rse.2011.09.027

Velásquez, R.M.A., & Lara, J.V.M. (2020). Gaussian approach for probability and correlation between the number of COVID-19 cases and air pollution in Lima. Urban Climate, 33, 100664. https://doi.org/10.1016/j.uclim.2020.100664

Venter, Z. S., Aunan, K., Chowdhury, S., & Lelieveld, J. (2020). COVID-19 lockdowns cause global air pollution declines. Proceedings of the National Academy of

Sciences of the United States of America, 117, 18984-18990. https://doi.org/10.1073/pnas.2006853117

Venter, Z. S., Aunan, K., Chowdhury, S., & Lelieveld, J. (2021). Air pollution declines during COVID-19 lockdowns mitigate the global health burden. Environmental Research, 192, 110403. https://doi.org/10.1016/j.envres.2020.110403

Wang, J., Sui, L., Yang, X., Wang, Z., Ge, D., Kang, J., Yang, F., Liu, Y., & Liu, B. (2019). Economic globalization impacts on the ecological environment of inland developing countries: A case study of Laos from the perspective of the land use/cover change. Sustainability, 11, 3940. https://doi.org/10.3390/su11143940

Wang, Q., & Su, M. (2020). A preliminary assessment of the impact of COVID-19 on environment – a case study of China. Science of The Total Environment, 728, 138915. https://doi.org/10.1016/j.scitotenv.2020.138915

Wang, Q., & Su, M. (2020). Preliminary assessment of the impact of COVID-19 on environment – a case study of China. Science of The Total Environment, 728, 138915. https://doi.org/10.1016/j.scitotenv.2020.138915

Wong, C.-M., Vichit-Vadakan, N., Kan, H., & Qian, Z. (2008). Public Health and Air Pollution in Asia (PAPA): A multicity study of short-term effects of air pollution on mortality. Environmental Health Perspectives, 116(9), 1195-1202. https://doi.org/10.1289/ehp.11257

Wetchayont, P. (2021). Investigation on the impacts of COVID-19 lockdown and influencing factors on air quality in greater Bangkok, Thailand. Advances in Meteorology, 2021, 1-11. https://doi.org/10.1155/2021/6697707

World Bank. (2002). Thailand - Environment monitor 2002: air quality (English). Retrieved January 12, 2021, from http://documents.worldbank.org/curated/en/710411468778515943/Thailand-Environment-monitor-2002-air-quality

World Health Organization. (2020). WHO Coronavirus (COVID-19) Dashboard. Retrieved June 12, 2021, from https://covid19.who.int/

World Health Organization. (2020). WHO Coronavirus (COVID-19) Thailand situation reports. Retrieved August 15, 2022, from https://www.who.int/docs/default-source/searo/thailand/2020-04-3-tha-sitrep-41-covid19-final.pdf?sfvrsn=9e14aebc_0.pdf

Worldometer. (n.d.). Worldometers.Info/World-Population. Retrieved February 8, 2023, from https://www.worldometers.info/world-population/

Xu, G., Xiu, T., Li, X., Liang, X., & Jiao, L. (2021). Lockdown induced night-time light dynamics during the COVID-19 epidemic in global megacities. International Journal of Applied Earth Observation and Geoinformation, 102, 102421. https://doi.org/10.1016/j.jag.2021.102421

Yin, S., Wang, X., Zhang, X., Guo, M., Miura, M., & Xiao, Y. (2019). Influence of biomass burning on local air pollution in mainland Southeast Asia from 2001 to 2016. Environmental Pollution, 254, 112949. https://doi.org/10.1016/j.envpol.2019.07.117

Zhang, R., Zhang, Y., Lin, H., Feng, X., Fu, T.-M., & Wang, Y. (2020). NOx emission reduction and recovery during COVID-19 in east China. Atmosphere, 11(4), 433. https://doi.org/10.3390/atmos11040433

Zhang, Z., Arshad, A., Zhang, C., Hussain, S., & Li, W. (2020b). Unprecedented temporary reduction in global air pollution associated with COVID-19 forced confinement: a continental and city-scale analysis. Remote Sensing, 12, 2420. https://doi.org/10.3390/rs12152420

Zhao, X., Yu, B., Liu, Y., Yao, S., Lian, T., Chen, L., & Wu, J. (2018). NPP-VIIRS DNB daily data in natural disaster assessment: Evidence from selected case studies. Remote Sensing, 10(10), 1526. https://doi.org/10.3390/rs10101526